



University of Dundee

Targeting Bacillosamine Biosynthesis in Bacterial Pathogens

De Schutter, Joris W.; Morrison, James P.; Morrison, Michael J.; Ciulli, Alessio; Imperiali, Barbara

Published in:
Journal of Medicinal Chemistry

DOI:
[10.1021/acs.jmedchem.6b01869](https://doi.org/10.1021/acs.jmedchem.6b01869)

Publication date:
2017

Document Version
Peer reviewed version

[Link to publication in Discovery Research Portal](#)

Citation for published version (APA):

De Schutter, J. W., Morrison, J. P., Morrison, M. J., Ciulli, A., & Imperiali, B. (2017). Targeting Bacillosamine Biosynthesis in Bacterial Pathogens: Development of Inhibitors to a Bacterial Amino-Sugar Acetyltransferase from *Campylobacter jejuni*. *Journal of Medicinal Chemistry*, 60(5), 2099-2118.
<https://doi.org/10.1021/acs.jmedchem.6b01869>

General rights

Copyright and moral rights for the publications made accessible in Discovery Research Portal are retained by the authors and/or other copyright owners and it is a condition of accessing publications that users recognise and abide by the legal requirements associated with these rights.

- Users may download and print one copy of any publication from Discovery Research Portal for the purpose of private study or research.
- You may not further distribute the material or use it for any profit-making activity or commercial gain.
- You may freely distribute the URL identifying the publication in the public portal.

Take down policy

If you believe that this document breaches copyright please contact us providing details, and we will remove access to the work immediately and investigate your claim.

Targeting Bacillosamine Biosynthesis in Bacterial Pathogens: Development of Inhibitors to a Bacterial Amino-Sugar Acetyltransferase from *Campylobacter jejuni*

Joris W. De Schutter, James P Morrison, Michael James Morrison, Alessio Ciulli, and Barbara Imperiali

J. Med. Chem., **Just Accepted Manuscript** • Publication Date (Web): 09 Feb 2017

Downloaded from <http://pubs.acs.org> on February 10, 2017

Just Accepted

“Just Accepted” manuscripts have been peer-reviewed and accepted for publication. They are posted online prior to technical editing, formatting for publication and author proofing. The American Chemical Society provides “Just Accepted” as a free service to the research community to expedite the dissemination of scientific material as soon as possible after acceptance. “Just Accepted” manuscripts appear in full in PDF format accompanied by an HTML abstract. “Just Accepted” manuscripts have been fully peer reviewed, but should not be considered the official version of record. They are accessible to all readers and citable by the Digital Object Identifier (DOI®). “Just Accepted” is an optional service offered to authors. Therefore, the “Just Accepted” Web site may not include all articles that will be published in the journal. After a manuscript is technically edited and formatted, it will be removed from the “Just Accepted” Web site and published as an ASAP article. Note that technical editing may introduce minor changes to the manuscript text and/or graphics which could affect content, and all legal disclaimers and ethical guidelines that apply to the journal pertain. ACS cannot be held responsible for errors or consequences arising from the use of information contained in these “Just Accepted” manuscripts.

Title

Targeting Bacillosamine Biosynthesis in Bacterial Pathogens: Development of Inhibitors to a Bacterial Amino-Sugar Acetyltransferase from *Campylobacter jejuni*[‡]

Authors

Joris W. De Schutter,¹ James P. Morrison,¹ Michael J. Morrison,¹ Alessio Ciulli,² Barbara Imperiali*^{1,3}

¹Department of Chemistry, Massachusetts Institute of Technology, 77 Massachusetts Ave., Cambridge, MA 02139, USA

²Division of Biological Chemistry and Drug Discovery, School of Life Sciences, University of Dundee, Dundee, Scotland

³Department of Biology, Massachusetts Institute of Technology, 77 Massachusetts Ave., Cambridge, MA 02139, USA

[‡]This paper is dedicated to the memory of Austin L. Travis

*To whom correspondence should be addressed

Abstract

The glycoproteins of selected microbial pathogens often include highly modified carbohydrates such as 2,4-diacetamidobacillosamine (diNAcBac). These glycoconjugates are involved in host cell interactions and may be associated with the virulence of medically-significant Gram-negative bacteria. In light of genetic studies demonstrating the attenuated virulence of bacterial strains in which modified carbohydrate biosynthesis enzymes have been

1
2
3 knocked out, we are developing small molecule inhibitors of selected enzymes as tools to evaluate
4
5 whether such compounds modulate virulence.
6

7
8 We performed fragment-based and high-throughput screens against an amino-sugar
9
10 acetyltransferase enzyme, PglD, involved in biosynthesis of UDP-diNAcBac in *C. jejuni*. Herein
11
12 we report optimization of the hits into potent small molecule inhibitors ($IC_{50} < 300$ nM).
13
14 Biophysical characterization shows that the best inhibitors are competitive with acetyl coenzyme
15
16 A and an X-ray co-crystal structure reveals that binding is biased towards occupation of the
17
18 adenine sub-pocket of the AcCoA binding site by an aromatic ring.
19
20
21
22
23
24
25
26
27
28
29
30
31
32
33
34
35
36
37
38
39
40
41
42
43
44
45
46
47
48
49
50
51
52
53
54
55
56
57
58
59
60

Introduction

Most clinically relevant antibiotics are targeted at essential bacterial survival functions including replication, transcription, translation, and cell wall biosynthesis.¹ This is an outcome of *in vitro* antibiotic screening and discovery, which has relied on observing cell death in culture in laboratory settings. The emergence of resistance against all major mechanisms of antibiotic action requires new paradigms for combating infectious disease. A potentially promising approach includes the development of agents that target bacterial virulence *in vivo* in human hosts. Such approaches may mitigate the effects of infectious disease, while potentially resulting in less selective pressure for resistance development.² Virulence factors are implicated in many bacterial processes including host-cell adhesion, invasion, and colonization, as well as quorum sensing and biofilm formation.²⁻⁵ In order to develop antivirulence agents, it is critical to identify validated pathogen-specific processes that cause virulence in the targeted human hosts.

Protein glycosylation is widespread in nature and regulates a variety of cellular functions including protein folding, cell-cell interactions, cell signaling, and the host immune response.⁶ Glycans are attached to proteins via either serine/threonine (O-linked) or the amide nitrogen of asparagine (N-linked). It is now recognized that selected bacteria possess the biosynthetic machinery for O- and/or N-glycosylation and that this modification may play a role in pathogenicity.⁷⁻¹¹ N-glycosylation was first discovered in *C. jejuni* in 1999 and the protein glycosylation (pgl) pathway has been characterized in detail for this organism (Figure 1).^{12,13} In *C. jejuni*, more than 60 proteins, including confirmed virulence factors, are modified with a conserved heptasaccharide.¹⁴

In a significant divergence between prokaryotes and eukaryotes, bacteria and archaea have specialized enzymatic processes to modify the structures of selected carbohydrates for incorporation into glycoconjugates. Furthermore, the discovery of unique prokaryote-specific

1
2
3 sugars is continuing with the pace of bacterial genome sequencing and bioanalytical methods
4
5 development.⁷ In contrast to the glycosyltransferase enzymes, which assemble complex glycans
6
7 and share common folds and mechanisms across domains of life, the specialized sugar-modifying
8
9 enzymes are attractive targets for developing targeted antivirulence agents because they tend not
10
11 to have mammalian homologs and because the associated glycoconjugates are linked with
12
13 bacterial pathogenicity.¹⁵ Of particular interest is di-N-acetylbacillosamine (diNAcBac),¹⁶ which
14
15 is derived from N-acetylglucosamine (GlcNAc). DiNAcBac is found, for example, at the reducing
16
17 end of O-linked glycans in selected strains of *N. gonorrhoeae* and *A. baumannii*, and N-linked
18
19 glycans in *C. jejuni*, highlighting the importance of diNAcBac biosynthesis pathways in these
20
21 Gram-negative pathogens.¹⁷ Intriguingly, while protein glycosylation pathways from these
22
23 pathogens glycosylate diverse proteins with different glycans, the reducing-end sugar is
24
25 diNAcBac.¹⁸⁻²⁰ The N-linked protein glycosylation (pgl) pathway of *C. jejuni* and steps leading to
26
27 diNAcBac biosynthesis are illustrated in Figure 1. The first two steps of UDP-diNAcBac
28
29 biosynthesis utilize an NAD⁺-dependent dehydratase (PglF) followed by a pyridoxal phosphate-
30
31 dependent aminotransferase (PglE) to produce a UDP-4-amino-sugar, which is then acetylated by
32
33 PglD using acetyl coenzyme A (AcCoA) as a co-substrate (Figure 1 inset).¹⁸ Subsequent glycan
34
35 assembly onto an undecaprenyl-diphosphate carrier, is catalyzed by a series of glycosyl
36
37 transferases. After assembly, the completed heptasaccharide is translocated across the inner
38
39 membrane and the glycan is transferred to protein substrates in the bacterial periplasm by the
40
41 oligosaccharyl transferase PglB.

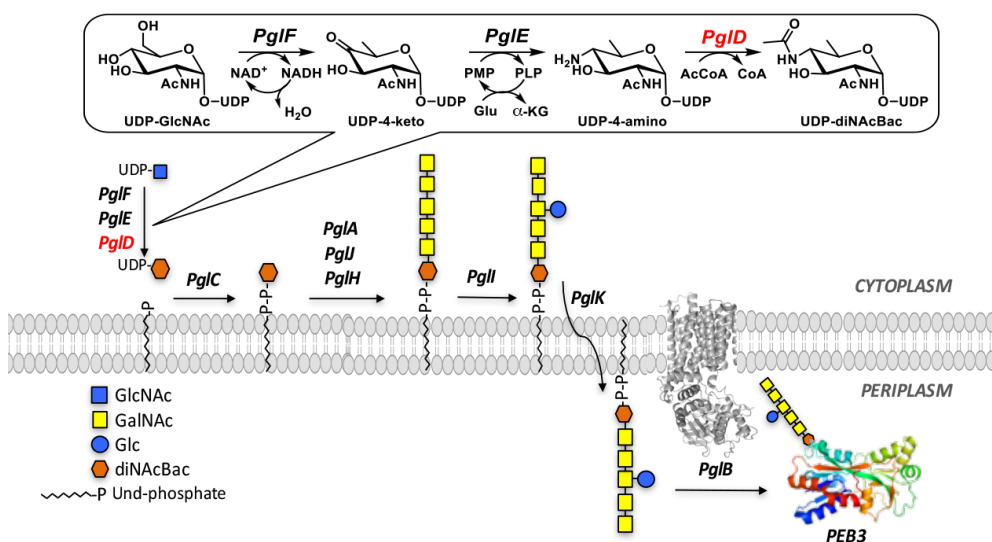
42
43
44
45
46
47
48
49
50 Studies have shown that disruption of genes responsible for diNAcBac biosynthesis (*pglF*,
51
52 *pglE*, *pglD*) perturb production of the native heptasaccharide glycosyl donor in *C. jejuni*.²¹ In
53
54 addition, Δ *pglD* and Δ *pglE* strains show greatly reduced colonization of the gastrointestinal tract
55
56 of 1-day-old chicks, thereby establishing a link between protein N-glycosylation and *C. jejuni*
57
58
59
60

1
2
3 pathogenicity in host cells.²² Further insight into these effects came from transposon mutagenesis
4
5 experiments, which identified *pglF* and *pglE* as essential genes for colonization. In mice,
6
7 mutation of *pglE* impaired invasion of intestinal epithelial cells and colonization of the gut.²³ The
8
9 causative glycoconjugates underpinning these findings remain unknown, but several molecular
10
11 associations between N-glycosylation and *C. jejuni* virulence have been defined. For example,
12
13 VirB10, a structural component to the type IV secretion system (TFSS), needs to be glycosylated
14
15 at Asn97, otherwise a 10-fold decrease in natural competency results.²⁴ Recently, 16 N-linked
16
17 glycoproteins were identified and found to be associated with *C. jejuni* outer membrane vesicles
18
19 (OMVs) including the PEB3 adhesin.²⁵ Pathogens deploy OMVs to deliver bacterial proteins into
20
21 host cells, making this an important finding in the relationship between periplasmic glycoproteins
22
23 and virulence.²⁶ Protein O-glycosylation is also associated with virulence; for example, loss of
24
25 glycosylation of Pile, a constituent of the type IV pilin in *N. gonorrhoeae*, leads to a significant
26
27 decrease in epithelial cell adhesion.²⁷
28
29
30
31
32

33
34 Herein we report the development of inhibitors targeting the *C. jejuni* PglD, a UDP-amino-
35
36 sugar acetyltransferase, which catalyzes the third step in diNAcBac biosynthesis. PglD represents
37
38 an attractive target for inhibitor development as it is well understood from a structural and
39
40 mechanistic perspective.^{28,29} Additionally, PglD is a soluble, well-expressed enzyme, which
41
42 makes it tractable for structure/activity-driven inhibitor discovery. Crystallographic analysis of
43
44 PglD reveals a homotrimeric structure with three equivalent active sites formed at the interfaces
45
46 between adjacent protomers.^{28,29} Like many other bacterial UDP-amino-sugar acetyltransferases,
47
48 PglD is a member of the left-handed β -helix family comprising two domains (Figure 2a); a N-
49
50 terminal domain with a β - α - β - α - β - α Rossmann fold motif that binds the UDP-4-amino-sugar,
51
52 and a C-terminal hexapeptide repeat motif that defines the left-handed β -helix that contributes to
53
54 the AcCoA binding site. PglD has been co-crystallized in the presence of the AcCoA and UDP-4-
55
56
57
58
59
60

amino-sugar substrates (Figure 2b).²⁸ The structural features of PglD and related homologs differentiate these prokaryotic AcCoA-dependent acetyltransferases from their mammalian counterparts, including for example HAT1 of the GCN5-related N-acetyltransferase (GNAT) superfamily.³⁰

Currently, many questions remain as to why modified carbohydrates, such as diNAcBac, are incorporated into bacterial glycoconjugates. Therefore, chemical tools such as small molecule inhibitors that selectively block diNAcBac biosynthesis would be valuable agents for understanding the significance of glycan diversification in selected bacteria. In addition, such tools could help to validate the *pgl* pathway enzymes as potential antivirulence targets. Consequently, we have established a program to develop inhibitors of diNAcBac biosynthesis with a focus on the well-characterized *C. jejuni* pathway. This Gram-negative pathogen is a common cause of gastroenteritis in humans and may also result in the development of Guillain-Barré syndrome, an auto-immune disease in which the peripheral nerves are attacked resulting in damage to the myelin insulation.^{31,32} In recent years, *C. jejuni* has shown increased resistance towards front-line antibiotics including the macrolides and fluoroquinolones, which inhibit protein synthesis and DNA unwinding, respectively.³³



1
2
3 **Figure 1:** Schematic representation of the *C. jejuni* N-linked protein glycosylation pathway.
4
5 Enzymes are shown in italics with the oligosaccharyl transferase PglB shown as determined in
6
7 PDB 3RCE. Also shown is an N-linked glycosylation substrate PEB3 (PDB: 2HXW), which is a
8
9 virulence factor in periplasm that is modified by N-linked glycosylation. Inset highlights the three
10
11 sugar-modifying enzymes that convert UDP-GlcNAc to UDP-diNAcBac.
12
13
14
15
16
17

18 **Results**

19 *Screening*

20
21
22 Initial hits for the development of inhibitors for PglD were identified by employing
23
24 fragment-based screening and high-throughput molecular library approaches.³⁴ The fragment-
25
26 based screen was performed with a fragment set that included a selection of the Maybridge Ro3
27
28 chemical library as described previously.³⁵ The primary screen involved differential scanning
29
30 fluorimetry (DSF) analysis against PglD to identify fragments that bind to and stabilize the
31
32 natively-folded protein. Following this, hits were confirmed by NMR spectroscopy
33
34 (WaterLOGSY and STD) and further validated using a UV-based biochemical assay, which
35
36 measures CoASH release following acetyl transfer to the UDP-4-amino-sugar.³⁶ Using this
37
38 workflow, 10 compound hits with IC₅₀ values in the 1-10 mM range and ligand efficiencies in the
39
40 0.29 – 0.32 range were validated. For example, compound **1** (Figure 2), which was analyzed by
41
42 X-ray in complex with PglD, binds to the central AcCoA binding groove occupying the
43
44 pantetheine site proximal to active-site residues involved in amino-sugar activation and thioester
45
46 attack (Figure 2c). Unfortunately, efforts to build upon this, and other validated fragments yielded
47
48 only modest improvements in affinity. Coincident with these studies a high-throughput screen
49
50 was performed in collaboration with the Broad Institute, using a Diversity-Orientated Synthesis
51
52 (DOS) compound collection (83,000) and the NIH Molecular Libraries Probe Production Centers
53
54
55
56
57
58
59
60

1
2
3 Network (MLPCN) library (276,000) of small molecules.³⁷ Compounds were screened at 10 μ M
4
5 using a PglD end-point assay monitoring the generation of CoASH from the acetyltransferase
6
7 reaction. Despite the low hit rate (defined as >20% inhibition) of 0.02% and 0.12% respectively,
8
9 the screen led to the discovery of thienopyrimidinone-6-carboxylate compound **2** as a promising
10
11 hit for further development. For direct comparison with the validated fragment hits, **2** was
12
13 deconstructed to the core structure **3**, which demonstrated a validated IC₅₀ value of 860 μ M and
14
15 LE of 0.31. In light of these results and the tractability of the core towards synthetic manipulation
16
17 at four points of diversification (C2, C4, C5, and C6; Scheme 1) this compound class became the
18
19 focus of our continuing medicinal chemistry efforts.
20
21
22
23

24 Preliminary structure activity studies to vary substitution at C2 generated analog **4** as the
25
26 best inhibitor with an IC₅₀ value of 1 μ M (LE 0.33). However, although this compound
27
28 represented a good improvement in potency, the candidate suffered from some disadvantages.
29
30 Specifically, **4** features a planar structure with poor solubility properties and a metabolic liability
31
32 due to the 1,3-unsubstituted indole and conjugated alkene systems. Furthermore, **4** and related
33
34 analogs showed poor long-term stability in solution. A significant effort was also made to
35
36 crystallize PglD with several of the thienopyrimidinone hits, however, this proved unsuccessful.
37
38 Therefore, we performed a docking study on fragment **3** to generate a computational model as a
39
40 guide for future synthetic efforts aimed at eliminating the compound liabilities while improving
41
42 potency.³⁸ The thienopyrimidinone-6-carboxylate core was predicted to occupy a binding site
43
44 overlapping with the panthetheine moiety of AcCoA, as had been previously observed in the co-
45
46 crystal structure of fragment **1** (PDB 5TYH), with similar placement of the carboxylate moiety
47
48 and close agreement between the positions of the furan oxygen of **1** and exocyclic oxygen of **2**
49
50 (compare Figure 2c and d). Given these observations, we exploited the computational model as a
51
52 guide for the design of the next generation of analogs, which recognized the opportunity to extend
53
54
55
56
57
58
59
60

the molecule *both* at the C2 position to interact with a hydrophobic region on the β -helix, and at the C4 position, by transitioning to the thienopyrimidine core, to further occupy the AcCoA binding groove (Scheme 1).

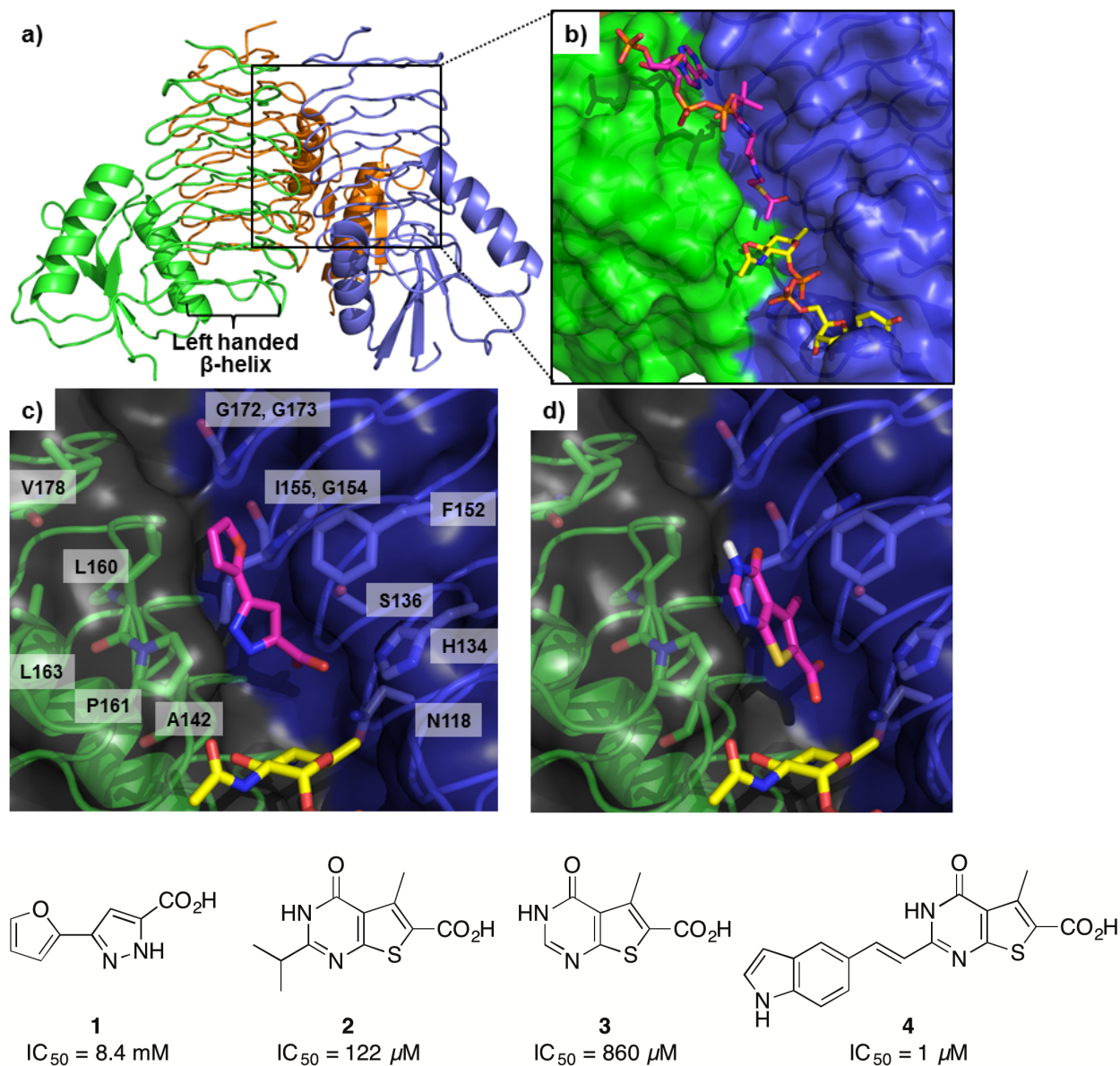
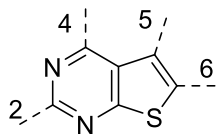


Figure 2: Structure analysis of *C. jejuni* PglD. (a) Crystal structure of the PglD homotrimer (PDB 3BSY) in cartoon representation; individual protomers are colored in green, blue and orange. (b) Expanded view of the PglD active site protein surface with the AcCoA substrate shown in stick representation (magenta, PDB 3BSY) as well as the UDP-4-amino-sugar substrate (yellow, PDB 3BSS). (c) Crystal structure of fragment **1** (magenta) bound to PglD with a semi-transparent

1
2
3 surface and selected side-chain residues shown in stick representation and annotated (PDB
4
5 5TYH). (d) Docking output pose generated for compound **3** (Glide, Maestro).³⁸
6
7
8



15
16 **Scheme 1:** General structure and numbering system of the thienopyrimidine core.
17

18
19 In order to reach cytoplasmic targets in Gram-negative pathogens, compounds may enter
20 cells through passive diffusion or pass through the bacterial porins to reach the periplasm and
21 then reach the cytoplasm *via* passive or active mechanisms.^{39,40} With these parameters in mind,
22 our overall goal was to develop potent ($IC_{50} < 500$ nM) inhibitors of *C. jejuni* PglD based on the
23 thienopyrimidine-6-carboxylate core with good ligand efficiency ($LE > 0.30$) together with
24 balanced physicochemical properties including cLogP values between 2 – 4.⁴¹
25
26
27
28
29
30
31
32
33

34 *Chemistry*

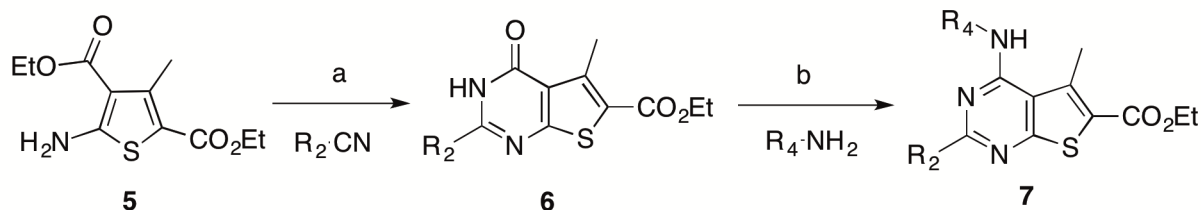
35
36
37 We developed modular synthetic routes to provide access to the target thienopyrimidine
38 carboxylic acids with readily-modifiable substitution at the C2 and C4 positions (Schemes 2 and
39
40
41
42 3).
43

44 For modification at the C2-position (Scheme 2, Route I), the synthesis was initiated by
45 condensation of commercially available thiophene, **5**, with nitriles bearing the desired R_2
46 substituent, under strongly acidic conditions. In most cases, the thienopyrimidone products of
47 general structure **6**, proved highly insoluble, and therefore chromatography and NMR
48 characterization was carried out after the subsequent step. In cases where nitriles with the
49 appropriate R_2 moiety were inaccessible, an alternative approach (Route II) was employed. This
50 route is somewhat longer and includes a Michaelis-Arbuzov reaction with triethyl phosphite and
51
52
53
54
55
56
57
58
59
60

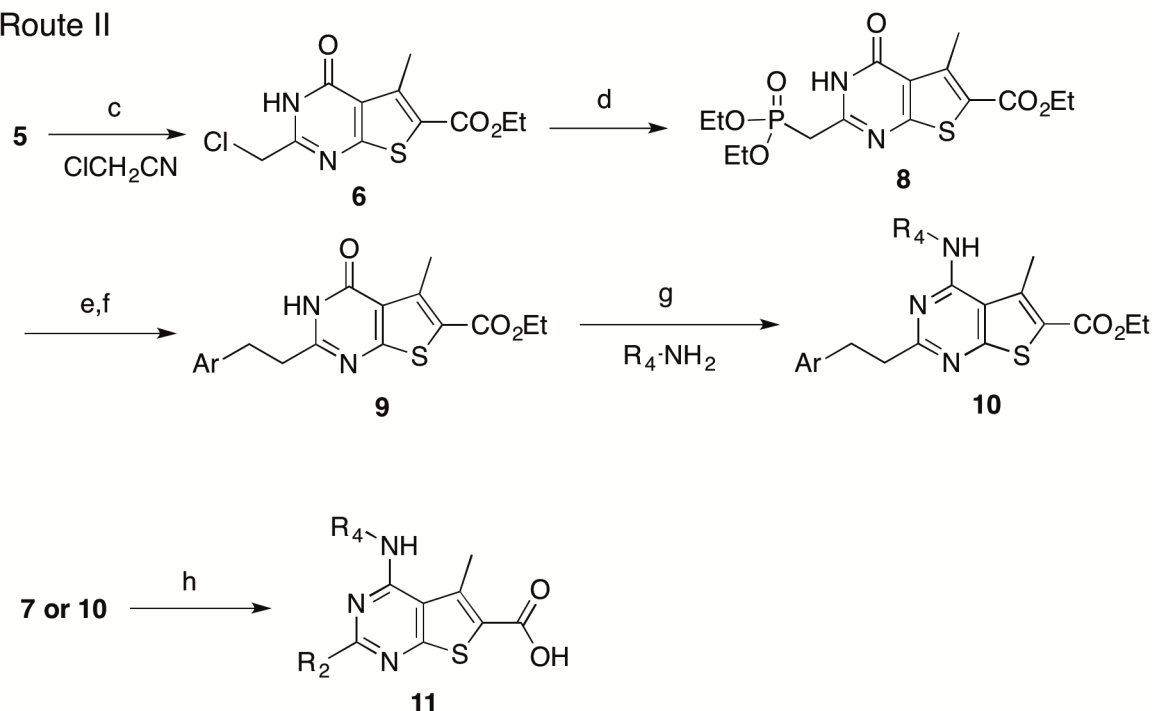
1
2
3 analog **6** (Core structure: R₂ = -CH₂Cl) to furnish phosphonate **8**. Subsequent Horner-Wadsworth-
4
5 Emmons (HWE) olefination and hydrogenation generated thienopyrimidinones of general
6
7 structure **9** with a variety of phenylethyl substituents at the C2-position.
8

9
10 Installation of a substituent at the C4-position of thienopyrimidines is typically
11
12 accomplished by transforming the C4 oxygen of the thienopyrimidone into chloride or bromide,
13
14 with POCl₃ and PBr₃ respectively, followed by a S_NAr reaction, both performed at high
15
16 temperatures. To avoid use of these harsh conditions and strong lachrymators, we instead
17
18 employed a one-step, room temperature reaction modified from chemistry developed by
19
20 researchers at Wyeth.⁴² Utilization of a sufficiently strong base, such as 1,8-
21
22 diazabicyclo[5.4.0]undec-7-ene (DBU), in excess solubilized the thienopyrimidinones in
23
24 acetonitrile and replacing the toxic and expensive BOP reagent for the readily available PyBOP,
25
26 allowed for robust formation of the desired pyrimidines of general structure **10** in good yields
27
28 (40-90%). These thienopyrimidines could be isolated by column chromatography in excellent
29
30 purity (>95% homogeneity as determined by LC-MS). The final saponification of
31
32 thioenopyrimidine esters represented by **7** and **10** was achieved in a THF/MeOH/H₂O mixture
33
34 containing NaOH; occasionally mild heating was required to achieve complete conversion. The
35
36 final inhibitors with core scaffold **11** were isolated by trituration as easy to handle solids.
37
38
39
40
41
42
43
44
45
46
47
48
49
50
51
52
53
54
55
56
57
58
59
60

Route I



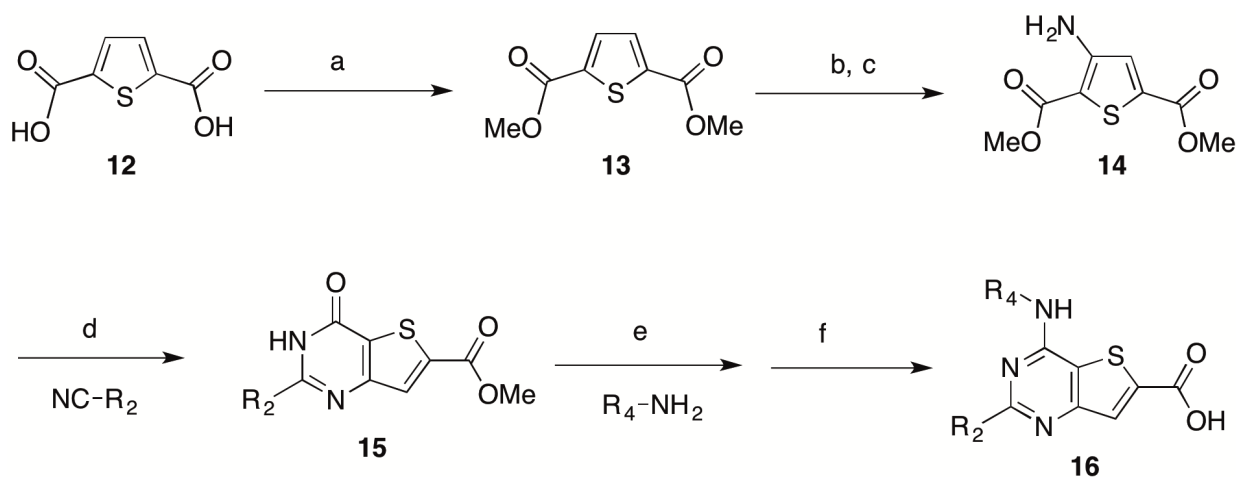
Route II

**Scheme 2:** Synthesis of inhibitors with thienopyrimidine-6-carboxylate core **11**

Conditions: (a) 1.2 equiv. R_2CN , 4 M HCl in 1,4-dioxane, 90°C (50-90%); (b) 1.5 equiv. R_4NH_2 , 1.3 equiv. PyBOP, 3 equiv. DBU, MeCN, RT (40-90%); (c) 1.2 equiv. $ClCH_2CN$, 4 M HCl in 1,4-dioxane, 90°C (50-90%) (d) 20 equiv. $P(OEt)_3$, 145°C (85%); (e) 1.5 equiv. NaH, 2 equiv. $ArCHO$, THF, RT (70-90%); (f) 10% $Pd(OH)_2/C$, THF/MeOH 1:1, 60°C (quant.); (g) 1.5 equiv. R_4NH_2 , 1.3 equiv. PyBOP, 3 equiv. DBU, MeCN, RT (40-90%) (h) 3 equiv. NaOH, THF/MeOH/H₂O 2:1:1, RT (50-80%).

A related thienopyrimidine isomer with general structure **16**, was accessed as described in Scheme 3. In this case, the thiophene starting material **14** is not commercially available but could

be readily prepared by the esterification of dicarboxylic acid **12** followed by nitration and hydrogenation. Condensation with nitriles provided thienopyrimidinones of general structure **15**, which differ from the scaffold **11** series in the relative location of the sulfur atom and the absence of a methyl group on the thiophene ring. Installation of substituents at C4 and saponification were performed as described previously, to provide inhibitors with core scaffold **16**.



Scheme 3: Synthesis of inhibitors with thienopyrimidine-6-carboxylate core **16**

Conditions: (a) 4 equiv. SOCl_2 , MeOH, 50°C (99%); (b) 2 equiv. HNO_3 , H_2SO_4 , RT; (c) 10% $\text{Pd}(\text{OH})_2/\text{C}$, THF/MeOH 1:1, RT (93% over 2 steps); (d) 1.2 equiv. R_2CN , 4 M HCl in 1,4-dioxane, 90°C (60-80%); (e) 1.5 equiv. R_4NH_2 , 1.3 equiv. PyBOP, 3 equiv. DBU, MeCN, RT (40-90%); (f) 3 equiv. NaOH in THF/MeOH/ H_2O 2:1:1, RT (50-80%).

Initial SAR analysis

All target thienopyrimidine carboxylic acids **11** and **16** (Figure 3) were assayed for inhibition of recombinantly-expressed and purified *C. jejuni* NCTC 11168 PglD acetyltransferase.¹⁸ The continuous assay monitors the release of CoASH using 5,5'-dithiobis-(2-

1
2
3 nitrobenzoic acid,³⁶ and was carried out at 300 μM AcCoA (K_m of 295 μM), and 500 μM UDP-4-
4
5 amino-sugar (K_m of 274 μM). IC_{50} values of selected compounds are summarized in Table 1. The
6
7 AcCoA concentration was aligned with reported physiologic concentrations in typical Gram-
8
9 negative bacteria.⁴³
10

11
12 Our initial strategy was to explore the C2- and C4-substituents individually and then
13
14 combine the optimal structural components from each series to capture advantageous synergistic
15
16 binding effects. We observed that short aliphatic chains and saturated carbocycles at C2 (with R_4
17
18 = Me) provided weak inhibitors with IC_{50} values in the 10 μM to 1 mM range (data not shown).
19
20 Based on these studies we selected an unsubstituted phenylethyl moiety (Figure 3, substituent **d**)
21
22 as a favorable C2-substituent in terms of potency gain *versus* added mass (e.g. **17**, IC_{50} = 2.2 μM ,
23
24 LE 0.35, Table 1). However, when we explored C4-substituents (with R_2 = H), these analogs
25
26 proved to be poor inhibitors (IC_{50} > 500 μM , data not shown) and SAR trends could not be well
27
28 defined from the data. Accordingly, we elected to directly prepare disubstituted analogs, with R_2
29
30 = phenylethyl (**d**), and iteratively build up the R_4 substituent in terms of length, sterics and
31
32 heteroatom substitution (e.g. inhibitors **18-35**; shorter and smaller substituents omitted for
33
34 brevity). In general, only modest gains in potency could be achieved, and all the gains were at the
35
36 cost of poorer ligand efficiencies. Ultimately, we observed that a phenylethyl moiety was also
37
38 well tolerated at the C4-position of the thienopyrimidine core (**20**, R_2 = R_4 = phenylethyl, IC_{50} =
39
40 1.4 μM).
41
42
43
44
45
46
47

48
49 In order to gain a better understanding of the binding behaviour of the inhibitors, we
50
51 examined the results of the phenyl scan on the R_4 substituent, which positioned moieties with
52
53 different characteristics (sterics, polarity and hydrogen-bonding capabilities) *ortho*, *meta* or *para*
54
55 on the aryl ring (inhibitors **21-35**). However, while we had predicted that these substitutions
56
57 would either complement or clash with the protein surface resulting in a measurable difference in
58
59
60

1
2
3 IC₅₀ values, we instead observed a “flat” SAR with inhibitors exhibiting IC₅₀ values around 0.5
4 μM (e.g. **21-35**). Indeed, only substitution with an acetamido group (**33-35**) elicited clear
5
6
7 variances, with the *ortho* substitution being the most disfavored (**35**, IC₅₀ = 9.0 μM). A potential
8
9 explanation for the flat SAR could be that if the aryl group occupies the AcCoA binding groove
10
11 then one edge would face the protein surface and the other would be solvent exposed, thus
12
13 precluding any interaction between the moieties on the R₄-aryl ring and the protein surface. This
14
15 hypothesis was tested by preparing analogs bearing two moieties on the aryl ring (inhibitors **36-**
16
17 **38**), however, potency remained at 0.5 μM.
18
19
20

21
22 In light of these data, we developed two hypotheses. One potential hypothesis was that the
23
24 compounds might have a different mode of action other than competitive inhibition with the
25
26 AcCoA substrate. We explored this by applying several biochemical and biophysical approaches,
27
28 which are presented in the next section (*vide infra*). The second possibility was that the inhibitor
29
30 binding mode differed significantly from that predicted by the computational model; for example,
31
32 either the ligands bind in a different location on the PglD protein surface or the enzyme itself
33
34 undergoes a significant conformational change. We also noted that the C₂,C₄-disubstituted
35
36 inhibitors were inherently quite symmetrical, with a pseudo C₂ axis of rotation in the plane of the
37
38 thienopyrimidine core (Figure 4a). This feature might explain the flat SAR observed for the
39
40 phenyl scan of the R₄-substituent since the effect of any moiety on the aryl group could
41
42 potentially be masked if the ligand flipped 180° and positioned the R₂-substituent in the AcCoA
43
44 binding groove instead. To test this hypothesis, we synthesized inhibitors **49** and **50**, which
45
46 included the quasi-regioisomeric thienopyrimidine core **16** and, if the binding orientation remains
47
48 true, should position the sulfur atom towards the protein surface. Indeed, these inhibitors had
49
50 similar potency to their parent analogs (compare **49** IC₅₀ = 3.9 μM vs. **17** IC₅₀ = 2.2 μM, and **50**
51
52 IC₅₀ = 1.4 μM vs. **41** IC₅₀ = 1.1 μM), suggesting the thienopyrimidine carboxylic core can bind in
53
54
55
56
57
58
59
60

1
2
3 either of two orientations into the AcCoA binding groove. To further validate this hypothesis, we
4
5 developed inhibitors that would be locked in a fixed conformation by introducing rigidifying
6
7 elements in the alkyl linkers between the thienopyrimidine core and substituent aryl groups.
8
9 Synthetically it was straightforward to add a methyl group on the second carbon of the R₂-
10
11 substituent and a methoxy group on the second carbon of the R₄-substituent; the prerequisite
12
13 starting materials were commercially available as both stereoisomers and could be easily
14
15 transformed into the corresponding nitrile or amine for the modular syntheses (Figure 4b). With
16
17 the four rigidified analogs we would expect to see data consistent with a matched/mismatched
18
19 phenomenon; either substituent should have an enantiomer that complements the protein surface
20
21 better than the other and when combined these effects should result in one poor inhibitor, two
22
23 moderate ones and a single preferred analog. Indeed, this was observed with compounds **51-54**
24
25 (Figure 4b), albeit in a modest IC₅₀ range. These combined results strongly suggested that the
26
27 inhibitors were capable of binding to the PglD active site with either the R₂-, or R₄-substituent in
28
29 the AcCoA groove.
30
31
32
33
34
35

36 Overall, the SAR data (Figure 4) shows that while binding may be somewhat promiscuous,
37
38 the R₂-substituent was far more important for binding potency. This experimental observation was
39
40 therefore inconsistent with our initial computational model, which had oriented this substituent
41
42 over the β-helix (and quite solvent exposed) and placed the R₄-substituent in the AcCoA groove.
43
44 These findings prompted us to investigate the binding mode in more detail, to provide a
45
46 foundation for the next synthetic and biochemical efforts.
47
48
49
50
51
52
53
54
55
56
57
58
59
60

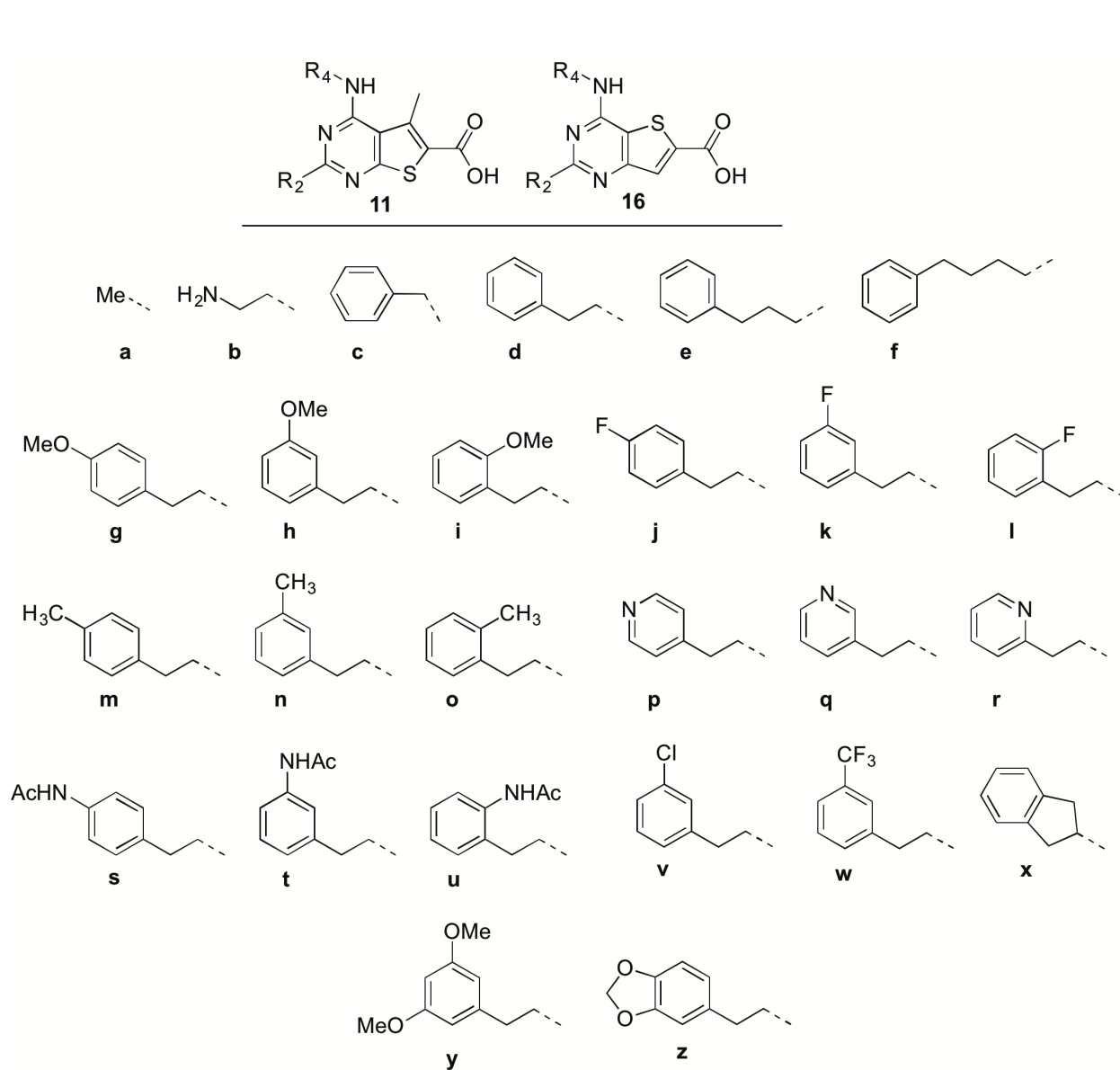


Figure 3: Representative examples of thienopyrimidine-6-carboxylate inhibitors of *C. jejuni*

PglD; Core 11: R₂ = a – z; R₄ = a – z; Core 16: R₂ = d, h; R₄ = a.

Compound #	Scaffold	R ₂	R ₄	IC ₅₀ (μ M)	LE	ΔT_m ($^{\circ}$ C)	cLogP
17	11	d	a	2.2 \pm 0.4	0.35	7.4	4.44
18	11	d	b	1.6	0.32	3.6	1.48
19	11	d	c	4.5	0.26	<i>nd</i>	5.89
20	11	d	d	1.4	0.27	13.2	6.54
21	11	d	g	0.54	0.27	<i>nd</i>	6.46
22	11	d	h	0.45	0.28	<i>nd</i>	6.46
23	11	d	i	0.48	0.28	13.7	6.46
24	11	d	j	0.42	0.29	<i>nd</i>	6.68
25	11	d	k	0.39	0.29	<i>nd</i>	6.68
26	11	d	l	0.48	0.29	13.2	6.68
27	11	d	m	0.72	0.28	<i>nd</i>	6.99
28	11	d	n	0.42	0.29	<i>nd</i>	6.99
29	11	d	o	0.25	0.30	14.3	6.99
30	11	d	p	0.39	0.30	12.0	5.04
31	11	d	q	0.34	0.30	12.0	5.04
32	11	d	r	0.42	0.30	12.5	5.04
33	11	s	a	2.4	0.29	<i>nd</i>	3.46
34	11	t	a	3.5	0.28	<i>nd</i>	3.46
35	11	u	a	9.0	0.26	<i>nd</i>	3.46
36	11	d	x	1.0	0.27	<i>nd</i>	6.42
37	11	d	y	0.37	0.26	<i>nd</i>	6.55
38	11	d	z	0.59	0.26	11.5	6.50

39	11	e	a	4.4	0.31	7.9	4.97
40	11	f	a	4.1	0.30	7.4	5.50
41	11	h	a	1.1 ± 0.2	0.33	8.4	4.36
42	11	k	a	2.3	0.33	8.9	4.58
43	11	q	a	0.46 ± 0.05	0.39	8.4	2.94
44	11	s	b	1.4	0.28	5.3	0.50
45	11	s	r	0.28	0.27	11.5	4.06
46	11	v	a	2.1	0.33	9.4	5.15
47	11	w	a	4.6	0.28	7.4	5.32
48	11	z	a	1.8	0.31	7.4	4.41
49	16	d	a	3.9	0.34	4.8	4.45
50	16	h	a	1.4	0.34	5.9	4.37
51	11	2PP(S)	2MPE(R)	2.0	0.24	9.4	6.50
52	11	2PP(S)	2MPE(S)	1.1	0.25	10.4	6.50
53	11	2PP(R)	2MPE(R)	0.87	0.27	<i>nd</i>	6.50
54	11	2PP(R)	2MPE(S)	0.42	0.27	9.9	6.50
55	11	s	2MPE(S)	0.27 ± 0.09	0.26	12.5	5.12

Table 1: Experimental data obtained for selected inhibitors (Figures 3 and 4): IC₅₀ values determined with the continuous *C. jejuni* PglD inhibition assay, calculated ligand efficiency (LE), thermal stabilization of the PglD/ligand complex with the DSF assay, and cLogP values calculated with built-in functionality of the ChemDraw[®] commercial software package. Compounds **51-54** (Figure 4): 2MPE: 2-methoxy-2-phenylethyl and 2PP: 2-phenylpropyl.

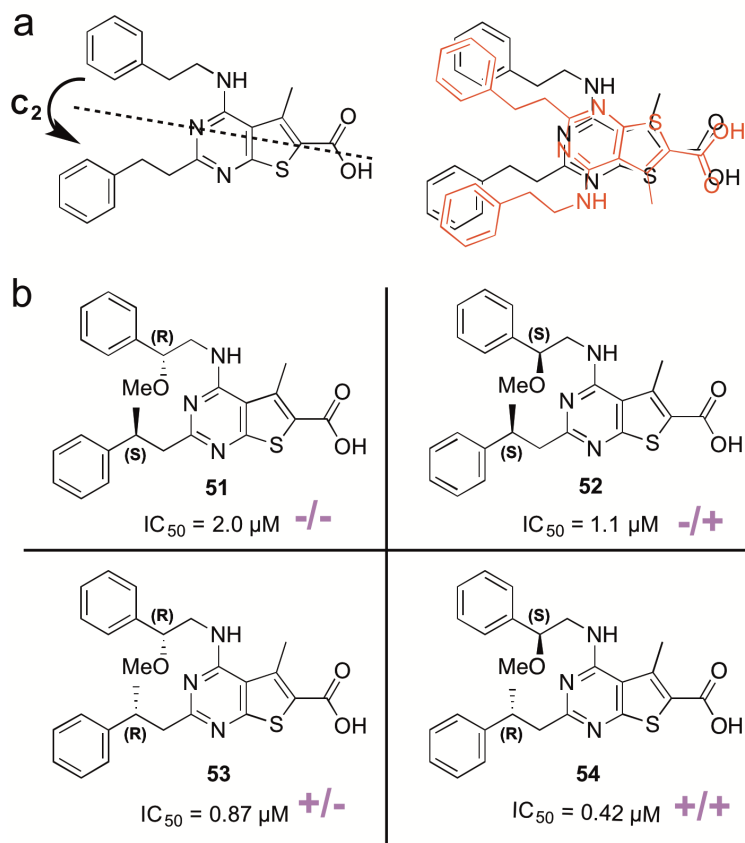


Figure 4: (a) Illustration of the quasi C_2 symmetry axis of the disubstituted inhibitors (b) SAR of inhibitors **51** – **54** with rigidified R_2 and R_4 substituents; magenta symbols represent stereochemical preference of R_2 and R_4 substituents with respect to the PglD protein surface and highlight the mismatched/matched pattern.

Biophysical characterization and inhibitor optimization

With the knowledge gained from SAR studies up to this point, we generated a potent *C. jejuni* PglD inhibitor, **55** (Figure 5), with an IC_{50} of 270 nM; however, this was at the cost of decreased ligand efficiency (0.26) and a high cLogP (5.12). In order to further optimize the potency and physicochemical properties of these compounds, we needed to better characterize their binding characteristics. Towards this end, we employed several complementary approaches

1
2
3 including the PglD inhibition assay with varying substrate concentrations, DSF analysis, dynamic
4
5 light scattering (DLS) and X-ray crystallography.
6

7 We had first initiated inhibitor development based on modeling studies, which suggested
8
9 that the thienopyrimidine carboxylate core competed with the AcCoA substrate for binding to the
10
11 PglD active site. To test this experimentally, we monitored inhibition in the presence of varying
12
13 concentrations of the two substrates. We observed that significantly higher concentrations of the
14
15 UDP-4-amino-sugar substrate had no measurable effect on the inhibition by a representative
16
17 analog of **11** (compound **37**, supporting information Table S2). In contrast, a 2-, and 5-fold
18
19 increase in AcCoA substrate concentration resulted in measured IC₅₀ values of 0.63 μM and 1.4
20
21 μM, respectively. These values represent a 2- and 4-fold decrease in potency and strongly suggest
22
23 that the thienopyrimidine carboxylate inhibitors compete with AcCoA for binding to the PglD
24
25 active site.
26
27
28
29
30

31 All of the data thus far has been based on the enzymatic inhibition assay and, despite the
32
33 judicious use of detergent and BSA to prevent aggregation phenomena,⁴⁴ may be prone to
34
35 artefacts that obscure binding trends. We therefore employed DSF as a qualitative secondary
36
37 assay to assess binding of inhibitors to the *C. jejuni* PglD. DSF employs a fluorescent dye, Sypro
38
39 Orange, to report on the thermal denaturation of a protein or protein/ligand complex.⁴⁵ Potent
40
41 inhibitors bind to their target enzyme more strongly than weak ones, resulting in a more stable
42
43 protein/ligand complex and higher measured melting temperature (T_m). Therefore, the thermal
44
45 stabilization (ΔT_m) of PglD can be used to provide an indirect measure of the *relative* binding
46
47 affinity of the *related* family of compounds. We selected a subset of inhibitors with a range of
48
49 IC₅₀ values and structural characteristics to analyze by DSF and plotted the ΔT_m vs IC₅₀ values
50
51 (Figure 6). The graph shows a positive correlation (R² = 0.72) between inhibition potency and
52
53 thermal stabilization over a range of IC₅₀ values indicating that the compounds stabilize the native
54
55
56
57
58
59
60

1
2
3 PglD homotrimer and that the more potent compounds, based on IC₅₀ values, indeed stabilize
4
5 PglD more effectively.
6

7
8 Next, we analyzed the enzyme quaternary structure in solution by dynamic light scattering
9
10 (DLS) and found the calculated hydrodynamic radius of apo PglD to be ~34 Å, consistent with the
11
12 crystal structures of trimeric PglD (supporting information Figure S1). In the presence of 10-fold
13
14 excess of inhibitor **55**, the measured radius was marginally larger, ~36 Å, yet still consistent with
15
16 the known trimeric structure. We also noted that the polydispersity index (PDI) of the PglD/**55**
17
18 complex (24 % PDI) was lower than apo PglD (31% PDI), providing strong support that the
19
20 inhibitor does not destabilize quaternary structure and indeed binds to the homotrimeric enzyme.
21
22
23

24
25 Throughout these efforts we also continued to pursue crystallization attempts to gain
26
27 structural insight on representative thienopyrimidine analogs. X-ray analysis of the *C. jejuni*
28
29 NCTC 11168 PglD enzyme has been successfully carried out in our group and others.^{28,29}
30
31 Typically, the reported precipitant solutions were either high ionic strength (1.9 M ammonium
32
33 sulfate) or contained acidic buffer components that were frequently observed to bind in the
34
35 enzyme active site (sulfate, phosphate, citrate).^{28,29} Despite numerous attempts, application of
36
37 previously published protocols did not yield co-crystal structures with the current
38
39 thienopyrimidine-6-carboxylate inhibitors and thus we screened for new conditions that would be
40
41 more compatible with the binding of small organic molecules. Ultimately, a crystallization hit
42
43 with PEG-3350 was successfully optimized to reliably produce high quality crystals. The crystals
44
45 develop as hollow, hexagonal rods that fill in from one end as they mature; producing either
46
47 “vase-like” or solid crystals (Figure S3). The diffraction quality did not appear to differ between a
48
49 solid or hollow end of such crystals. The crystals were tolerant of DMSO in concentrations up to
50
51 10%, but tended to be rather fragile and could break upon looping. Therefore, we employed an
52
53
54
55
56
57
58
59
60

1
2
3 “in-drop soaking” protocol, in which a solution of the inhibitor is directly added to the drop
4
5 containing the crystals.
6

7
8 Using these crystallization conditions, we were able to obtain high-quality diffraction data
9
10 and successfully solve the co-crystal structure of the PglD/**17** complex (Figure 7 and S4). From
11
12 the structure, two significant observations were immediately evident. Firstly, as anticipated from
13
14 the SAR studies, the thienopyrimidine core was flipped 180° compared to the computational
15
16 model developed with the core fragment, with the R₂-substituent binding in the AcCoA groove
17
18 (Figure 7, panel b). This position of the thienopyrimidine core directs the R₄-substituent away
19
20 from the AcCoA groove and into solvent where it makes no significant interactions with the PglD
21
22 protein surface (Figure S5, LigPlot⁴⁶). This observation is consistent with our SAR findings that
23
24 R₄-substituent makes small contributions to inhibitor potency at the expense of ligand efficiency
25
26 (Table 1). Secondly, the most surprising observation was that the ligand was bound 3.9 Å further
27
28 along the AcCoA groove, relocating the carboxylate distal to the acetyltransferase active site
29
30 where the AcCoA thioester is normally accommodated. This observation was rather unexpected as
31
32 we assumed that the Asn118, H134 and S136 residues would be preferred hydrogen-bonding
33
34 partners for the inhibitor carboxylic acid moiety. Furthermore, this displacement precludes a T-
35
36 shaped π -stacking between the side chain of Phe152 and the thienopyrimidine core; instead the
37
38 binding mode positions Phe152 at an offset angle over the inhibitor carboxylate (Figure S4). To
39
40 compensate, inhibitor **17** makes several other key interactions with the PglD surface; the
41
42 carboxylic acid moiety is positioned at a favorable distance and orientation to form hydrogen
43
44 bonds with the Ser136 side chain and the backbone amide NH of Ile155. Similarly, the
45
46 thienopyrimidine N1 atom is well placed to interact with Gly173. From the structure it appears
47
48 that a definitive interaction may be the placement of the R₂ phenyl ring within the AcCoA adenine
49
50 binding sub-pocket, displacing solvent waters from a relatively hydrophobic protein cavity. The
51
52
53
54
55
56
57
58
59
60

1
2
3 ligand binding mode is also internally favorable (low torsion) as the bound conformation adopts
4
5 an anti-periplanar angle of approximately 160° along the benzylidene bond between the
6
7 thienopyridimine core and R₂ phenyl ring (Figure 7c).
8

9
10 Armed with this new structural information we set out to further optimize the inhibitor
11
12 series. First we investigated the possibility of simultaneously placing the R₂ phenyl ring in the
13
14 adenine sub-pocket and the carboxylate in the active site hot spot by increasing the linker length
15
16 between the inhibitor core and R₂-substituent. This did not prove successful as analogs **39** and **40**
17
18 (with a 3- and 4-carbon linker respectively) demonstrated lower *in vitro* potency; presumably due
19
20 to internal strain of unfavorable torsion angles of the alkyl linker. Secondly we noted that
21
22 although the R₂ phenyl group fits well in the adenine sub-pocket, it does not fully occupy the
23
24 volume of the [6,5]-fused ring cavity and there was unoccupied space at the *meta* position relative
25
26 to the linker (Figure 7c). We explored several moieties at this position (**41** –OMe, **42** –F, **46** –Cl
27
28 and **47** –CF₃, Table 1), but only gained a minor improvement in potency with compound **41** (IC₅₀
29
30 = 1.1 μM). Finally upon closer inspection of the adenine sub-pocket we speculated that if the
31
32 aromatic carbon at a position *ortho* to the linker is replaced by a nitrogen and protonated, it would
33
34 be well-oriented to form a hydrogen bond with the backbone oxygen of Gly173, as it does with
35
36 the exocyclic amine of the adenine of the AcCoA substrate (PDB ID 3BSY).²⁸ While the resultant
37
38 pyridine nitrogen is only weakly basic, it could potentially be protonated in the microenvironment
39
40 of the enzyme and lead to an order of magnitude improvement in potency. For example, the
41
42 pyridine derivative risedronic acid is a ~300-fold more potent inhibitor of the human farnesyl
43
44 pyrophosphate synthase than the corresponding phenyl analog.⁴⁷ Although not as significant, the
45
46 4.8-fold fold enhancement we observed between inhibitor **43** (IC₅₀ = 0.46 μM) and **17** (IC₅₀ = 2.2
47
48 μM) is very interesting considering the minor nature of the structural change. Although **43** is not
49
50 the most potent inhibitor, it exhibits the best ligand efficiency, 0.39, and has a cLogP of 2.94,
51
52
53
54
55
56
57
58
59
60

within the -0.5 - 3 range that is thought to be ideal to reach cytoplasmic targets of Gram-negative bacteria; with these characteristics **43** represents our best candidate to date with balanced physicochemical properties.

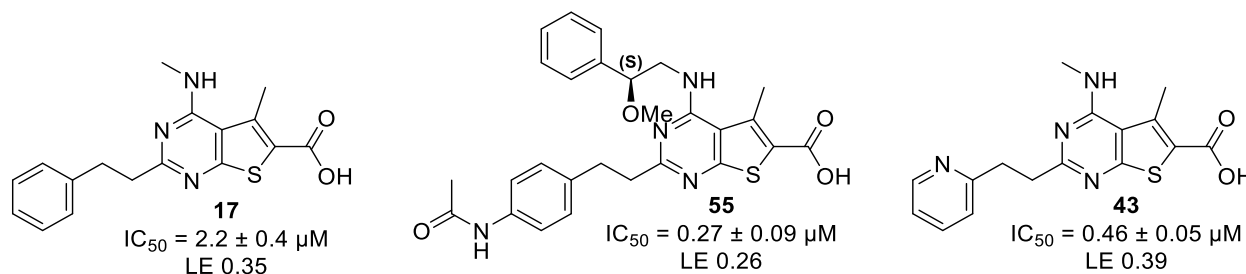


Figure 5: Structures of key inhibitors discussed in this section: **17**, **43** and **55**.

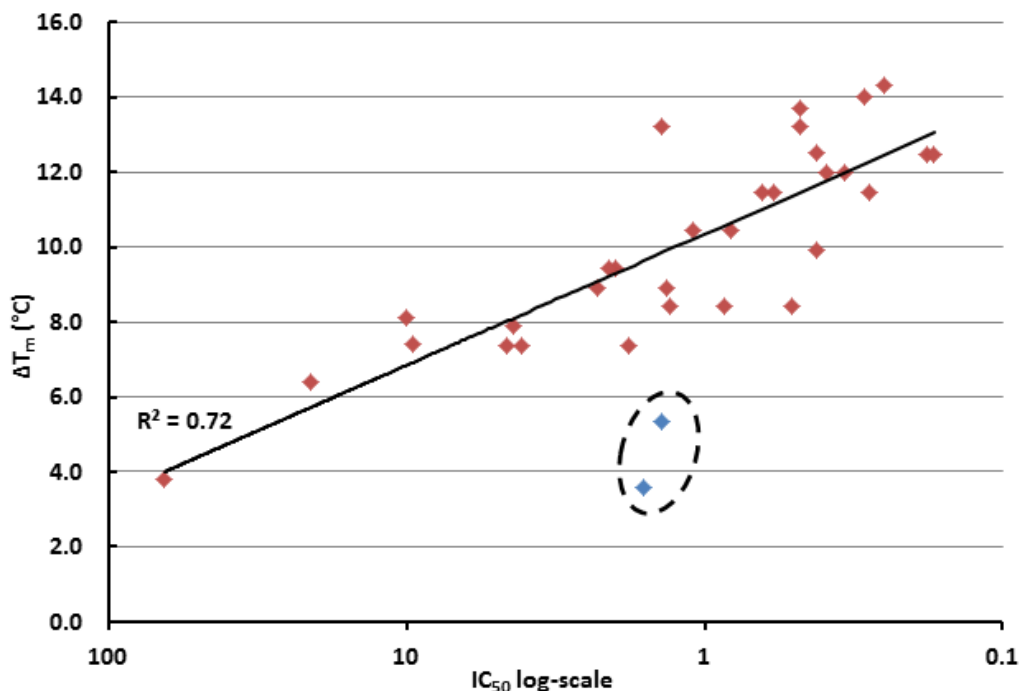
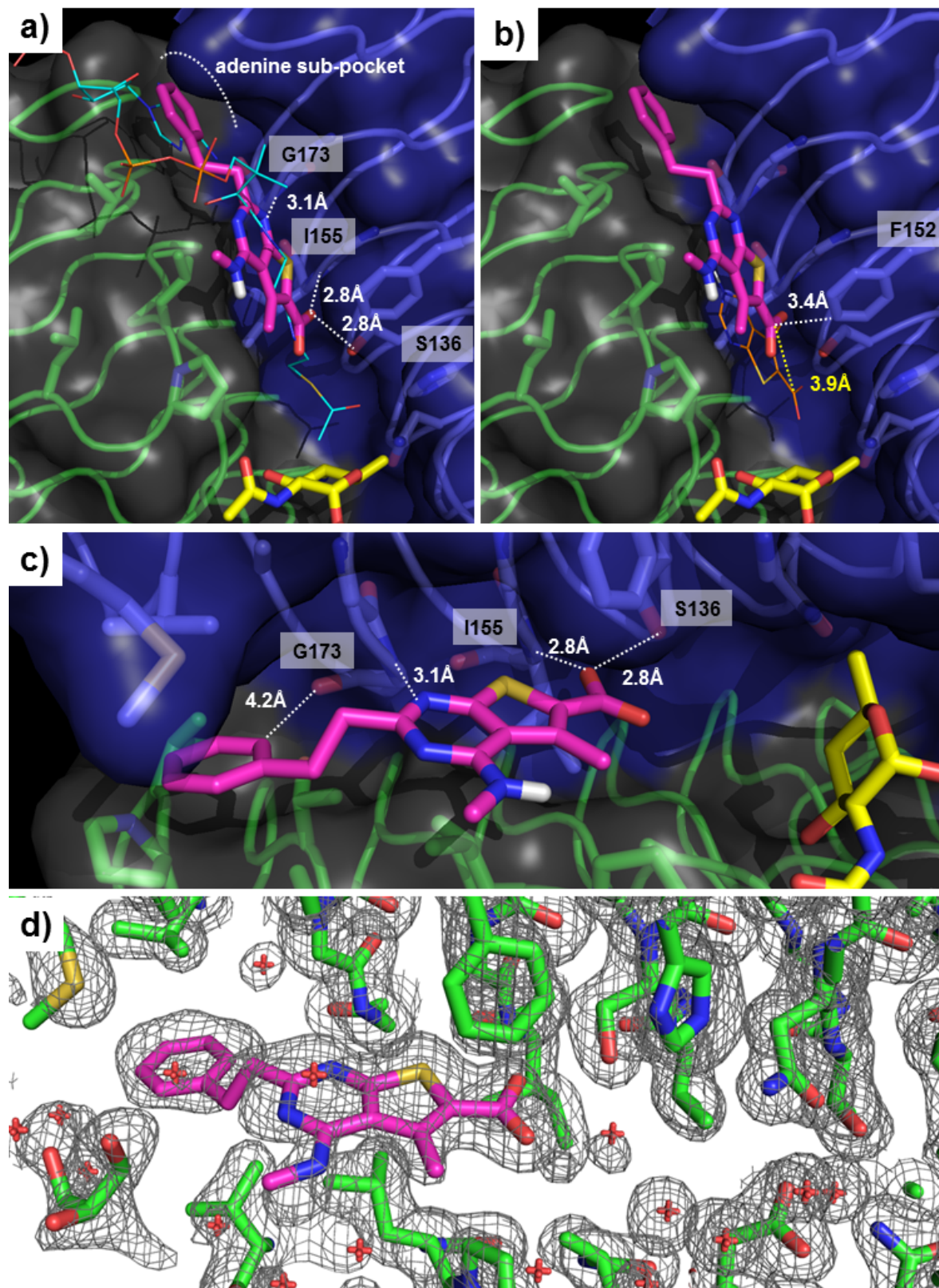


Figure 6: Correlation between the *in vitro* potency against PglD and the T_m (calculated from the first derivative of the thermal melting curve) of the PglD/inhibitor complexes with core **11**; thermal melt assays were performed with 10 μM PglD and 100 μM compound. Correlation

1
2
3 coefficient provided for all data indicated by red diamond. Inhibitors with $R_4 = \mathbf{b}$ (ethylamine)
4
5 (blue diamond, circled) appear as outliers and are omitted from the calculation of the correlation
6
7 coefficient.
8
9
10
11
12
13
14
15
16
17
18
19
20
21
22
23
24
25
26
27
28
29
30
31
32
33
34
35
36
37
38
39
40
41
42
43
44
45
46
47
48
49
50
51
52
53
54
55
56
57
58
59
60



1
2
3 **Figure 7:** Co-crystal structure of the PglD/17 complex (PDB 5T2Y). (a) Inhibitor 17 shown in
4 sticks presentation (magenta) and overlaid with AcCoA substrate in lines (cyan, PDB 3BSY)
5 and sugar substrate in sticks (yellow, PDB 3BSS). (b) overlay with the computational docking
6 pose of compound 2 in line representation (orange). (c) Side-view highlighting the AcCoA
7 adenine sub-pocket and interaction between 17 and residues Gly173, Ile155 and Ser136. White
8 dashed lines indicate distances between 17 and PglD side-chain residues; yellow dashed line
9 shows distance between the carboxylate computational docking pose and crystal structure. (d)
10 Composite omit map $2F_o - F_c$ contoured at 1.0σ generated with the built in functionality of the
11 PHENIX software and image generated in PYMOL.
12
13
14
15
16
17
18
19
20
21
22
23
24
25
26
27
28
29
30
31
32
33
34
35
36
37
38
39
40
41
42
43
44
45
46
47
48
49
50
51
52
53
54
55
56
57
58
59
60

Discussion and Conclusions

In the development of inhibitors of the *C. jejuni* UDP-4-amino-sugar acetyltransferase, PglD, we initially screened both fragment-based and HTS libraries. These studies led to the identification of a thienopyrimidine-6-carboxylate core as a promising hit. Over the course of the SAR studies we found substitution at the C2-position of the core to be most impactful and that the binding mode appeared to be poorly predicted *in silico*. By combining data from substrate competition assays, DSF, and DLS we confirmed that the inhibitors bind exclusively to the AcCoA binding groove of the active site without disrupting the homo-trimeric structure of PglD.

Critically, crystallographic analysis reveals a 180° flip of the thienopyrimidine core to place the R₂-substituent in the AcCoA groove, as was anticipated from the SAR data. However, in contrast to previously characterized small fragments, we observed a 3.9 Å displacement of the inhibitor further along the AcCoA groove away from the known thioester binding site. Notably, in this new binding mode, the inhibitor makes several hydrogen-bonding interactions that compensate for the ones that would have been formed with the key catalytic residues (Asn118 & His134), but also precludes a stabilizing T-shaped π -interaction between the thienopyrimidine core and Phe152. Ultimately, it appears that placement of the R₂-phenyl into the adenine sub-pocket of AcCoA binding site may be the main driving force of ligand binding and indeed further optimization of this interaction resulted in to our most promising lead. Specifically, inhibitor **43** (IC₅₀ = 0.46 μ M) shows an excellent ligand efficiency of 0.39 and a favorable clogP of 2.94. To the best of our knowledge this is the first competitive inhibitor with an IC₅₀ value < 1 μ M for a bacterial amino-sugar-modifying enzyme. A selection of inhibitors from the series presented herein was also tested against the structurally homologous amino-sugar acetyltransferase from *N. gonorrhoeae* (PglC in that O-linked glycosylation pathway) and no significant inhibition was

1
2
3 observed even at 100 μ M. This observation was not surprising considering the significant
4
5 differences between the AcCoA binding sites of the two enzymes.⁴⁸
6

7
8 With respect to biological analysis, the *in vivo* analysis of inhibitors that target bacterial
9
10 virulence factors requires more complex experimental approaches than the simple estimation of
11
12 minimal inhibitory concentrations (MICs) used in assessing bacterial viability with antibiotics
13
14 that are targeted at cell survival processes. We are therefore pursuing multiple strategies to
15
16 investigate *in vivo* efficacy both directly in *C. jejuni*, by assessing the impact of the inhibitors on
17
18 glycoprotein biosynthesis, and in cell culture models of mammalian gut endothelia assessing *C.*
19
20 *jejuni* adhesion and invasion. Currently, despite robust *in vitro* activity, we do not observe a
21
22 reduction in glycosylation of periplasmic and cell surface proteins upon treatment of *C. jejuni*
23
24 with the current inhibitors. This observation may be the result of insufficient inhibition potency
25
26 against the target and/or may result from limited cellular uptake or efflux. In this context, *C.*
27
28 *jejuni* features both a formidable cell wall including inner and outer cell membranes flanking a
29
30 peptidoglycan barrier together with a dense external glycocalyx, as well as an active CmeABC
31
32 efflux pump system to guard against external chemical agents.⁴⁹ With respect to potency, the X-
33
34 ray analysis of PglD with compound **17** provides an excellent foundation for further structure-
35
36 guided optimization of the thienopyrimidine core. Concerning cellular uptake and efflux, which
37
38 are common impediments to antibiotic activity in Gram-negative pathogens, the presented
39
40 thienopyrimidine core also offers considerable opportunities. In particular, we are exploring
41
42 several strategies including bioisosteric replacement of the carboxylate moiety and development
43
44 of pro-drug analogs in consideration of the fact that the negative charge of the carboxylic acid
45
46 moiety might acting as an impediment for compound uptake into the cytoplasm, which is the site
47
48 of PglD activity. Additionally, the C4-substituent of the thienopyrimidine series represents a
49
50 valuable handle for modulating the cLogP of the inhibitor, since we have demonstrated that
51
52
53
54
55
56
57
58
59
60

1
2 substitution at this site can be varied without adversely perturbing PglD inhibition. As elegantly
3 demonstrated in a recent study of another Gram-negative pathogen, researchers have shown that
4 fine-tuning the physical properties of inhibitors, in this case to mimic the zwitterionic charge
5 distribution of amino acids, allowed novel carbapenem analogs to pass through the OccD1
6 membrane porin of *P. aeruginosa*.⁵⁰ Thus the thienopyrimidine compounds in this report are
7 amenable to further such optimizations and current efforts are focused on overcoming the *C.*
8 *jejuni* defenses to validate PglD as a potential antivirulence target in the biological context of
9 infection.
10
11
12
13
14
15
16
17
18
19
20

21 Overall the studies presented herein support further development of small molecule
22 inhibitors as tools for investigating of the role diNAcBac in bacterial glycosylation and how it
23 relates to pathogenicity. Promising candidates targeting important virulence factors have already
24 been documented, including agents inhibiting pilus assembly in uropathogenic *E. coli*⁵¹ and
25 bacterial motility by inhibiting disulfide formation of periplasmic proteins.⁵² Progress has also
26 been made towards modulators of quorum sensing.⁵³ Closely related to the work in this paper, the
27 Sulea and Logan research groups have reported an inhibitor that targets the pseudaminic acid
28 biosynthetic pathway found in *H. pylori* and *C. jejuni*.⁵⁴ The “sialic-acid like” nonulosonate sugar
29 product is required for the glycosylation of structural flagellin proteins and exposure to inhibitors
30 attenuated flagellin production at concentrations of ≥ 100 μM . The flagella are required for
31 persistent infections of *H. pylori* and this work demonstrates the link between bacterial
32 glycosylation and pathogenicity using chemical tools (as opposed to genetic modification). The
33 most advanced antivirulence work has been accomplished with N-phenyl-4-(3-
34 phenylthioureido)benzenesulfonamide, **56** (LED209), a prodrug agent that covalently inhibits
35 QseC, a receptor involved in signaling between many Gram-negative pathogens and the infected
36 host.⁵⁵ Treatment with **56** in a mouse infection model showed prophylactic efficacy against *S.*
37
38
39
40
41
42
43
44
45
46
47
48
49
50
51
52
53
54
55
56
57
58
59
60

1
2
3 *typhimurium* and provided protection against *F. tularensis* both pre- and post-infection.
4
5 Furthermore, **56** was not toxic at therapeutic doses and did not affect pathogen growth *in vitro*.
6
7 These promising *in vivo* results are compelling evidence that killing is not necessarily required for
8
9 treatment of bacterial infection and alternate therapeutic intervention strategies are worth
10
11 exploring.
12

13
14 In conclusion, herein we disclose the hit-to-lead development of a new series of
15
16 thienopyrimidine-6-carboxylate inhibitors of the *C. jejuni* PglD UDP-amino-sugar
17
18 acetyltransferase enzyme, which, upon further optimization could represent valuable chemical
19
20 tools for unraveling the intricate biological role(s) of highly modified sugars in bacteria and
21
22 potentially may lead to new agents with targeted antivirulence activity.
23
24
25
26
27

28 29 **Experimental section**

30 31 32 33 *General Procedures for Characterization of Compounds.*

34
35 All intermediate compounds were purified by normal phase flash column chromatography on
36
37 silica gel using a CombiFlash instrument. The homogeneity of all final compounds was confirmed
38
39 to $\geq 95\%$ by analytical reverse-phase LC-MS using an Agilent Series 1100 HPLC instrument
40
41 equipped with a YMC AQ12S03-1003WT C18 column and a Finnigan LCQ Deca electrospray
42
43 ionization mass spectrometer, using a gradient of 5-95% in 20 min of acetonitrile in water with
44
45 0.1% TFA. Each final compound was fully characterized by ^1H and ^{13}C NMR and HRMS.
46
47 Chemical shifts (δ) are reported in ppm relative to the internal deuterated solvent (^1H , ^{13}C), unless
48
49 indicated otherwise. The high-resolution MS spectra of final products were recorded using direct
50
51 analysis in real time (DART) ionization on a Bruker Daltonics APEXIV 4.7 Tesla Fourier
52
53 Transform Ion Cyclotron Resonance Mass Spectrometer (FT-ICR-MS).
54
55
56
57
58
59
60

1
2
3
4
5 *General procedure for the formation of thienopyrimidinones – Parent structure 6*
6

7 A pressure vessel washed charged with aminothiophene (1 equivalent) and nitrile (1-1.2
8 equivalents) and 4M HCl in dioxane was added via syringe. The pressure vessel was tightly
9 sealed with a Teflon screw cap stopper and the reaction was stirred at 80°C until the reaction was
10 complete, as judged by TLC. The reaction mixture was cooled to room temperature, transferred to
11 an Erlenmeyer flask in an ice-bath with a minimum volume of methanol and diluted with water
12 (10-fold of solvent volume). The pH was brought to ~8 with ammonium hydroxide solution (25%)
13 resulting in precipitate formation. The mixture was held on ice for 15-60 min and then filtered
14 over filter paper; washing with distilled water. The residue was dried under vacuum to afford the
15 desired thienopyrimidine in sufficient purity for the subsequent step. Due to the poor solubility of
16 these compounds, full characterization was performed after the next synthetic step and
17 purification.
18
19
20
21
22
23
24
25
26
27
28
29
30
31
32
33
34
35

36 *Ethyl 2-((diethoxyphosphoryl)methyl)-5-methyl-4-oxo-3,4-dihydrothieno[2,3-d]pyrimidine-6-*
37 *carboxylate (8)*
38

39 A 100 mL RBF was charged with ethyl 2-(chloromethyl)-5-methyl-4-oxo-3,4-dihydrothieno[2,3-
40 d]pyrimidine-6-carboxylate (900 mg, 3.13 mmol) (6) and triethylphosphite (10.4 g, 10.8 mL, 62.8
41 mmol) was added *via* syringe and the reaction was heated at 145 °C for 2 h. The reaction mixture
42 was cooled down, diluted with 100 mL diethyl ether and stirred for 1 h on ice. The suspension
43 was filtered, washed with copious amounts of ether and petroleum ether. The obtained residue
44 was dried on high vacuum to furnish the desired the product as a fine, free-flowing white powder,
45 994 mg (82%). ¹H NMR (500 MHz, DMSO) δ 12.62 (s, NH), 4.28 (q, *J* = 7.1 Hz, 2H), 4.10 –
46 3.99 (m, 4H), 3.37 (d, *J* = 22.2 Hz, 2H), 2.79 (s, 3H), 1.28 (t, *J* = 7.1 Hz, 3H), 1.21 (t, *J* = 7.0 Hz,
47
48
49
50
51
52
53
54
55
56
57
58
59
60

1
2
3 6H). ^{13}C NMR (126 MHz, DMSO) δ 166.99 (d, $J = 3.0$ Hz), 162.98, 159.97, 154.77 (d, $J = 8.6$
4 Hz), 144.46, 122.93, 122.17, 63.42 (d, $J = 6.3$ Hz), 62.28, 33.99 (d, $J = 131.2$ Hz), 17.30 (d, $J =$
5 6.0 Hz), 15.95, 15.29. ^{31}P NMR (121 MHz, DMSO) δ 21.87. MS (ESI): calcd. 389.09; found
6 389.07 $[\text{M}+\text{H}]^+$.
7
8
9

10
11
12
13
14 *General procedure for the Horner-Wadsworth-Emmons reactions:*
15

16
17 To an ice-cooled solution of phosphonate **8** (1 equivalent) and aldehyde (3 equivalents) in
18 anhydrous THF was added sodium hydride (60% suspension in mineral oil, 3 equivalents) in
19 small portions. The reaction was stirred at RT until complete consumption of starting material, as
20 determined by TLC. The crude product was poured into ice-water (5 times the reaction solvent
21 volume), filtered and washed with water. The filter-cake was washed with ice-cold ethanol,
22 diethyl ether and pentanes. The residue was dried on high vacuum to furnish the desired product
23 in sufficient purity for subsequent reactions.
24
25
26
27
28
29
30
31
32

33
34
35
36 *General procedure for the hydrogenation reactions:*
37

38 A round bottom flask was charged with the alkene product from the HWE reaction, suspended in
39 MeOH/THF/ NH_4OH 10:2:1 and purged with nitrogen. Pearlman's catalyst was added (20%
40 $\text{Pd}(\text{OH})_2/\text{C}$, 0.5 equivalents, CAS 12135-22-7), and the reaction mixture was purged with H_2 gas
41 and equipped with an H_2 -filled balloon. The reaction was stirred at 60°C until complete
42 consumption of starting material, as determined by TLC, replenishing the H_2 balloon as needed.
43 The reaction mixture was purged with nitrogen and filtered through a plug of Celite, rinsing with
44 EtOAc. The filtrate was concentrated *in vacuo* and the obtained material was used without further
45 purification.
46
47
48
49
50
51
52
53
54
55
56
57
58
59
60

1
2
3 *General procedure for the formation of ester precursors (10)*

4
5 To a solution of or thienopyrimidinone (1 equivalent) and (benzotriazol-1-yloxy)-
6
7 tripyrrolidinophosphonium hexafluorophosphate (PyBOP, 1.3 equivalents) in anhydrous
8
9 acetonitrile was added 1,8-diazabicyclo[5.4.0]undec-7-ene (1.5 equivalents, 3 equivalents in case
10
11 of amine-HCl salts) *via* syringe. The mixture was stirred at RT for 5 min, after which the
12
13 nucleophile (1.5 equivalents) was added and the reaction stirred at RT until complete
14
15 consumption of starting material, as determined by TLC. The solvent was removed *in vacuo* and
16
17 the crude residue was purified by column chromatography on silica gel using a gradient of EtOAc
18
19 in 1:1 Hex/CH₂Cl₂. *Note*: Substituent **b** was introduced as a mono-Boc-protected diamine; the Boc
20
21 protecting group was expediently removed by treating the compound with 4 M HCl in 1,4-
22
23 dioxane followed by precipitation with cold diethyl ether and filtration.
24
25
26
27
28
29
30

31 *Ethyl 5-methyl-4-(methylamino)-2-phenethylthieno[2,3-d]pyrimidine-6-carboxylate 10(d,a)*

32
33 Isolated 80 mg (77% yield) as a white solid. ¹H NMR (500 MHz, DMSO) δ 7.27 – 7.19 (m, 4H),
34
35 7.17 – 7.12 (m, 1H), 7.09 (m, NH), 4.28 (q, *J* = 7.1 Hz, 2H), 3.09 – 3.04 (m, 2H), 3.02 – 2.97 (m,
36
37 5H), 2.86 (s, 3H), 1.28 (t, *J* = 7.1 Hz, 3H). ¹³C NMR (126 MHz, DMSO) δ 168.26, 167.97,
38
39 163.50, 159.84, 142.72, 141.08, 129.47, 129.39, 126.92, 120.08, 115.95, 62.16, 41.31, 34.42,
40
41 29.27, 16.74, 15.34. MS (ESI): calcd. 356.14; found 356.27 [M+H]⁺.
42
43
44
45
46
47

48 *Ethyl 4-((2-aminoethyl)amino)-5-methyl-2-phenethylthieno[2,3-d]pyrimidine-6-carboxylate*

49
50 **10(d,b)**

51
52 Isolated 70 mg (92% yield) as a white powder. ¹H NMR (500 MHz, DMSO) δ 8.00 (br. s., NH₂),
53
54 7.48 (m, NH), 7.29 – 7.24 (m, 4H), 7.19 – 7.14 (m, 1H), 4.30 (q, *J* = 7.1 Hz, 2H), 3.81 (q, *J* = 5.6
55
56 Hz, 2H), 3.12 – 3.03 (m, 6H), 2.95 (s, 3H), 1.30 (t, *J* = 7.1 Hz, 3H). ¹³C NMR (75 MHz, DMSO) δ
57
58
59
60

1
2
3 165.02, 162.48, 159.04, 141.38, 140.89, 129.04, 128.98, 126.75, 121.53, 116.43, 62.15, 38.60,
4
5 38.41, 33.27, 16.21, 14.79. MS (ESI): calcd. 385.170; found 385.20 [M+H]⁺.
6
7

8
9
10 *Ethyl 4-(benzylamino)-5-methyl-2-phenethylthieno[2,3-d]pyrimidine-6-carboxylate 10(d,c)*

11 Isolated 80 mg (79% yield) as an off-white solid. ¹H NMR (500 MHz, DMSO) δ 7.70 (m, NH₂),
12
13 7.40 (d, *J* = 7.7 Hz, 2H), 7.29 (t, *J* = 7.6 Hz, 2H), 7.23 – 7.15 (m, 3H), 7.09 (m, 3H), 4.75 (d, *J* =
14
15 5.8 Hz, 2H), 4.27 (q, *J* = 7.1 Hz, 2H), 2.93 (m, 7H), 1.28 (t, *J* = 7.1 Hz, 3H). ¹³C NMR (126 MHz,
16
17 DMSO) δ 168.26, 168.09, 163.46, 159.24, 142.59, 141.04, 140.88, 129.38, 129.33, 128.52,
18
19 127.77, 126.85, 120.39, 115.86, 62.19, 45.07, 41.25, 34.27, 16.88, 15.31. MS (ESI): calcd.
20
21 432.17; found 432.33 [M+H]⁺.
22
23
24
25
26
27

28
29 *Ethyl 5-methyl-2-phenethyl-4-(phenethylamino)thieno[2,3-d]pyrimidine-6-carboxylate 10(d,d)*

30 Isolated 106 mg (91% yield) as a pale yellow solid. ¹H NMR (500 MHz, DMSO) δ 7.32 – 7.16
31
32 (m, 8H & NH), 7.16 – 7.07 (m, 2H), 4.26 (q, *J* = 7.0 Hz, 2H), 3.72 (dd, *J* = 14.0, 6.3 Hz, 2H),
33
34 3.13 – 3.05 (m, 2H), 3.05 – 2.96 (m, 2H), 2.94 – 2.86 (m, 2H), 2.79 (s, 3H), 1.27 (t, *J* = 7.1 Hz,
35
36 3H). ¹³C NMR (126 MHz, DMSO) δ 168.22, 168.19, 163.44, 159.23, 142.67, 140.85, 140.67,
37
38 129.82, 129.55, 129.40, 129.37, 127.29, 126.93, 120.27, 115.77, 62.14, 43.49, 41.29, 35.77,
39
40 34.47, 16.60, 15.30. MS (ESI): calcd. 446.19; found 446.40 [M+H]⁺.
41
42
43
44
45
46
47

48
49 *Ethyl 4-((4-methoxyphenethyl)amino)-5-methyl-2-phenethylthieno[2,3-d]pyrimidine-6-
50
51 carboxylate 10(d,g)*

52 Isolated 172 mg (83% yield) as an off-white solid. ¹H NMR (500 MHz, DMSO) δ 7.26 – 7.20 (m,
53
54 4H), 7.18 – 7.09 (m, 3H & NH), 6.86 (d, *J* = 8.6 Hz, 2H), 4.28 (q, *J* = 7.1 Hz, 2H), 3.71 – 3.66
55
56 (m, 5H), 3.12 – 3.07 (m, 2H), 3.03 – 2.99 (m, 2H), 2.86 – 2.80 (m, 5H), 1.28 (t, *J* = 7.1 Hz, 3H).
57
58
59
60

¹³C NMR (75 MHz, CDCl₃) δ 168.07, 163.30, 158.99, 158.70, 142.08, 138.32, 130.92, 130.03, 128.70, 128.55, 126.07, 121.47, 115.33, 114.46, 61.45, 55.53, 42.47, 41.16, 34.55, 34.46, 15.70, 14.58. MS (ESI): calcd. 476.20; found 476.40 [M+H]⁺.

Ethyl 4-((3-methoxyphenethyl)amino)-5-methyl-2-phenethylthieno[2,3-d]pyrimidine-6-carboxylate **10(d,h)**

Isolated 182 mg (87% yield) as a pale yellow solid. ¹H NMR (500 MHz, DMSO) δ 7.27 – 7.19 (m, 6H), 7.17 – 7.11 (m, 1H 7 NH), 6.82 (m, 2H), 4.28 (q, *J* = 7.1 Hz, 2H), 3.73 (m, 2H), 3.69 (s, 3H), 3.10 (m, 2H), 3.01 (m, 2H), 2.91 – 2.86 (m, 2H), 2.82 (s, 3H), 1.28 (t, *J* = 7.1 Hz, 3H). ¹³C NMR (75 MHz, CDCl₃) δ 168.05, 163.28, 160.23, 158.96, 142.08, 140.67, 138.35, 130.10, 128.70, 128.56, 126.08, 121.47, 121.36, 115.34, 114.92, 112.13, 61.45, 55.39, 42.27, 41.18, 35.41, 34.56, 15.66, 14.58. MS (ESI): calcd. 476.20; found 476.47 [M+H]⁺.

Ethyl 4-((2-methoxyphenethyl)amino)-5-methyl-2-phenethylthieno[2,3-d]pyrimidine-6-carboxylate **10(d,i)**

Isolated 198 mg (95% yield) as a beige solid. ¹H NMR (500 MHz, DMSO) δ 7.25 – 7.11 (m, 7H), 7.08 (m, NH), 6.95 (d, *J* = 7.6 Hz, 1H), 6.86 (td, *J* = 7.4, 1.0 Hz, 1H), 4.28 (q, *J* = 7.1 Hz, 2H), 3.74 (s, 3H), 3.73 – 3.68 (m, 2H), 3.09 (m, 2H), 3.00 (m, 2H), 2.92 (t, *J* = 7.3 Hz, 2H), 2.81 (s, 3H), 1.30 – 1.26 (m, 3H). ¹³C NMR (75 MHz, CDCl₃) δ 168.04, 163.38, 159.12, 157.72, 142.17, 138.59, 130.92, 128.72, 128.54, 128.39, 127.51, 126.04, 121.11, 115.32, 110.79, 61.40, 55.61, 41.84, 41.19, 34.53, 29.65, 15.62, 14.59. MS (ESI): calcd. 476.20; found 476.27 [M+H]⁺.

Ethyl 4-((4-fluorophenethyl)amino)-5-methyl-2-phenethylthieno[2,3-d]pyrimidine-6-carboxylate **10(d,j)**.

1
2
3 Isolated 183 mg (90% yield) as a pale yellow solid. ^1H NMR (300 MHz, CDCl_3) δ 7.32 – 7.23 (m,
4 4H), 7.21 – 7.12 (m, 3H), 7.02 (m, 2H), 5.61 (t, $J = 5.5$ Hz, NH), 4.34 (q, $J = 7.1$ Hz, 2H), 3.85
5 (dd, $J = 12.5, 6.8$ Hz, 2H), 3.22 – 3.14 (m, 4H), 2.94 (m, 2H), 2.71 (s, 3H), 1.38 (t, $J = 7.1$ Hz,
6 3H). ^{13}C NMR (75 MHz, CDCl_3) δ 168.02, 163.25, 161.95 (d, $J = 245.0$ Hz), 158.92, 142.03,
7 138.10, 134.79 (d, $J = 3.3$ Hz), 130.55, 130.44, 128.67, 128.57, 126.09, 121.68, 115.82 (d, $J =$
8 21.2 Hz), 115.30, 61.49, 42.44, 41.14, 34.63, 34.54, 15.71, 14.57. MS (ESI): calcd. 464.18; found
9 464.47 $[\text{M}+\text{H}]^+$.

10
11
12
13
14
15
16
17
18
19
20
21
22 *Ethyl 4-((3-fluorophenethyl)amino)-5-methyl-2-phenethylthieno[2,3-d]pyrimidine-6-carboxylate*

23
24 **10(d,k)**

25
26 Isolated 168 mg (83% yield) as a pale yellow solid. ^1H NMR (300 MHz, CDCl_3) δ 7.34 – 7.23 (m,
27 5H), 7.18 (m, 1H), 7.05 – 6.89 (m, 3H), 5.63 (t, $J = 5.4$ Hz, NH), 4.34 (q, $J = 7.1$ Hz, 2H), 3.87
28 (dd, $J = 12.5, 6.8$ Hz, 2H), 3.23 – 3.15 (m, 4H), 2.96 (m, 2H), 2.72 (s, 3H), 1.38 (t, $J = 7.1$ Hz,
29 3H). ^{13}C NMR (75 MHz, CDCl_3) δ 168.01, 163.27 (d, $J = 246.3$ Hz), 163.23, 158.88, 142.02,
30 141.77 (d, $J = 7.1$ Hz), 138.14, 130.49 (d, $J = 8.3$ Hz), 128.68, 128.57, 126.09, 124.78, 124.75,
31 121.68, 115.90 (d, $J = 20.9$ Hz), 115.31, 113.88 (d, $J = 21.0$ Hz), 61.48, 42.17, 41.16, 35.21,
32 34.56, 15.69, 14.57. MS (ESI): calcd. 464.18; found 464.47 $[\text{M}+\text{H}]^+$.

33
34
35
36
37
38
39
40
41
42
43
44
45 *Ethyl 4-((2-fluorophenethyl)amino)-5-methyl-2-phenethylthieno[2,3-d]pyrimidine-6-carboxylate*

46
47 **10(d,l)**

48
49 Isolated 170 mg (84% yield) as an off-white solid. ^1H NMR (300 MHz, CDCl_3) δ 7.32 – 7.02 (m,
50 9H), 5.69 (t, $J = 5.4$ Hz, NH), 4.35 (q, $J = 7.1$ Hz, 2H), 3.89 (dd, $J = 12.4, 6.6$ Hz, 2H), 3.23 –
51 3.12 (m, 4H), 3.04 (m, 2H), 2.76 (s, 3H), 1.39 (t, $J = 7.1$ Hz, 3H). ^{13}C NMR (75 MHz, CDCl_3) δ
52 168.00, 163.30, 161.51 (d, $J = 244.8$ Hz), 158.99, 142.10, 138.29, 131.46 (d, $J = 4.9$ Hz), 128.86,
53 54 55 56 57 58 59 60

1
2
3 128.75, 128.70, 128.55, 126.08 (d, $J = 16.0$ Hz), 126.06, 124.60 (d, $J = 3.5$ Hz), 121.55, 115.75
4
5 (d, $J = 22.0$ Hz), 115.31, 61.46, 41.41, 41.16, 34.52, 29.03, 15.68, 14.58. MS (ESI): calcd.
6
7 464.18; found 464.47 [M+H]⁺.
8
9

10
11
12 *Ethyl 5-methyl-4-((4-methylphenethyl)amino)-2-phenethylthieno[2,3-d]pyrimidine-6-carboxylate*

13
14 **10(d,m)**

15
16
17 Isolated 103 mg (77% yield) as a white solid. ¹H NMR (300 MHz, CDCl₃) δ 7.34 – 7.10 (m, 9H),
18
19 5.61 (t, $J = 5.3$ Hz, NH), 4.35 (q, $J = 7.1$ Hz, 2H), 3.88 (dd, $J = 12.2, 6.6$ Hz, 2H), 3.24 – 3.13 (m,
20
21 4H), 2.95 (t, $J = 6.7$ Hz, 2H), 2.69 (s, 3H), 2.36 (s, 3H), 1.40 (t, $J = 7.1$ Hz, 3H). ¹³C NMR (75
22
23 MHz, CDCl₃) δ 168.09, 163.33, 159.00, 142.11, 138.36, 136.59, 135.89, 129.76, 128.96, 128.71,
24
25 128.56, 126.07, 121.45, 115.34, 61.44, 42.41, 41.19, 34.93, 34.57, 21.32, 15.68, 14.59. MS (ESI):
26
27 calcd. 460.21; found 460.47 [M+H]⁺.
28
29
30
31
32

33
34 *Ethyl 5-methyl-4-((3-methylphenethyl)amino)-2-phenethylthieno[2,3-d]pyrimidine-6-carboxylate*

35
36 **10(d,n)**

37
38 Isolated 113 mg (84% yield) as an off-white solid. ¹H NMR (300 MHz, CDCl₃) δ 7.34 – 7.16 (m,
39
40 6H), 7.07 (m, 3H), 5.61 (t, $J = 5.3$ Hz, NH), 4.35 (q, $J = 7.1$ Hz, 2H), 3.89 (dd, $J = 12.2, 6.6$ Hz,
41
42 2H), 3.19 (m, 4H), 2.95 (t, $J = 6.7$ Hz, 2H), 2.69 (s, 3H), 2.36 (s, 3H), 1.39 (t, $J = 7.1$ Hz, 3H).
43
44 ¹³C NMR (75 MHz, CDCl₃) δ 168.09, 163.31, 159.00, 142.11, 138.97, 138.74, 138.33, 129.89,
45
46 129.03, 128.71, 128.56, 127.79, 126.09, 126.07, 121.46, 115.36, 61.45, 42.36, 41.20, 35.29,
47
48 34.58, 21.66, 15.61, 14.58. MS (ESI): calcd. 460.21; found 460.50 [M+H]⁺.
49
50
51
52
53

54
55 *Ethyl 5-methyl-4-((2-methylphenethyl)amino)-2-phenethylthieno[2,3-d]pyrimidine-6-carboxylate*

56
57 **10(d,o)**
58
59
60

1
2
3 Isolated 101 mg (75% yield) as a pale yellow solid. ^1H NMR (300 MHz, CDCl_3) δ 7.33 – 7.14 (m,
4 9H), 5.68 (t, $J = 5.5$ Hz, NH), 4.36 (q, $J = 7.1$ Hz, 2H), 3.87 (dd, $J = 12.8, 7.0$ Hz, 2H), 3.19 (m,
5 4H), 3.01 (t, $J = 7.1$ Hz, 2H), 2.76 (s, 3H), 2.41 (s, 3H), 1.40 (t, $J = 7.1$ Hz, 3H). ^{13}C NMR (75
6 MHz, CDCl_3) δ 168.10, 163.32, 159.09, 142.07, 138.29, 137.10, 136.71, 130.94, 129.79, 128.70,
7 128.57, 127.16, 126.48, 126.09, 121.56, 115.35, 61.47, 41.30, 41.13, 34.69, 32.99, 19.71, 15.79,
8 14.59. MS (ESI): calcd. 460.21; found 460.47 $[\text{M}+\text{H}]^+$.
9
10
11
12
13
14
15
16
17
18

19 *Ethyl 5-methyl-2-phenethyl-4-((2-(pyridin-4-yl)ethyl)amino)thieno[2,3-d]pyrimidine-6-*
20 *carboxylate* **10(d,p)**
21
22
23

24 Isolated 70 mg (72% yield) as a pale yellow solid. ^1H NMR (500 MHz, DMSO) δ 8.45 (d, $J = 5.9$
25 Hz, 2H), 7.25 (d, $J = 6.0$ Hz, 2H), 7.22 (m, 4H), 7.18 (br. t, $J = 5.8$ Hz, NH), 7.13 (m, 1H), 4.28
26 (q, $J = 7.1$ Hz, 2H), 3.77 (dd, $J = 13.5, 6.5$ Hz, 2H), 3.10 – 3.05 (m, 2H), 3.03 – 2.98 (m, 2H),
27 (q, $J = 7.1$ Hz, 2H), 3.77 (dd, $J = 13.5, 6.5$ Hz, 2H), 3.10 – 3.05 (m, 2H), 3.03 – 2.98 (m, 2H),
28 2.92 (dd, $J = 10.3, 4.0$ Hz, 2H), 2.81 (s, 3H), 1.29 (t, $J = 7.1$ Hz, 3H). ^{13}C NMR (126 MHz,
29 DMSO) δ 168.27, 159.30, 150.69, 149.70, 140.91, 129.45, 127.00, 125.50, 62.28, 42.30, 35.00,
30 34.48, 16.68, 15.37. MS (ESI): calcd. 447.185; found 447.20 $[\text{M}+\text{H}]^+$.
31
32
33
34
35
36
37
38
39

40 *Ethyl 5-methyl-2-phenethyl-4-((2-(pyridin-3-yl)ethyl)amino)thieno[2,3-d]pyrimidine-6-*
41 *carboxylate* **10(d,q)**
42
43
44

45 Isolated 54 mg (41% yield) as a pale yellow solid. ^1H NMR (500 MHz, DMSO) δ 8.46 (s, 1H),
46 8.41 (d, $J = 4.5$ Hz, 1H), 7.64 (d, $J = 7.8$ Hz, 1H), 7.31 (dd, $J = 7.7, 4.8$ Hz, 1H), 7.25 – 7.21 (m,
47 4H), 7.19 – 7.12 (m, NH, 1H), 4.28 (q, $J = 7.1$ Hz, 2H), 3.76 (dd, $J = 13.1, 6.7$ Hz, 2H), 3.10 –
48 3.05 (m, 2H), 3.00 (dd, $J = 8.4, 6.2$ Hz, 2H), 2.93 (t, $J = 7.1$ Hz, 2H), 2.81 (s, 3H), 1.29 (t, $J = 7.1$
49 Hz, 3H). ^{13}C NMR (126 MHz, DMSO) δ 168.19, 163.47, 159.26, 151.00, 148.56, 142.66, 140.86,
50
51
52
53
54
55
56
57
58
59
60

1
2
3 137.49, 136.20, 129.41, 126.95, 124.63, 120.37, 115.78, 62.21, 42.92, 41.25, 34.48, 32.87, 16.65,
4
5 15.32. MS (ESI): calcd. 447.185; found 447.27 [M+H]⁺.
6
7
8

9
10 *Ethyl 5-methyl-2-phenethyl-4-((2-(pyridin-2-yl)ethyl)amino)thieno[2,3-d]pyrimidine-6-*
11
12 *carboxylate 10(d,r)*
13

14 Isolated 118 mg (90% yield) as a pale yellow solid. ¹H NMR (300 MHz, CDCl₃) δ 8.52 (dd, *J* =
15 5.8, 1.7 Hz, 1H), 7.62 (td, *J* = 7.7, 1.8 Hz, 1H), 7.49 (s, NH), 7.31 – 7.23 (m, 4H), 7.21 – 7.13 (m,
16 3H), 4.34 (q, *J* = 7.1 Hz, 2H), 4.02 (dd, *J* = 11.5, 5.2 Hz, 2H), 3.19 – 3.06 (m, 6H), 2.97 (s, 3H),
17 1.38 (t, *J* = 7.1 Hz, 3H). ¹³C NMR (75 MHz, CDCl₃) δ 168.08, 168.01, 163.46, 160.33, 158.80,
18 149.13, 142.21, 139.20, 137.12, 128.71, 128.51, 126.00, 123.76, 122.02, 120.96, 115.53, 61.35,
19 41.19, 40.27, 36.09, 34.56, 15.79, 14.60. MS (ESI): calcd. 447.19; found 447.40 [M+H]⁺.
20
21
22
23
24
25
26
27
28
29
30

31 *Ethyl 4-((2,3-dihydro-1H-inden-2-yl)amino)-5-methyl-2-phenethylthieno[2,3-d]pyrimidine-6-*
32
33 *carboxylate 10(d,x)*
34
35

36 Isolated 105 mg (79% yield) as a pale yellow solid. ¹H NMR (300 MHz, CDCl₃) δ 7.33 – 7.17 (m,
37 9H), 5.82 (d, *J* = 6.7 Hz, NH), 5.13 (m, 1H), 4.36 (q, *J* = 7.1 Hz, 2H), 3.52 (d, *J* = 7.3 Hz, 2H),
38 3.46 (d, *J* = 7.2 Hz, 2H), 2.95 (d, *J* = 5.4 Hz, 2H), 2.89 (d, *J* = 5.5 Hz, 2H), 2.84 (s, 3H), 1.40 (t, *J*
39 = 7.1 Hz, 3H). ¹³C NMR (75 MHz, CDCl₃) δ 168.03, 163.28, 158.79, 142.05, 141.03, 138.10,
40 128.71, 128.57, 127.14, 126.08, 125.10, 121.73, 115.31, 61.49, 52.48, 41.12, 40.45, 34.57,
41 15.88, 14.58. MS (ESI): calcd. 458.19; found 458.47 [M+H]⁺.
42
43
44
45
46
47
48
49
50
51

52 *Ethyl 4-((3,5-dimethoxyphenethyl)amino)-5-methyl-2-phenethylthieno[2,3-d]pyrimidine-6-*
53
54 *carboxylate 10(d,y)*
55
56
57
58
59
60

1
2
3 Isolated 77 mg (52% yield) as a pale yellow solid. ^1H NMR (500 MHz, DMSO) δ 7.23 (m, 4H),
4 7.16 – 7.09 (m, 1H, NH), 6.41 (s, 2H), 6.33 (s, 1H), 4.28 (q, $J = 7.1$ Hz, 2H), 3.73 (dd, $J = 13.7$,
5 6.3 Hz, 2H), 3.67 (s, 6H), 3.10 (m, 2H), 3.04 – 2.98 (m, 2H), 2.88 – 2.79 (m, 5H), 1.29 (t, $J = 7.1$
6 7 Hz, 3H). ^{13}C NMR (126 MHz, DMSO) δ 168.21, 168.18, 163.44, 161.61, 159.23, 142.96, 142.67,
7 140.85, 129.39, 129.37, 126.94, 120.26, 115.78, 107.80, 99.12, 62.15, 56.10, 43.39, 41.34, 36.05,
8 34.48, 16.60, 15.29. MS (ESI): calcd. 506.21; found 506.53 $[\text{M}+\text{H}]^+$
9
10
11
12
13
14
15
16
17
18

19 *Ethyl 4-((2-(benzo[d][1,3]dioxol-5-yl)ethyl)amino)-5-methyl-2-phenethylthieno[2,3-d]pyrimidine-*
20 *6-carboxylate* **10(d,z)**
21
22
23

24 Isolated 94 mg (66% yield) as a pale yellow solid. ^1H NMR (500 MHz, DMSO) δ 7.27 – 7.20 (m,
25 4H), 7.10 (s, 1H, NH), 6.85 – 6.79 (m, 2H), 6.68 (d, $J = 7.9$ Hz, 1H), 5.95 (s, 2H), 4.28 (q, $J = 7.1$
26 Hz, 2H), 3.69 (dd, $J = 14.1$, 6.3 Hz, 2H), 3.12 – 3.05 (m, 2H), 3.05 – 2.95 (m, 2H), 2.85 – 2.78
27 (m, 5H), 1.29 (t, $J = 7.1$ Hz, 3H). ^{13}C NMR (126 MHz, DMSO) δ 168.19, 163.45, 159.23, 148.42,
28 146.70, 142.67, 140.87, 134.41, 129.40, 129.38, 126.94, 122.67, 120.25, 115.76, 110.12, 109.30,
29 101.84, 62.15, 43.63, 41.32, 35.45, 34.49, 16.62, 15.31. MS (ESI): calcd. 490.18; found 490.47
30 $[\text{M}+\text{H}]^+$.
31
32
33
34
35
36
37
38
39
40
41
42

43 *Ethyl 5-methyl-4-(methylamino)-2-(3-phenylpropyl)thieno[2,3-d]pyrimidine-6-carboxylate*
44 **10(e,a)**
45
46

47 Isolated 52 mg (33% yield) as a yellow oil. ^1H NMR (300 MHz, CDCl_3) δ 7.26 – 7.14 (m, 5H),
48 5.67 (m, NH), 4.33 (q, $J = 7.1$ Hz, 2H), 3.12 (d, $J = 4.8$ Hz, 3H), 2.88 (s, 3H), 2.84 (m, 2H), 2.75
49 – 2.67 (m, 2H), 2.22 – 2.11 (m, 2H), 1.37 (t, $J = 7.1$ Hz, 3H). ^{13}C NMR (75 MHz, CDCl_3) δ
50 168.72, 167.83, 163.32, 159.61, 142.63, 138.32, 128.75, 128.45, 125.88, 121.25, 115.33, 61.42,
51 39.21, 35.91, 30.26, 28.33, 15.93, 14.56. MS (ESI): calcd. 370.159; found 370.33 $[\text{M}+\text{H}]^+$
52
53
54
55
56
57
58
59
60

1
2
3
4
5 *Ethyl 5-methyl-4-(methylamino)-2-(4-phenylbutyl)thieno[2,3-d]pyrimidine-6-carboxylate* **10(f,a)**
6

7 Isolated 88 mg (43 % yield) as a pale yellow syrup. ¹H NMR (300 MHz, CDCl₃) δ 7.29 – 7.13 (m,
8 5H), 5.64 (br. m, NH), 4.34 (q, *J* = 7.1 Hz, 2H), 3.11 (d, *J* = 4.8 Hz, 3H), 2.89 (s, 3H), 2.88 – 2.81
9 (m, 2H), 2.70 – 2.63 (m, 2H), 1.95 – 1.83 (m, 2H), 1.78 – 1.67 (m, 2H), 1.38 (t, *J* = 7.1 Hz, 3H).
10
11
12
13
14 ¹³C NMR (75 MHz, CDCl₃) δ 168.96, 167.88, 163.35, 159.64, 142.89, 138.27, 128.65, 128.43,
15
16 125.80, 121.27, 115.32, 61.42, 39.51, 36.06, 31.51, 28.30, 15.95, 14.57. MS (ESI): calcd.
17 384.175; found 384.27 [M+H]⁺.
18
19
20
21
22
23

24 *Ethyl 2-(3-methoxyphenethyl)-5-methyl-4-(methylamino)thieno[2,3-d]pyrimidine-6-carboxylate*
25

26 **10(h,a)**
27

28 Isolated 163 mg (83% yield) as a pale yellow solid. ¹H NMR (300 MHz, CDCl₃) δ 7.16 (t, *J* = 7.8
29 Hz, 1H), 6.84 (m, 2H), 6.70 (dd, *J* = 8.1, 2.5 Hz, 1H), 5.66 (br. m, NH), 4.33 (q, *J* = 7.1 Hz, 2H),
30
31 3.75 (s, 3H), 3.15 – 3.08 (m, 7H), 2.86 (s, 3H), 1.37 (t, *J* = 7.1 Hz, 3H). ¹³C NMR (75 MHz,
32
33 CDCl₃) δ 167.96, 163.29, 159.77, 159.61, 143.75, 138.29, 129.46, 121.37, 121.09, 115.41,
34
35 114.25, 111.53, 61.44, 55.32, 41.06, 34.48, 28.32, 15.90, 14.56. MS (ESI): calcd. 386.154; found
36
37 386.27 [M+H]⁺.
38
39
40
41
42
43
44

45 *Ethyl 2-(3-fluorophenethyl)-5-methyl-4-(methylamino)thieno[2,3-d]pyrimidine-6-carboxylate*
46

47 **10(k,a)**
48

49 Isolated 141 mg (54% yield) as a pale yellow oil. ¹H NMR (300 MHz, CDCl₃) δ 7.21 – 7.13 (m,
50
51 1H), 7.05 – 6.92 (m, 2H), 6.84 (td, *J* = 8.5, 2.6 Hz, 1H), 5.66 (br. m, NH), 4.33 (q, *J* = 7.1 Hz,
52
53 2H), 3.17 – 3.06 (m, 7H), 2.88 (s, 3H), 1.37 (t, *J* = 7.1 Hz, 3H). ¹³C NMR (75 MHz, CDCl₃) δ
54
55 167.80, 167.58, 164.66, 163.28, 161.41, 159.61, 144.70 (d, *J* = 7.2 Hz), 138.21, 129.85 (d, *J* = 8.4
56
57
58
59
60

1
2
3 Hz), 124.34 (d, $J = 2.6$ Hz), 121.51, 115.42 (d, $J = 3.6$ Hz), 112.84 (d, $J = 21.0$ Hz), 61.46, 40.67,
4
5 34.02, 28.32, 15.92, 14.54. MS (ESI): calcd. 374.134; found 374.20 [M+H]⁺.
6
7

8
9
10 *Ethyl 5-methyl-4-(methylamino)-2-(2-(pyridin-2-yl)ethyl)thieno[2,3-d]pyrimidine-6-carboxylate*

11
12 **10(q,a)**

13
14 Isolated 585 mg (57% yield) as a white solid. ¹H NMR (300 MHz, CDCl₃) δ 8.54 (ddd, $J = 5.0$,
15 1.7, 0.8 Hz, 1H), 7.65 (td, $J = 7.7$, 1.8 Hz, 1H), 7.29 (d, $J = 7.9$ Hz, 1H), 7.17 (ddd, $J = 7.5$, 5.0,
16 1.1 Hz, 1H), 5.68 (br. m, NH), 4.34 (q, $J = 7.1$ Hz, 2H), 3.45 – 3.35 (m, 2H), 3.29 (m, 2H), 3.08
17 (d, $J = 4.7$ Hz, 3H), 2.91 (s, 3H), 1.38 (t, $J = 7.1$ Hz, 3H). ¹³C NMR (75 MHz, CDCl₃) δ 167.41,
18 163.29, 161.18, 159.61, 148.18, 138.21, 137.73, 123.64, 121.71, 121.59, 115.48, 61.47, 38.68,
19 35.79, 28.39, 15.96, 14.55. MS (ESI): calcd. 357.139; found 357.20 [M+H]⁺.
20
21
22
23
24
25
26
27
28
29
30
31
32

33
34 *Ethyl 2-(4-acetamidophenethyl)-5-methyl-4-(methylamino)thieno[2,3-d]pyrimidine-6-carboxylate*

35
36 **10(s,a)**

37
38 Isolated 38 mg (68% yield) as a beige solid. ¹H NMR (500 MHz, DMSO) δ 9.83 (s, NHAc), 7.41
39 (d, $J = 8.4$ Hz, 2H), 7.13 (d, $J = 8.2$ Hz, 2H), 7.09 (m, NH), 4.27 (q, $J = 7.1$ Hz, 2H), 3.02 – 2.94
40 (m, 7H), 2.86 (s, 3H), 1.98 (s, 3H), 1.28 (t, $J = 7.1$ Hz, 3H). ¹³C NMR (126 MHz, CDCl₃ +
41 CD₃OD) δ 174.50, 172.26, 171.43, 167.85, 164.01, 143.40, 142.04, 140.74, 133.30, 125.53,
42 124.67, 119.90, 65.95, 45.18, 38.26, 32.49, 28.11, 19.95, 18.70. MS (ESI): calcd. 413.16; found
43 413.33 [M+H]⁺.
44
45
46
47
48
49
50
51
52
53

54
55 *Ethyl 2-(4-acetamidophenethyl)-4-((2-aminoethyl)amino)-5-methylthieno[2,3-d]pyrimidine-6-*

56
57 *carboxylate* **10(s,b)**
58
59
60

1
2
3 Isolated 51 mg (83 % yield) as a white solid. ¹H NMR (300 MHz, DMSO) δ 9.81 (s, NHAc), 7.43
4 (d, *J* = 8.4 Hz, 2H), 7.14 (d, *J* = 8.4 Hz, 2H), 7.07 – 6.96 (m, NH), 4.26 (q, *J* = 7.0 Hz, 2H), 3.57
5 (dd, *J* = 11.0, 5.5 Hz, 2H), 3.23 (dd, *J* = 11.6, 6.1 Hz, 2H), 3.03 – 2.90 (m, 4H), 2.86 (s, 3H), 1.99
6 (s, 3H), 1.27 (t, *J* = 7.1 Hz, 3H). ¹³C NMR (75 MHz, DMSO) δ 167.69, 162.98, 159.06, 156.71,
7 140.62, 137.83, 136.80, 129.09, 119.63, 115.35, 78.38, 61.67, 33.38, 24.59, 21.41, 16.11, 14.81.
8 MS (ESI): calcd. 442.191; found 442.27 [M+H]⁺.
9
10
11
12
13
14
15
16
17
18

19 *Ethyl 2-(4-acetamidophenethyl)-5-methyl-4-((2-(pyridin-4-yl)ethyl)amino)thieno[2,3-*
20 *d]pyrimidine-6-carboxylate 10(s,p)*
21
22
23

24 Isolated 86 mg (68% yield) as a pale yellow solid. ¹H NMR (500 MHz, DMSO) δ 9.83 (s, NHAc),
25 8.46 (d, *J* = 4.7 Hz, 2H), 7.45 (d, *J* = 8.2 Hz, 2H), 7.24 (m, 2H, NH), 7.12 (d, *J* = 8.2 Hz, 2H),
26 4.26 (q, *J* = 7.0 Hz, 2H), 3.76 (dd, *J* = 12.7, 6.4 Hz, 2H), 3.07 – 2.90 (m, 6H), 2.79 (s, 3H), 2.00
27 (s, 3H), 1.28 (t, *J* = 7.0 Hz, 3H). ¹³C NMR (126 MHz, DMSO) δ 169.24, 168.18, 163.44, 159.18,
28 150.63, 149.67, 140.79, 138.35, 137.19, 129.51, 129.43, 129.38, 125.41, 120.15, 115.75, 62.17,
29 46.92, 41.32, 34.98, 33.91, 25.05, 16.61, 15.28. MS (ESI): calcd. 504.207; found 504.13 [M+H]⁺.
30
31
32
33
34
35
36
37
38
39

40 *Ethyl 2-(4-acetamidophenethyl)-5-methyl-4-((2-(pyridin-3-yl)ethyl)amino)thieno[2,3-*
41 *d]pyrimidine-6-carboxylate 10(s,q)*
42
43
44

45 Isolated 79 mg (63% yield) as a pale yellow solid. ¹H NMR (500 MHz, DMSO) δ 9.83 (s, NHAc),
46 8.41 (d, *J* = 4.7 Hz, 1H), 7.63 (d, *J* = 7.7 Hz, 1H), 7.46 (m, *J* = 15.7, 8.4 Hz, 3H), 7.30 (dd, *J* =
47 7.7, 4.8 Hz, 1H), 7.18 – 7.10 (m, 2H, NH), 4.27 (q, *J* = 7.0 Hz, 2H), 3.76 (dd, *J* = 12.9, 6.6 Hz,
48 2H), 3.06 – 2.91 (m, 6H), 2.80 (s, 3H), 2.00 (s, 3H), 1.29 (t, *J* = 7.1 Hz, 3H). ¹³C NMR (126 MHz,
49 DMSO) δ 168.20, 163.45, 159.23, 151.01, 148.58, 140.83, 137.41, 137.19, 136.19, 129.62,
50
51
52
53
54
55
56
57
58
59
60

1
2
3 129.52, 124.60, 120.22, 120.13, 115.75, 62.18, 47.02, 33.93, 32.88, 27.10, 25.06, 16.63, 15.30.

4
5 MS (ESI): calcd. 504.207; found 504.27 [M+H]⁺.

6
7
8
9
10 *Ethyl 2-(4-acetamidophenethyl)-5-methyl-4-((2-(pyridin-2-yl)ethyl)amino)thieno[2,3-*
11 *d]pyrimidine-6-carboxylate* **10(s,r)**

12
13
14 Isolated 55 mg (44% yield) as a pale yellow solid. ¹H NMR (500 MHz, DMSO) δ 9.83 (s, NHAc),
15 8.52 (d, *J* = 4.1 Hz, 1H), 7.71 (t, *J* = 7.6 Hz, 1H), 7.43 (m, 2H, NH), 7.28 (d, *J* = 7.4 Hz, 1H),
16 7.24 (dd, *J* = 7.4, 4.9 Hz, 1H), 7.14 (d, *J* = 8.3 Hz, 2H), 4.27 (q, *J* = 7.1 Hz, 2H), 3.88 (dd, *J* =
17 12.3, 6.4 Hz, 2H), 3.09 (m, 2H), 3.05 – 2.99 (m, 2H), 2.96 (dd, *J* = 8.2, 6.3 Hz, 2H), 2.84 (s, 3H),
18 2.00 (s, 3H), 1.29 (t, *J* = 7.1 Hz, 3H). ¹³C NMR (126 MHz, DMSO) δ 169.20, 168.29, 168.13,
19 163.46, 160.72, 159.20, 150.13, 140.80, 138.33, 137.87, 137.24, 129.56, 124.47, 122.79, 120.33,
20 120.14, 115.79, 62.17, 41.60, 41.33, 37.36, 33.85, 25.09, 16.52, 15.31. MS (ESI): calcd. 504.207;
21 found 504.20 [M+H]⁺.

22
23
24
25
26
27
28
29
30
31
32
33
34
35
36 *Ethyl 2-(3-acetamidophenethyl)-5-methyl-4-(methylamino)thieno[2,3-d]pyrimidine-6-carboxylate*
37 **10(t,a)**

38
39
40 Isolated 45 mg (81% yield) as a white powder. ¹H NMR (500 MHz, DMSO) δ 9.84 (s, NHAc),
41 7.47 (s, 1H), 7.36 (d, *J* = 7.7 Hz, 1H), 7.14 (t, *J* = 7.8 Hz, 1H), 7.11 (m, *J* = 4.5 Hz, NH), 6.90 (d,
42 *J* = 7.6 Hz, 1H), 4.28 (q, *J* = 7.1 Hz, 2H), 3.04 – 2.94 (m, 7H), 2.87 (s, 3H), 2.00 (s, 3H), 1.28 (t,
43 *J* = 7.1 Hz, 3H). ¹³C NMR (126 MHz, CDCl₃ + CD₃OD) δ 174.50, 172.26, 171.43, 167.85,
44 164.01, 143.40, 142.04, 140.74, 133.30, 125.53, 124.67, 119.90, 65.95, 45.18, 38.26, 32.49,
45 28.11, 19.95, 18.70. MS (ESI): calcd. 413.16; found 413.30 [M+H]⁺.

1
2
3 *Ethyl 2-(2-acetamidophenethyl)-5-methyl-4-(methylamino)thieno[2,3-d]pyrimidine-6-carboxylate*

4
5 **10(u,a)**

6
7 Isolated 35 mg (63% yield) as a white powder. ¹H NMR (500 MHz, DMSO) δ 9.43 (s, NHAc),
8 7.29 (d, *J* = 7.8 Hz, 1H), 7.24 (d, *J* = 7.6 Hz, 1H), 7.13 (t, *J* = 7.5 Hz, 1H), 7.08 (m, NH, 1H),
9 4.27 (q, *J* = 7.1 Hz, 2H), 3.03 (m, 2H), 2.97 (d, *J* = 4.5 Hz, 3H), 2.93 (m, 2H), 2.86 (s, 3H), 2.03
10 (s, 3H), 1.27 (t, *J* = 7.1 Hz, 3H). ¹³C NMR (126 MHz, CDCl₃ + CD₃OD) δ 175.11, 172.05,
11 171.24, 167.71, 164.02, 143.67, 139.66, 139.37, 134.36, 131.18, 130.57, 130.32, 125.54, 120.05,
12 66.02, 44.45, 33.67, 32.49, 28.01, 19.89, 18.71. MS (ESI): calcd. 413.16; found 413.10 [M+H]⁺.
13
14
15
16
17
18
19
20
21
22
23

24 *Ethyl 2-(3-chlorophenethyl)-5-methyl-4-(methylamino)thieno[2,3-d]pyrimidine-6-carboxylate*

25
26 **10(v,a)**

27
28 Isolated 122 mg (47% yield) as a pale yellow oil. ¹H NMR (300 MHz, CDCl₃) δ 7.26 (m, 1H),
29 7.15 – 7.08 (m, 3H), 5.65 (br. m, NH), 4.32 (q, *J* = 7.1 Hz, 2H), 3.13 – 3.08 (m, 7H), 2.87 (s, 3H),
30 1.36 (t, *J* = 7.1 Hz, 3H). ¹³C NMR (75 MHz, CDCl₃) δ 167.77, 167.51, 163.26, 159.59, 144.15,
31 138.23, 134.13, 129.73, 128.89, 126.89, 126.17, 121.49, 115.43, 61.46, 40.65, 33.94, 28.33,
32 15.91, 14.55. MS (ESI): calcd. 390.104; found 390.20 [M+H]⁺.
33
34
35
36
37
38
39
40
41
42
43
44

45 *Ethyl 5-methyl-4-(methylamino)-2-(3-(trifluoromethyl)phenethyl)thieno[2,3-d]pyrimidine-6-*
46 *carboxylate* **10(w,a)**

47
48 Isolated 128 mg (50% yield) as a pale yellow semi-solid. ¹H NMR (300 MHz, CDCl₃) δ 7.52 (s,
49 1H), 7.37 (m, 3H), 5.66 (br. m, NH), 4.32 (q, *J* = 7.1 Hz, 2H), 3.25 – 3.11 (m, 4H), 3.09 (d, *J* =
50 4.8 Hz, 3H), 2.87 (s, 3H), 1.36 (t, *J* = 7.1 Hz, 3H). ¹³C NMR (75 MHz, CDCl₃) δ 167.77, 167.36,
51 163.25, 159.60, 142.95, 138.20, 132.09, 130.62 (d, *J* = 31.9 Hz), 128.88, 125.52 (d, *J* = 3.8 Hz),
52
53
54
55
56
57
58
59
60

1
2
3 122.87 (d, $J = 3.8$ Hz), 121.55, 115.43, 61.46, 40.61, 34.04, 28.26, 15.88, 14.51. MS (ESI): calcd.
4
5 424.131; found 424.27 [M+H]⁺.
6
7

8
9
10 *Ethyl 2-(2-(benzo[d][1,3]dioxol-5-yl)ethyl)-5-methyl-4-(methylamino)thieno[2,3-d]pyrimidine-6-*
11
12 *carboxylate 10(z,a)*
13

14 Isolated 62 mg (41% yield) as a pale yellow solid. ¹H NMR (500 MHz, DMSO) δ 7.08 (m, NH),
15 6.81 (s, 1H), 6.76 (dd, $J = 7.9, 2.0$ Hz, 1H), 6.67 (d, $J = 7.9$ Hz, 1H), 5.92 (s, 2H), 4.27 (q, $J = 7.1$
16 Hz, 2H), 3.33 (s, 3H), 3.02 – 2.93 (m, 7H), 2.86 (s, 3H), 1.28 (t, $J = 7.1$ Hz, 3H). ¹³C NMR (126
17 MHz, DMSO) δ 168.23, 167.95, 163.50, 159.82, 148.24, 146.36, 141.08, 136.55, 122.20, 120.06,
18 115.93, 109.95, 109.16, 101.71, 62.16, 41.56, 34.09, 29.27, 16.73, 15.33. MS (ESI): calcd.
19 400.13; found 400.40 [M+H]⁺.
20
21
22
23
24
25
26
27
28
29

30
31 *Dimethyl thiophene-2,5-dicarboxylate (13)*
32

33 An ice-cooled pressure vessel was charged with thiophene-2,5-carboxylic acid (2.5 g, 14.5 mmol)
34 and 50 mL anhydrous MeOH; thionyl chloride (4.2 mL, 58 mmol) was added dropwise via
35 syringe and once gas evolution had ceased the vessel was tightly sealed with a Teflon screw cap.
36 The reaction was stirred 1h at RT and 3h at 60°C. The reaction mixture was cooled to RT and
37 stirred open to air for 1h. The crude reaction mixture was diluted with 100 mL DCM, stirred for
38 1h and decanted. The residue was collected by filtration and washed with DCM to obtain the
39 desired product as a whit powder, 2.9 g (99% yield). ¹H NMR (300 MHz, DMSO) δ 7.81 (s, 2H),
40 3.85 (s, 6H). ¹³C NMR (126 MHz, DMSO) δ 162.40, 139.25, 134.94, 53.99.
41
42
43
44
45
46
47
48
49
50
51
52
53
54

55 *Dimethyl 3-aminothiophene-2,5-dicarboxylate (14)*
56
57
58
59
60

1
2
3 An ice-cooled round-bottom flask was charged with **12** (1.0 g, 5.0 mmol), followed by 5 mL
4
5 sulfuric acid. Nitric acid (0.50 mL, 6.2 mmol) was added slowly dropwise via syringe and the
6
7 reaction was stirred at RT for 1 h. The crude reaction mixture was carefully poured on ice-water
8
9 and stirred for 1h. The suspension was filtered, washed with water and dried on high vacuum to
10
11 furnish dimethyl 3-nitrothiophene-2,5-dicarboxylate as a white solid, 1.1 g (93% yield). ¹H NMR
12
13 (500 MHz, DMSO) δ 8.22 (s, 1H), 3.88 (s, 6H). ¹³C NMR (126 MHz, DMSO) δ 161.14, 159.81,
14
15 148.22, 136.58, 133.46, 129.26, 55.05, 54.53.
16
17

18
19 A round-bottom flask was charged with dimethyl 3-nitrothiophene-2,5-dicarboxylate (1.0 g, 4.1
20
21 mmol), suspended in MeOH/THF 2:1 and purged with nitrogen. Pearlman's catalyst was added
22
23 (286 mg, 2.0 mmol, 20% Pd(OH)₂/C, CAS 12135-22-7), and the reaction mixture was purged
24
25 with H₂ gas and equipped with an H₂-filled balloon. The reaction was stirred at RT until complete
26
27 consumption of starting material, as determined by TLC. The reaction mixture was purged with
28
29 nitrogen and filtered through a plug of Celite, rinsing with EtOAc. The filtrate was concentrated
30
31 *in vacuo* and the obtained material was used as such without further purification. Isolated 900 mg
32
33 (100% yield) as a yellow powder. ¹H NMR (500 MHz, DMSO) δ 7.22 (s, 1H), 6.62 (s, NH₂), 3.80
34
35 (s, 3H), 3.74 (s, 3H). ¹³C NMR (126 MHz, DMSO) δ 164.82, 162.69, 155.01, 136.68, 126.34,
36
37 103.33, 53.84, 52.61.
38
39
40
41
42
43
44

45 Thienopyrimidinone formation, amine coupling and ester saponification performed as described
46
47 in the general procedures.
48

49 *Methyl 4-(methylamino)-2-phenethylthieno[3,2-d]pyrimidine-6-carboxylate* **16(d,a)**

50
51 Isolated 106 mg (51% yield) as a white solid. ¹H NMR (500 MHz, DMSO) δ 7.98 (m, NH), 7.84
52
53 (s, 1H), 7.22 (m, 4H), 7.12 (m, 1H), 3.87 (s, 3H), 3.13 – 3.04 (m, 4H), 2.98 (d, *J* = 4.5 Hz, 3H).
54
55 ¹³C NMR (126 MHz, DMSO) δ 167.61, 163.19, 159.25, 158.42, 142.92, 137.95, 130.96, 129.43,
56
57
58
59
60

1
2
3 129.35, 126.84, 117.58, 54.06, 34.81, 26.99, 26.93. MS (ESI): calcd. 328.11; found 328.27
4
5 [M+H]⁺.
6
7
8

9
10 *Methyl 2-(3-methoxyphenethyl)-4-(methylamino)thieno[3,2-d]pyrimidine-6-carboxylate* **16(h,a)**

11
12 Isolated 100 mg (64% yield) as a pale yellow oil. MS (ESI): calcd. 358.123; found 358.27

13
14 [M+H]⁺
15
16
17

18
19 *General procedure for the saponification of esters:*

20
21 To solution of ester (1 equivalent) in 2:1 THF/MeOH was added 1 M NaOH (3 equivalents) and
22
23 water to bring the final solvent ratio to 2:1:1 THF/MeOH/H₂O. In cases where the starting
24
25 material was not fully dissolved, the solution was heated to 50 °C as necessary. The reaction was
26
27 stirred at RT until complete consumption of starting material as determined by TLC. The reaction
28
29 mixture was acidified to pH~3 with 1 M HCl and concentrated *in vacuo*. The resultant slurry was
30
31 diluted with 5 mL water, filtered and washed successively with deionized water, and purification
32
33 grade pentane. The obtained residue was dried on high vacuum to furnish the desired free
34
35
36
37
38
39
40
41
42
43
44
45
46
47
48
49
50
51
52
53
54
55
56
57
58
59
60

43 *5-Methyl-4-(methylamino)-2-phenethylthieno[2,3-d]pyrimidine-6-carboxylic acid* (**17**)

44
45 Isolated 32 mg (87% yield) as a white powder. ¹H NMR (500 MHz, DMSO) δ 7.27 – 7.23 (m,
46
47 4H), 7.16 (m, 1H), 7.07 (br. d, *J* = 4.4 Hz, NH), 3.10 – 3.06 (m, 2H), 3.02 – 2.98 (m, 5H), 2.87 (s,
48
49 3H). ¹³C NMR (126 MHz, DMSO) δ 166.82, 166.58, 164.06, 158.71, 141.62, 138.94, 128.33,
50
51 128.26, 125.79, 120.64, 115.00, 40.18, 33.32, 28.11, 15.44. HRMS (ESI): calcd. 328.11197 for
52
53 C₁₇H₁₈N₃O₂S; found 328.1112 [M+H]⁺.
54
55
56
57
58
59
60

1
2
3 *4-((2-Aminoethyl)amino)-5-methyl-2-phenethylthieno[2,3-d]pyrimidine-6-carboxylic acid (18)*

4
5 Isolated 15 mg (35% yield) as a white powder. ¹H NMR (500 MHz, DMSO) δ 7.28 – 7.14 (m,
6 4H), 7.04 (br. s, NH), 3.51 (m, 2H), 3.28 (m, 2H), 3.12 – 3.03 (m, 2H), 3.06 – 2.93 (m, 5H), 2.58
7 (s, 3H). ¹³C NMR (126 MHz, DMSO) δ 166.91, 166.32, 163.82, 158.03, 142.57, 139.42, 128.65,
8 128.97, 126.02, 120.41, 114.63, 47.69, 41.31, 33.89, 25.16, 16.46.

9
10 HRMS (ESI): calcd. 357.13852 for C₁₈H₂₁N₄O₂S; found 357.1389 [M+H]⁺.
11
12
13

14
15
16
17
18
19 *4-(Benzylamino)-5-methyl-2-phenethylthieno[2,3-d]pyrimidine-6-carboxylic acid (19)*

20
21 Isolated 40 mg (86% yield) as a white crystalline material. ¹H NMR (500 MHz, DMSO) δ 7.96
22 (br. s, NH), 7.41 (d, *J* = 7.1 Hz, 2H), 7.32 (t, *J* = 7.6 Hz, 2H), 7.25 – 7.21 (m, 1H), 7.19 (d, *J* = 7.5
23 Hz, 2H), 7.15 – 7.08 (m, 3H), 4.79 (d, *J* = 5.8 Hz, 2H), 2.96 (m, 4H), 2.95 (s, 3H). ¹³C NMR (126
24 MHz, DMSO) δ 164.72, 163.63, 157.97, 140.85, 139.07, 138.84, 128.29, 128.29, 128.25, 127.47,
25 126.84, 125.94, 122.31, 115.31, 44.39, 38.54, 32.66, 15.43. HRMS (ESI): calcd. 404.14327 for
26 C₂₃H₂₂N₃O₂S; found 404.1432 [M+H]⁺.
27
28
29
30
31
32
33
34
35
36
37

38 *5-Methyl-2-phenethyl-4-(phenethylamino)thieno[2,3-d]pyrimidine-6-carboxylic acid (20)*

39
40 Isolated 28 mg (60% yield) as a white crystalline material. ¹H NMR (500 MHz, DMSO) δ 7.34 –
41 7.19 (m, 9H), 7.17 – 7.13 (m, 1H), 7.11 (br. t, *J* = 5.7 Hz, NH), 3.74 (dd, *J* = 14.6, 6.0 Hz, 2H),
42 3.11 (dd, *J* = 8.5, 6.3 Hz, 2H), 3.03 (dd, *J* = 8.5, 6.2 Hz, 2H), 2.95 – 2.89 (m, 2H), 2.81 (s, 3H).
43
44
45
46
47 ¹³C NMR (126 MHz, DMSO) δ 166.79, 164.03, 158.14, 141.56, 139.58, 138.76, 128.73, 128.45,
48 128.30, 128.28, 126.19, 125.83, 120.89, 114.87, 42.33, 40.13, 34.66, 33.37, 15.33. HRMS (ESI):
49 calcd. 418.15892 for C₂₄H₂₄N₃O₂S; found 418.1557 [M+H]⁺.
50
51
52
53
54
55
56
57
58
59
60

1
2
3 *4-((4-Methoxyphenethyl)amino)-5-methyl-2-phenethylthieno[2,3-d]pyrimidine-6-carboxylic acid*
4
5 **(21)**

6
7 Isolated 36 mg (55% yield) as an off white powder. ¹H NMR (500 MHz, DMSO) δ 7.52 (m, NH),
8 7.27 – 7.22 (m, 4H), 7.15 (m, *J* = 7.5 Hz, 3H), 6.86 (d, *J* = 8.7 Hz, 2H), 3.72 (dd, *J* = 14.3, 6.4
9 Hz, 2H), 3.70 (s, 3H), 3.13 – 3.09 (m, 2H), 3.06 (m, 2H), 2.87 – 2.82 (m, 2H), 2.82 (s, 3H). ¹³C
10 NMR (126 MHz, DMSO) δ 164.45, 158.96, 158.84, 141.58, 139.77, 131.93, 130.86, 129.57,
11 129.40, 127.30, 116.56, 115.02, 56.16, 44.42, 34.63, 33.54, 16.15. HRMS (ESI): calcd. 448.16949
12 for C₂₅H₂₆N₃O₃S; found 448.1695 [M+H]⁺.
13
14
15
16
17
18
19
20
21
22
23

24 *4-((3-Methoxyphenethyl)amino)-5-methyl-2-phenethylthieno[2,3-d]pyrimidine-6-carboxylic acid*
25
26 **(22)**

27
28 Isolated 45 mg (68% yield) as an off white powder. ¹H NMR (500 MHz, DMSO) δ 7.31 (m, NH),
29 7.25 – 7.19 (m, 5H), 7.16 – 7.12 (m, 1H), 6.81 (m, 2H), 6.77 (m, 1H), 3.75 (dd, *J* = 14.0, 6.4 Hz,
30 2H), 3.69 (s, 3H), 3.13 – 3.08 (m, 2H), 3.06 – 3.01 (m, 2H), 2.88 (t, *J* = 7.4 Hz, 2H), 2.81 (s, 3H).
31 ¹³C NMR (126 MHz, DMSO) δ 164.79, 160.49, 159.06, 142.11, 141.96, 139.82, 130.61, 129.49,
32 129.39, 127.13, 122.13, 116.29, 115.49, 112.80, 56.01, 43.78, 35.68, 34.00, 16.28. HRMS (ESI):
33 calcd. 448.16949 for C₂₅H₂₆N₃O₃S; found 448.1684 [M+H]⁺.
34
35
36
37
38
39
40
41
42
43
44

45 *4-((2-Methoxyphenethyl)amino)-5-methyl-2-phenethylthieno[2,3-d]pyrimidine-6-carboxylic acid*
46
47 **(23)**

48
49 Isolated 28 mg (60% yield) as an off white powder. ¹H NMR (500 MHz, DMSO) δ 7.26 – 7.13
50 (m, 7H, NH), 6.95 (d, *J* = 7.7 Hz, 1H), 6.86 (t, *J* = 7.3 Hz, 1H), 3.73 (m, 5H), 3.10 (m, 2H), 3.01
51 (m, 2H), 2.92 (t, *J* = 7.1 Hz, 2H), 2.81 (s, 3H). ¹³C NMR (126 MHz, DMSO) δ 164.67, 159.08,
52 158.45, 141.93, 139.86, 131.43, 129.53, 129.39, 128.95, 128.07, 127.19, 121.48, 116.36, 111.85,
53
54
55
56
57
58
59
60

1
2
3 56.38, 42.62, 33.72, 30.29, 16.20. HRMS (ESI): calcd. 448.16949 for C₂₅H₂₆N₃O₃S; found
4
5 448.1681 [M+H]⁺.
6
7
8

9
10 *4-((4-Fluorophenethyl)amino)-5-methyl-2-phenethylthieno[2,3-d]pyrimidine-6-carboxylic acid*
11
12 **(24)**
13

14 Isolated 23 mg (35% yield) as an off white powder. ¹H NMR (500 MHz, DMSO) δ 7.28 – 7.20
15 (m, 5H, NH), 7.12 (m, 4H), 3.71 (dd, *J* = 13.8, 6.2 Hz, 2H), 3.11 – 3.06 (m, 2H), 3.03 – 2.98 (m,
16 2H), 2.89 (t, *J* = 7.4 Hz, 2H), 2.80 (s, 3H). ¹³C NMR (126 MHz, DMSO) δ 165.01, 162.00 (d, *J* =
17 241.5 Hz), 159.18, 142.45, 139.87, 136.73 (d, *J* = 3.0 Hz), 131.63 (d, *J* = 7.9 Hz), 129.44, 129.40,
18 127.01, 116.24 (d, *J* = 21.0 Hz), 116.08, 43.52, 34.82, 34.30, 16.41. HRMS (ESI): calcd.
19 436.14950 for C₂₄H₂₃FN₃O₂S; found 436.1473 [M+H]⁺.
20
21
22
23
24
25
26
27
28
29
30

31 *4-((3-Fluorophenethyl)amino)-5-methyl-2-phenethylthieno[2,3-d]pyrimidine-6-carboxylic acid*
32
33 **(25)**
34
35

36 Isolated 30 mg (46% yield) as an off white powder. ¹H NMR (500 MHz, DMSO) δ 7.41 (m, NH),
37 7.32 (dd, *J* = 14.4, 7.8 Hz, 1H), 7.26 – 7.21 (m, 4H), 7.16 – 7.12 (m, 1H), 7.07 (m, 2H), 7.02 (td,
38 *J* = 8.8, 2.5 Hz, 1H), 3.77 (dd, *J* = 13.9, 6.3 Hz, 2H), 3.12 – 3.07 (m, 2H), 3.06 – 3.02 (m, 2H),
39 2.93 (t, *J* = 7.3 Hz, 2H), 2.81 (s, 3H). ¹³C NMR (126 MHz, DMSO) δ 164.44, 163.37 (d, *J* = 243.2
40 Hz), 158.87, 143.12 (d, *J* = 7.4 Hz), 141.59, 139.72, 131.41 (d, *J* = 8.3 Hz), 129.54, 129.39,
41 127.28, 126.12, 126.10, 124.37, 116.64 (d, *J* = 14.6 Hz), 116.54, 114.25 (d, *J* = 20.8 Hz), 43.76,
42 38.43, 35.12, 33.58, 16.14. HRMS (ESI): calcd. 436.14950 for C₂₄H₂₃FN₃O₂S; found 436.1479
43
44
45
46
47
48
49
50
51 [M+H]⁺.
52
53
54
55
56
57
58
59
60

1
2
3 4-((2-Fluorophenethyl)amino)-5-methyl-2-phenethylthieno[2,3-d]pyrimidine-6-carboxylic acid
4
5 (26)
6

7 Isolated 21 mg (32% yield) as an off white powder. ^1H NMR (500 MHz, DMSO) δ 7.32 – 7.19
8 (m, 6H, NH), 7.12 (m, 3H), 3.76 (dd, $J = 13.8, 6.7$ Hz, 2H), 3.08 (m, 2H), 3.02 – 2.93 (m, 4H),
9
10 (m, 6H, NH), 7.12 (m, 3H), 3.76 (dd, $J = 13.8, 6.7$ Hz, 2H), 3.08 (m, 2H), 3.02 – 2.93 (m, 4H),
11
12 2.81 (s, 3H). ^{13}C NMR (126 MHz, DMSO) δ 164.90, 161.97 (d, $J = 243.3$ Hz), 159.18, 142.33,
13
14 139.88, 132.52 (d, $J = 5.0$ Hz), 129.59, 129.53, 129.47, 129.39, 127.10 (d, $J = 16.1$ Hz), 127.06,
15
16 125.55 (d, $J = 3.3$ Hz), 116.32 (d, $J = 21.8$ Hz), 116.16, 42.24, 34.08, 29.25, 16.34. HRMS (ESI):
17
18 calcd. 436.14950 for $\text{C}_{24}\text{H}_{23}\text{FN}_3\text{O}_2\text{S}$; found 436.1476 $[\text{M}+\text{H}]^+$.
19
20
21
22
23

24 *5-Methyl-4-((4-methylphenethyl)amino)-2-phenethylthieno[2,3-d]pyrimidine-6-carboxylic acid*
25
26 (27)
27

28 Isolated 48 mg (73% yield) as an off white powder. ^1H NMR (500 MHz, DMSO) δ 7.33 (m, NH),
29
30 7.26 – 7.21 (m, 4H), 7.16 – 7.09 (m, 5H), 3.72 (dd, $J = 14.4, 6.2$ Hz, 2H), 3.12 – 3.08 (m, 2H),
31
32 3.06 – 3.02 (m, 2H), 2.88 – 2.83 (m, 2H), 2.81 (s, 3H), 2.25 (s, 3H). ^{13}C NMR (126 MHz, DMSO)
33
34 δ 164.64, 158.94, 141.90, 139.78, 137.16, 136.36, 130.15, 129.73, 129.52, 129.38, 127.19,
35
36 116.37, 44.09, 35.17, 33.81, 21.80, 16.25. HRMS (ESI): calcd. 432.17457 for $\text{C}_{25}\text{H}_{26}\text{N}_3\text{O}_2\text{S}$;
37
38 found 432.1719 $[\text{M}+\text{H}]^+$.
39
40
41
42
43
44

45 *5-Methyl-4-((3-methylphenethyl)amino)-2-phenethylthieno[2,3-d]pyrimidine-6-carboxylic acid*
46
47 (28)
48

49 Isolated 42 mg (64% yield) as an off white powder. ^1H NMR (500 MHz, DMSO) δ 7.45 (m, NH),
50
51 7.25 – 7.22 (m, 4H), 7.20 – 7.13 (m, 2H), 7.07 (s, 1H), 7.02 (m, 2H), 3.74 (dd, $J = 14.6, 6.1$ Hz,
52
53 2H), 3.12 (m, 2H), 3.06 (m, 2H), 2.89 – 2.84 (m, 2H), 2.81 (s, 3H), 2.25 (s, 3H). ^{13}C NMR (126
54
55 MHz, DMSO) δ 164.43, 158.82, 141.57, 140.02, 139.73, 138.61, 130.58, 129.56, 129.50, 129.38,
56
57
58
59
60

1
2
3 128.09, 127.30, 126.94, 116.59, 44.26, 38.35, 35.44, 33.55, 22.15, 16.12. HRMS (ESI): calcd.
4
5 432.17457 for C₂₅H₂₆N₃O₂S; found 432.1728 [M+H]⁺.
6
7

8
9
10 *5-Methyl-4-((2-methylphenethyl)amino)-2-phenethylthieno[2,3-d]pyrimidine-6-carboxylic acid*
11
12 **(29)**

13
14 Isolated 55 mg (84% yield) as an off white powder. ¹H NMR (500 MHz, DMSO) δ 7.42 (m, NH),
15
16 7.27 – 7.21 (m, 4H), 7.17 – 7.12 (m, 3H), 7.12 – 7.08 (m, 2H), 3.68 (dd, *J* = 15.5, 5.8 Hz, 2H),
17
18 3.11 – 3.06 (m, 2H), 3.04 – 2.99 (m, 2H), 2.93 – 2.88 (m, 2H), 2.85 (s, 3H), 2.40 (s, 3H). ¹³C
19
20 NMR (126 MHz, DMSO) δ 164.75, 159.07, 142.05, 139.79, 138.43, 137.20, 131.24, 130.55,
21
22 129.52, 129.33, 127.51, 127.16, 127.08, 116.25, 42.76, 34.25, 33.47, 20.10, 16.39. HRMS (ESI):
23
24 calcd. 432.17457 for C₂₅H₂₆N₃O₂S; found 432.1746 [M+H]⁺.
25
26
27
28
29

30
31 *5-Methyl-2-phenethyl-4-((2-(pyridin-4-yl)ethyl)amino)thieno[2,3-d]pyrimidine-6-carboxylic acid*
32
33 **(30)**

34
35 Isolated 42 mg (64% yield) as a white powder. ¹H NMR (500 MHz, DMSO) δ 8.47 (d, *J* = 5.8 Hz,
36
37 2H), 7.28 (d, *J* = 5.7 Hz, 2H), 7.25 – 7.20 (m, 4H), 7.13 (m, NH, 1H), 3.77 (dd, *J* = 13.4, 6.6 Hz,
38
39 2H), 3.09 – 3.05 (m, 2H), 3.00 (m, 2H), 2.93 (t, *J* = 7.2 Hz, 2H), 2.80 (s, 3H). ¹³C NMR (126
40
41 MHz, DMSO) δ 168.00, 167.89, 165.14, 159.23, 150.30, 142.65, 139.84, 129.42, 129.41, 126.95,
42
43 125.59, 122.11, 116.00, 42.20, 41.19, 35.03, 34.47, 16.48. HRMS (ESI): calcd. 419.15417 for
44
45 C₂₃H₂₃N₄O₂S; found 419.1537 [M+H]⁺.
46
47
48
49
50

51
52 *5-Methyl-2-phenethyl-4-((2-(pyridin-3-yl)ethyl)amino)thieno[2,3-d]pyrimidine-6-carboxylic acid*
53
54 **(31)**
55
56
57
58
59
60

1
2
3 Isolated 41 mg (87% yield) as a white powder. ^1H NMR (500 MHz, DMSO) δ 8.45 (s, 1H), 8.40
4 (d, $J = 4.7$ Hz, 1H), 7.63 (d, $J = 7.8$ Hz, 1H), 7.30 (dd, $J = 7.7, 4.8$ Hz, 1H), 7.25 – 7.20 (m, 4H),
5
6 (d, $J = 4.7$ Hz, 1H), 7.63 (d, $J = 7.8$ Hz, 1H), 7.30 (dd, $J = 7.7, 4.8$ Hz, 1H), 7.25 – 7.20 (m, 4H),
7
8 7.13 (m, 1H, NH), 3.75 (dd, $J = 13.3, 6.7$ Hz, 2H), 3.07 (dd, $J = 8.4, 6.1$ Hz, 2H), 2.99 (dd, $J =$
9
10 8.5, 6.3 Hz, 2H), 2.92 (t, $J = 7.2$ Hz, 2H), 2.80 (s, 3H). ^{13}C NMR (126 MHz, DMSO) δ 168.00,
11
12 167.89, 165.15, 159.25, 151.01, 148.56, 142.67, 139.82, 137.49, 136.22, 129.41, 126.94, 124.63,
13
14 122.11, 115.97, 42.86, 41.23, 34.49, 32.89, 16.47. HRMS (ESI): calcd. 419.15417 for
15
16 $\text{C}_{23}\text{H}_{23}\text{N}_4\text{O}_2\text{S}$; found 419.1537 $[\text{M}+\text{H}]^+$.
17
18
19
20

21
22 *5-Methyl-2-phenethyl-4-((2-(pyridin-2-yl)ethyl)amino)thieno[2,3-d]pyrimidine-6-carboxylic acid*
23
24 **(32)**
25

26 Isolated 57 mg (87% yield) as an off white solid. ^1H NMR (500 MHz, DMSO) δ 8.56 (d, $J = 4.9$
27
28 Hz, 1H), 7.83 (m, NH), 7.41 – 7.32 (m, 3H), 7.24 – 7.21 (m, 4H), 7.15 – 7.11 (m, 1H), 3.89 (dd, J
29
30 = 12.4, 6.6 Hz, 2H), 3.12 (t, $J = 6.7$ Hz, 2H), 3.05 (m, 2H), 2.96 (m, 2H), 2.84 (s, 3H). ^{13}C NMR
31
32 (126 MHz, DMSO) δ 167.80, 165.14, 159.92, 159.17, 148.62, 142.70, 139.82, 139.46, 129.42,
33
34 129.38, 126.90, 125.32, 123.35, 122.12, 115.99, 41.44, 41.17, 36.77, 34.40, 16.42. MS (ESI):
35
36 calcd. 419.15417 for $\text{C}_{23}\text{H}_{23}\text{N}_4\text{O}_2\text{S}$; found 419.1545 $[\text{M}+\text{H}]^+$
37
38
39
40
41

42
43 *2-(4-Acetamidophenethyl)-5-methyl-4-(methylamino)thieno[2,3-d]pyrimidine-6-carboxylic acid*
44
45 **(33)**
46

47 Isolated 27 mg (72% yield) as an off white powder. ^1H NMR (500 MHz, DMSO) δ 9.85 (s,
48
49 NHAc), 7.46 (m, NH), 7.44 (d, $J = 8.3$ Hz, 2H), 7.15 (d, $J = 8.3$ Hz, 2H), 3.03 (m, 7H), 2.87 (s,
50
51 3H), 1.99 (s, 3H). ^{13}C NMR (126 MHz, DMSO) δ 169.25, 164.47, 159.15, 139.96, 138.66,
52
53 136.03, 129.62, 124.20, 120.16, 116.72, 38.55, 33.04, 30.12, 25.10, 16.22. HRMS (ESI): calcd.
54
55 385.13344 for $\text{C}_{19}\text{H}_{21}\text{N}_4\text{O}_3\text{S}$; found 385.1336 $[\text{M}+\text{H}]^+$.
56
57
58
59
60

1
2
3
4
5 *2-(3-Acetamidophenethyl)-5-methyl-4-(methylamino)thieno[2,3-d]pyrimidine-6-carboxylic acid*

6
7
8 **(34)**

9
10 Isolated 23 mg (62% yield) as a white powder. ¹H NMR (500 MHz, DMSO) δ 9.84 (s, NHAc),
11 7.47 (s, 1H), 7.37 (d, *J* = 8.3 Hz, 1H), 7.15 (t, *J* = 7.8 Hz, 1H), 7.08 (m, NH), 6.90 (d, *J* = 7.9 Hz,
12 1H), 3.05 – 2.94 (m, 7H), 2.86 (s, 3H), 2.00 (s, 3H). ¹³C NMR (126 MHz, DMSO) δ 169.33,
13 167.60, 165.14, 159.80, 143.12, 140.46, 140.07, 129.69, 124.16, 121.93, 120.00, 117.75, 116.19,
14 34.57, 29.33, 25.18, 16.55. HRMS (ESI): calcd. 385.13344 for C₁₉H₂₁N₄O₃S; found 385.1333
15
16
17
18
19
20
21 [M+H]⁺.
22
23
24
25

26 *2-(2-Acetamidophenethyl)-5-methyl-4-(methylamino)thieno[2,3-d]pyrimidine-6-carboxylic acid*

27
28
29 **(35)**

30
31 Isolated 13 mg (46% yield) as an off white powder. ¹H NMR (500 MHz, DMSO) δ 9.40 (s,
32 NHAc), 7.32 (d, *J* = 7.8 Hz, 1H), 7.25 (d, *J* = 7.6 Hz, 1H), 7.14 (m, NH), 7.08 (m, 2H), 3.08 –
33 3.02 (m, 2H), 2.98 (d, *J* = 4.4 Hz, 3H), 2.96 – 2.91 (m, 2H), 2.86 (s, 3H), 2.04 (s, 3H). ¹³C NMR
34 3.02 (m, 2H), 2.98 (d, *J* = 4.4 Hz, 3H), 2.96 – 2.91 (m, 2H), 2.86 (s, 3H), 2.04 (s, 3H). ¹³C NMR
35 (126 MHz, DMSO) δ 169.54, 168.12, 165.17, 159.83, 140.10, 137.22, 136.98, 130.26, 127.28,
36 126.57, 121.82, 116.18, 30.04, 29.25, 24.42, 16.58. HRMS (ESI): calcd. 385.13344 for
37 C₁₉H₂₁N₄O₃S; found 385.1331 [M+H]⁺.
38
39
40
41
42
43
44
45
46

47 *4-((2,3-Dihydro-1H-inden-2-yl)amino)-5-methyl-2-phenethylthieno[2,3-d]pyrimidine-6-*
48
49 *carboxylic acid (36)*

50
51 Isolated 47 mg (72% yield) as an off white powder. ¹H NMR (500 MHz, DMSO) δ 7.25 – 7.19
52 (m, 5H, NH), 7.17 – 7.12 (m, 3H), 6.91 (d, *J* = 7.0 Hz, 1H), 5.07 – 4.98 (m, 1H), 3.36 – 3.28 (m,
53 2H), 3.09 – 3.04 (m, 3H), 3.01 (m, 3H), 2.87 (s, 3H). ¹³C NMR (126 MHz, DMSO) δ 168.05,
54
55
56
57
58
59
60

1
2
3 167.84, 165.15, 159.46, 142.65, 142.33, 140.06, 129.41, 129.37, 127.58, 126.91, 125.53, 122.21,
4
5 116.24, 53.03, 41.21, 39.86, 34.49, 16.39. HRMS (ESI): calcd. 430.15892 for C₂₅H₂₄N₃O₂S;
6
7 found 430.1562 [M+H]⁺.
8
9

10
11
12 *4-((3,5-Dimethoxyphenethyl)amino)-5-methyl-2-phenethylthieno[2,3-d]pyrimidine-6-carboxylic*
13
14 *acid (37)*
15

16
17 Isolated 31 mg (82% yield) as an off white powder. ¹H NMR (500 MHz, DMSO) δ 7.24 – 7.22
18
19 (m, 4H), 7.16 – 7.09 (m, 1H, NH), 6.41 (d, *J* = 2.2 Hz, 2H), 6.33 (t, *J* = 2.2 Hz, 1H), 3.73 (dd, *J* =
20
21 14.5, 6.4 Hz, 2H), 3.67 (s, 6H), 3.10 (m, 2H), 3.01 (m, 2H), 2.87 – 2.82 (m, 2H), 2.81 (s, 3H). ¹³C
22
23 NMR (126 MHz, DMSO) δ 165.08, 161.61, 159.21, 142.94, 142.57, 139.84, 129.42, 129.38,
24
25 126.99, 116.05, 107.83, 99.15, 56.13, 43.42, 36.02, 34.40, 16.41. MS (ESI): calcd. 478.18005 for
26
27 C₂₆H₂₈N₃O₄S; found 478.1782 [M+H]⁺.
28
29
30
31
32

33
34 *4-((2-(Benzo[d][1,3]dioxol-5-yl)ethyl)amino)-5-methyl-2-phenethylthieno[2,3-d]pyrimidine-6-*
35
36 *carboxylic acid (38)*
37

38
39 Isolated 22 mg (47% yield) as a white solid. ¹H NMR (500 MHz, DMSO) δ 7.27 – 7.18 (m, 5H,
40
41 NH), 7.16 – 7.12 (m, 1H), 6.82 (m, 2H), 6.68 (dd, *J* = 7.9, 1.6 Hz, 1H), 5.95 (s, 2H), 3.70 (dd, *J* =
42
43 14.0, 6.0 Hz, 1H), 3.13 – 3.06 (m, 2H), 3.02 (m, 2H), 2.85 – 2.78 (m, 5H). ¹³C NMR (126 MHz,
44
45 DMSO) δ 164.83, 159.07, 148.43, 146.76, 142.18, 139.85, 134.16, 129.49, 129.40, 127.12,
46
47 122.76, 116.24, 110.19, 109.33, 101.86, 43.92, 35.33, 34.07, 16.31. HRMS (ESI): calcd.
48
49 462.14875 for C₂₅H₂₄N₃O₄S; found 462.1486 [M+H]⁺.
50
51
52

53
54
55 *5-Methyl-4-(methylamino)-2-(3-phenylpropyl)thieno[2,3-d]pyrimidine-6-carboxylic acid (39)*
56
57
58
59
60

1
2
3 Isolated 36 mg (78% yield) as a white powder. ^1H NMR (500 MHz, DMSO) δ 7.25 (m, 2H), 7.19
4 (m, 2H), 7.14 (m, 1H, NH), 2.97 (d, $J = 4.4$ Hz, 3H), 2.84 (s, 3H), 2.69 (t, $J = 7.5$ Hz, 2H), 2.62
5 (t, $J = 7.6$ Hz, 2H), 2.05 – 1.97 (m, 2H). ^{13}C NMR (126 MHz, DMSO) δ 168.13, 165.10, 159.76,
6 143.09, 140.03, 129.53, 129.38, 126.84, 121.96, 116.11, 38.83, 35.90, 30.49, 29.34, 16.50. MS
7 (ESI): calcd 342.12762 for $\text{C}_{18}\text{H}_{20}\text{N}_3\text{O}_2\text{S}$; found 342.1256 $[\text{M}+\text{H}]^+$.
8
9
10
11
12
13
14
15
16

17 *5-Methyl-4-(methylamino)-2-(4-phenylbutyl)thieno[2,3-d]pyrimidine-6-carboxylic acid (40)*

18
19 Isolated 60 mg (86% yield) as white powder. ^1H NMR (500 MHz, DMSO) δ 7.23 (t, $J = 7.5$ Hz,
20 2H), 7.13 (m, 3H), 7.03 (br. m, NH), 2.94 (d, $J = 4.4$ Hz, 3H), 2.84 (s, 3H), 2.69 (t, $J = 7.5$ Hz,
21 2H), 2.58 (t, $J = 7.6$ Hz, 2H), 1.76 – 1.68 (m, 2H), 1.63 – 1.55 (m, 2H). ^{13}C NMR (126 MHz,
22 DMSO) δ 168.72, 167.39, 165.17, 159.83, 143.33, 140.06, 129.42, 129.34, 126.74, 121.71,
23 116.03, 39.49, 36.12, 31.86, 29.21, 28.41, 16.53. HRMS (ESI): calcd 356.14327 for
24 $\text{C}_{19}\text{H}_{22}\text{N}_3\text{O}_2\text{S}$; found 356.1413 $[\text{M}+\text{H}]^+$.
25
26
27
28
29
30
31
32
33
34
35

36 *2-(3-Methoxyphenethyl)-5-methyl-4-(methylamino)thieno[2,3-d]pyrimidine-6-carboxylic acid (41)*

37
38 Isolated 66 mg (71% yield) as a white powder. ^1H NMR (500 MHz, DMSO) δ 7.12 (t, $J = 8.0$ Hz,
39 1H), 7.01 (m, NH), 6.77 (m, 2H), 6.68 (dd, $J = 9.0, 1.6$ Hz, 1H), 3.05 – 2.93 (m, 7H), 2.82 (s,
40 3H). OCH_3 signal obscured by water peak. ^{13}C NMR (126 MHz, DMSO) δ 167.90, 167.48,
41 165.15, 160.29, 159.80, 144.29, 140.03, 130.39, 121.82, 121.70, 116.09, 115.03, 112.39, 55.95,
42 41.03, 34.37, 29.19, 16.48. MS (ESI): calc. 358.12254 for $\text{C}_{18}\text{H}_{20}\text{N}_3\text{O}_3\text{S}$; found 358.1208 $[\text{M}+\text{H}]^+$.
43
44
45
46
47
48
49
50
51

52 *2-(3-Fluorophenethyl)-5-methyl-4-(methylamino)thieno[2,3-d]pyrimidine-6-carboxylic acid (42)*

53
54 Isolated 77 mg (83% yield) as a white powder. ^1H NMR (500 MHz, DMSO) δ 7.24 (m, 1H), 7.02
55 (m, 2H, NH), 6.93 (m, 1H), 3.06 (t, $J = 7.5$ Hz, 2H), 3.00 – 2.95 (m, 2H), 2.94 (d, $J = 4.5$ Hz,
56
57
58
59
60

1
2
3 3H), 2.81 (s, 3H). ^{13}C NMR (126 MHz, DMSO) δ 167.64, 167.50, 165.14, 163.28 (d, $J = 242.8$
4 Hz), 159.77, 145.69 (d, $J = 7.3$ Hz), 140.01, 131.16 (d, $J = 8.4$ Hz), 125.58 (d, $J = 2.6$ Hz),
5
6 121.85, 116.12 (d, $J = 20.7$ Hz), 116.09, 113.65 (d, $J = 20.9$ Hz), 40.65, 33.89, 29.17, 16.47.
7
8 HRMS (ESI): calcd. 346.10255 for $\text{C}_{17}\text{H}_{17}\text{FN}_3\text{O}_2\text{S}$; found 346.1006 $[\text{M}+\text{H}]^+$.
9
10
11

12
13
14 *5-Methyl-4-(methylamino)-2-(2-(pyridin-2-yl)ethyl)thieno[2,3-d]pyrimidine-6-carboxylic acid*

15
16
17 **(43)**

18
19 Isolated 46 mg (84% yield) as a white powder. ^1H NMR (300 MHz, DMSO) δ 8.75 (d, $J = 4.9$ Hz,
20 1H), 8.41 (td, $J = 7.9, 1.5$ Hz, 1H), 7.95 (d, $J = 8.0$ Hz, 1H), 7.82 (t, $J = 6.3$ Hz, 1H), 7.17 (br. m,
21 NH), 3.47 (t, $J = 7.1$ Hz, 2H), 3.27 (t, $J = 7.1$ Hz, 2H), 2.80 (m, 6H). ^{13}C NMR (75 MHz, DMSO)
22
23 δ 165.80, 165.33, 164.51, 159.13, 157.64, 146.10, 142.19, 139.47, 127.38, 125.11, 121.94,
24
25 115.76, 36.57, 31.33, 28.73, 15.89. HRMS (ESI): calcd. 329.10722 for $\text{C}_{16}\text{H}_{17}\text{N}_4\text{O}_2\text{S}$; found
26
27 329.1067 $[\text{M}+\text{H}]^+$.
28
29
30
31
32
33

34
35
36 *2-(4-Acetamidophenethyl)-4-((2-aminoethyl)amino)-5-methylthieno[2,3-d]pyrimidine-6-*
37
38 *carboxylic acid (44)*

39
40 Isolated 17 mg (36% yield) as a white powder. ^1H NMR (500 MHz, DMSO) δ 9.84 (s, NHAc),
41
42 8.50 (br. s, NH_2), 7.56 (br. s, NH), 7.44 (d, $J = 8.3$ Hz, 2H), 7.15 (d, $J = 8.4$ Hz, 2H), 3.82 (m,
43
44 2H), 3.15 (m, 2H), 3.03 (s, 3H), 3.00 (d, $J = 7.2$ Hz, 2H), 2.94 (d, $J = 7.8$ Hz, 2H), 2.00 (s, 3H).
45
46 HRMS (ESI): calcd. 414.15999 for $\text{C}_{20}\text{H}_{24}\text{N}_5\text{O}_3\text{S}$; found 414.1591 $[\text{M}+\text{H}]^+$.
47
48
49
50

51
52 *2-(4-Acetamidophenethyl)-5-methyl-4-((2-(pyridin-2-yl)ethyl)amino)thieno[2,3-d]pyrimidine-6-*
53
54 *carboxylic acid (45)*
55
56
57
58
59
60

1
2
3 Isolated 33 mg (64% yield) as a white powder. ^1H NMR (500 MHz, DMSO) δ 9.83 (s, NH), 8.51
4 (d, $J = 4.9$ Hz, 1H), 7.71 (tt, $J = 7.7, 1.9$ Hz, 1H), 7.42 (d, $J = 6.8$ Hz, 2H), 7.36 (br. t, $J = 4.8$ Hz,
5 NH), 7.28 (d, $J = 7.8$ Hz, 1H), 7.25 – 7.20 (m, 1H), 7.13 (d, $J = 6.9$ Hz, 2H), 3.87 (dd, $J = 12.2,$
6 5.5 Hz, 2H), 3.08 (t, $J = 6.5$ Hz, 2H), 3.04 – 2.99 (m, 2H), 2.97 – 2.93 (m, 2H), 2.85 (s, 3H), 1.99
7 (s, 3H). ^{13}C NMR (126 MHz, DMSO) δ 169.20, 167.80, 165.22, 160.73, 159.22, 150.13, 138.30,
8 137.87, 137.25, 129.57, 124.49, 122.79, 120.13, 116.03, 41.56, 41.31, 37.42, 33.89, 25.07, 16.32.
9
10
11
12
13
14
15
16
17 HRMS (ESI): calcd. 476.17564 for $\text{C}_{25}\text{H}_{26}\text{N}_5\text{O}_3\text{S}$; found 476.1761 $[\text{M}+\text{H}]^+$
18
19
20
21

22 *2-(3-Chlorophenethyl)-5-methyl-4-(methylamino)thieno[2,3-d]pyrimidine-6-carboxylic acid (46)*
23

24 Isolated 62 mg (67% yield) as a white powder. ^1H NMR (500 MHz, DMSO) δ 7.28 (s, 1H), 7.25 –
25 7.21 (m, 1H), 7.18 – 7.14 (m, 2H), 7.03 (m, NH), 3.07 – 3.02 (m, 2H), 2.97 (m, 2H), 2.94 (d, $J =$
26 4.5 Hz, 3H), 2.81 (s, 3H). ^{13}C NMR (126 MHz, DMSO) δ 167.47, 167.21, 165.11, 159.74, 145.25,
27 140.00, 133.93, 131.16, 129.37, 128.21, 126.90, 121.93, 116.10, 40.51, 33.75, 29.20, 16.46.
28
29
30
31
32
33
34
35
36
37
38
39
40
41
42

43 *5-Methyl-4-(methylamino)-2-(3-(trifluoromethyl)phenethyl)thieno[2,3-d]pyrimidine-6-carboxylic*
44 *acid (47)*
45

46 Isolated 80 mg (86% yield) as a white powder. ^1H NMR (500 MHz, DMSO) δ 7.55 (s, 1H), 7.46
47 (m, 3H), 7.04 (br. m, NH), 3.14 (t, $J = 7.5$ Hz, 2H), 3.02 (t, $J = 7.5$ Hz, 2H), 2.92 (d, $J = 4.4$ Hz,
48 3H), 2.81 (s, 3H). ^{13}C NMR (126 MHz, DMSO) δ 167.36, 167.13, 165.10, 159.73, 144.05,
49 139.97, 133.66, 130.31, 130.16, 129.91, δ 126.06 (q, $J = 3.8$ Hz), 123.66 (q, $J = 3.9$ Hz), 121.96,
50 116.09, 33.79, 29.14, 16.44. HRMS (ESI): calcd. 396.09936 for $\text{C}_{18}\text{H}_{17}\text{F}_3\text{N}_3\text{O}_2\text{S}$; found 396.0975
51
52
53
54
55
56
57
58
59
60

1
2
3 *2-(2-(Benzo[d][1,3]dioxol-5-yl)ethyl)-5-methyl-4-(methylamino)thieno[2,3-d]pyrimidine-6-*
4
5 *carboxylic acid (48)*
6

7 Isolated 25 mg (54% yield) as white solid. ¹H NMR (500 MHz, DMSO) δ 7.13 (br. s, NH), 6.82
8 (s, 1H), 6.77 (d, *J* = 7.9 Hz, 1H), 6.67 (d, *J* = 7.9 Hz, 1H), 5.93 (s, 2H), 3.02 – 2.93 (m, 7H), 2.86
9 (s, 3H). ¹³C NMR (126 MHz, DMSO) δ 167.45, 165.09, 159.73, 148.25, 146.39, 140.07, 136.42,
10 122.21, 122.05, 116.18, 109.95, 109.18, 101.72, 41.21, 34.01, 29.36, 16.53. HRMS (ESI): calcd.
11 372.10180 for C₁₈H₁₈N₃O₄S; found 372.1021 [M+H]⁺.
12
13
14
15
16
17
18
19

20
21
22 *4-(methylamino)-2-phenethylthieno[3,2-d]pyrimidine-6-carboxylic acid (49)*
23

24 Isolated 40 mg (84% yield) as an off-white powder. ¹H NMR (500 MHz, DMSO) δ 7.99 (m, NH),
25 7.81 (s, 1H), 7.27 – 7.23 (m, 4H), 7.16 (m, 1H), 3.12 – 3.07 (m, 2H), 3.05 – 3.01 (m, 2H), 2.99 (d,
26 *J* = 4.0 Hz, 3H). ¹³C NMR (126 MHz, DMSO) δ 167.38, 164.21, 158.49, 142.88, 130.23, 129.48,
27 129.39, 126.90, 41.32, 34.82, 28.44. HRMS (ESI): calcd. 314.09632 for C₁₆H₁₆N₃O₂S; found
28 314.0962 [M+H]⁺.
29
30
31
32
33
34
35
36
37

38 *2-(3-Methoxyphenethyl)-4-(methylamino)thieno[3,2-d]pyrimidine-6-carboxylic acid (50)*
39

40 Isolated 78 mg (81% yield) as a white powder. ¹H NMR (500 MHz, DMSO) δ 8.11 (br. d, *J* = 4.3
41 Hz, 1H), 7.76 (s, 1H), 7.13 (t, *J* = 7.8 Hz, 1H), 6.81 – 6.75 (m, 2H), 6.68 (dd, *J* = 8.3, 1.7 Hz,
42 1H), 3.04 – 2.99 (m, 4H), 2.97 (d, *J* = 4.4 Hz, 3H). OCH₃ signal obscured by water peak. ¹³C
43 NMR (126 MHz, DMSO) δ 167.10, 164.14, 160.30, 144.29, 130.40, 129.32, 121.72, 121.68,
44 115.03, 112.40, 55.95, 40.79, 34.69. HRMS (ESI): calcd. 344.10689 for C₁₇H₁₈N₃O₃S; found
45 344.1072 [M+H]⁺.
46
47
48
49
50
51
52
53
54
55
56
57
58
59
60

1
2
3 *Ethyl 4-(((R)-2-methoxy-2-phenylethyl)amino)-5-methyl-2-((S)-2-phenylpropyl)thieno[2,3-*
4
5 *d]pyrimidine-6-carboxylate – 51* (precursor)

6
7 Isolated 101 mg (53% yield) as a colorless syrup. ¹H NMR (500 MHz, DMSO) δ 7.38 (m, 2H),
8
9 7.34 – 7.28 (m,), 7.22 (m, 5H), 7.10 (t, *J* = 6.8 Hz, 1H), 6.96 (br. t, *J* = 5.5 Hz, NH), 4.54 (dd, *J* =
10
11 7.5, 5.3 Hz, 1H), 4.27 (q, *J* = 7.1 Hz, 2H), 3.76 – 3.69 (m, 1H), 3.69 – 3.61 (m, 1H), 3.43 (m, 1H),
12
13 3.18 (s, 3H), 2.96 (m, 2H), 2.76 (s, 3H), 1.28 (t, *J* = 7.1 Hz, 3H), 1.20 (d, *J* = 6.9 Hz, 3H). ¹³C
14
15 NMR (75 MHz, DMSO) δ 167.65, 167.15, 162.87, 158.58, 147.31, 140.51, 140.03, 129.07,
16
17 128.85, 128.46, 127.41, 127.19, 126.50, 120.06, 115.15, 81.57, 79.84, 61.61, 57.16, 47.51, 39.04,
18
19 22.62, 15.94, 14.75. MS (ESI): calcd. 490.22; found 490.33 [M+H]⁺.

20
21
22
23
24
25
26 *4-(((R)-2-methoxy-2-phenylethyl)amino)-5-methyl-2-((S)-2-phenylpropyl)thieno[2,3-*
27
28 *d]pyrimidine-6-carboxylic acid (51)*

29
30 Isolated 13 mg (28% yield) as white solid. ¹H NMR (500 MHz, DMSO) δ 7.38 (m, 2H), 7.31 (m,
31
32 3H), 7.22 (m, 4H), 7.12 – 7.08 (m, 1H), 6.85 (br. s, NH), 4.54 (m, 1H), 3.72 (m, 1H), 3.68 – 3.60
33
34 (m, 1H), 3.18 (s, 3H), 3.02 – 2.86 (m, 3H), 2.75 (s, 3H), 1.20 (d, *J* = 6.9 Hz, 3H). ¹³C NMR (126
35
36 MHz, DMSO) δ 167.68, 167.10, 165.30, 159.07, 147.85, 141.06, 129.60, 129.40, 128.99, 127.97,
37
38 127.75, 127.04, 115.94, 82.06, 57.70, 47.98, 47.61, 39.57, 23.21, 16.17. HRMS (ESI): calcd.
39
40 462.18514 for C₂₆H₂₈N₃O₃S; found 462.1853 [M+H]⁺

41
42
43
44
45
46
47 *Ethyl 4-(((S)-2-methoxy-2-phenylethyl)amino)-5-methyl-2-((S)-2-phenylpropyl)thieno[2,3-*
48
49 *d]pyrimidine-6-carboxylate 52* (precursor)

50
51 Isolated 31 mg (16% yield) as a colorless syrup. ¹H NMR (500 MHz, DMSO) δ 7.41 – 7.36 (m,
52
53 2H), 7.31 (m, 3H), 7.25 – 7.20 (m, 4H), 7.10 (m, 1H), 6.99 (br. t, *J* = 5.4 Hz, NH), 4.51 (dd, *J* =
54
55 7.8, 4.7 Hz, 1H), 4.27 (q, *J* = 7.1 Hz, 2H), 3.79 – 3.73 (m, 1H), 3.62 (m, 1H), 3.44 (m, 1H), 3.17
56
57
58
59
60

1
2
3 (s, 3H), 2.95 (m, 2H), 2.78 (s, 3H), 1.28 (t, $J = 7.1$ Hz, 3H), 1.22 (d, $J = 7.0$ Hz, 3H). ^{13}C NMR
4
5 (75 MHz, DMSO) δ 167.62, 167.17, 162.90, 158.60, 147.27, 140.52, 140.12, 129.11, 128.88,
6
7 128.51, 127.45, 127.20, 126.54, 120.05, 115.17, 81.63, 61.68, 57.21, 47.49, 36.87, 24.96, 22.71,
8
9 16.00, 14.80. MS (ESI): calcd. 490.22; found 490.40 $[\text{M}+\text{H}]^+$.

14
15 *4-(((S)-2-Methoxy-2-phenylethyl)amino)-5-methyl-2-((S)-2-phenylpropyl)thieno[2,3-*
16
17 *d]pyrimidine-6-carboxylic acid (52)*

18
19 Isolated 15 mg (53% yield) as a white solid. ^1H NMR (500 MHz, DMSO) δ 7.39 (m, 2H), 7.31
20
21 (m, 3H), 7.21 (m, 4H), 7.10 (m, 1H), 6.97 (m, NH), 4.51 (dd, $J = 7.7, 4.4$ Hz, 1H), 3.76 (m, 1H),
22
23 3.62 (m, 1H), 3.17 (s, 3H), 2.95 (m, 3H), 2.77 (s, 3H), 1.22 (d, $J = 6.9$ Hz, 3H). ^{13}C NMR (126
24
25 MHz, DMSO) δ 167.30, 165.07, 159.10, 147.75, 141.02, 139.64, 129.62, 129.40, 129.02, 127.97,
26
27 127.73, 127.07, 122.30, 115.88, 82.12, 57.72, 47.89, 47.70, 39.49, 23.24, 16.32. HRMS (ESI):
28
29 calcd. 462.18514 for $\text{C}_{26}\text{H}_{28}\text{N}_3\text{O}_3\text{S}$; found 462.1857 $[\text{M}+\text{H}]^+$.

33
34
35
36 *Ethyl 4-(((R)-2-methoxy-2-phenylethyl)amino)-5-methyl-2-((R)-2-phenylpropyl)thieno[2,3-*
37
38 *d]pyrimidine-6-carboxylate 53 (precursor)*

39
40 Isolated 65 mg (63% yield) as pale yellow syrup. ^1H NMR (300 MHz, CDCl_3) δ 7.46 – 7.20 (m,
41
42 9H), 7.16 – 7.09 (m, 1H), 6.11 (br. t, NH), 4.41 – 4.31 (m, 3H), 4.08 (ddd, $J = 13.8, 7.2, 4.0$ Hz,
43
44 1H), 3.56 – 3.44 (m, 2H), 3.30 (s, 3H), 3.17 – 2.96 (m, 2H), 2.87 (s, 3H), 1.39 (t, $J = 7.1$ Hz, 3H),
45
46 1.29 (d, $J = 7.0$ Hz, 3H). ^{13}C NMR (75 MHz, CDCl_3) δ 163.33, 158.77, 147.18, 139.30, 138.36,
47
48 128.97, 128.57, 128.47, 127.27, 126.87, 126.13, 115.37, 82.07, 61.45, 57.25, 47.11, 39.30, 24.96,
49
50 22.09, 15.71, 14.56. MS (ESI): calcd. 490.22; found 490.33 $[\text{M}+\text{H}]^+$.

1
2
3 4-(((*R*)-2-Methoxy-2-phenylethyl)amino)-5-methyl-2-((*R*)-2-phenylpropyl)thieno[2,3-
4
5 *d*]pyrimidine-6-carboxylic acid (**53**)

6
7 Isolated 43 mg (76% yield) as white solid. ¹H NMR (500 MHz, DMSO) δ 7.39 (m, 2H), 7.31 (m,
8 3H), 7.25 – 7.18 (m, 4H), 7.12 – 7.07 (m, 1H), 7.04 (br. t, *J* = 5.4 Hz, NH), 4.50 (dd, *J* = 7.9, 4.7
9 Hz, 1H), 3.80 – 3.73 (m, 1H), 3.66 – 3.61 (m, 1H), 3.17 (s, 3H), 2.96 (m, 4H), 2.77 (s, 3H), 1.22
10 (d, *J* = 7.0 Hz, 3H). ¹³C NMR (126 MHz, DMSO) δ 167.06, 165.01, 159.08, 147.65, 140.95,
11 139.63, 129.63, 129.42, 129.04, 127.96, 127.73, 127.10, 122.47, 115.92, 82.10, 68.17, 57.72,
12 47.73, 39.47, 23.22, 16.28. HRMS (ESI): calcd. 462.18514 for C₂₆H₂₈N₃O₃S; found 462.1847
13 [M+H]⁺.
14
15
16
17
18
19
20
21
22
23
24
25

26 Ethyl 4-(((*S*)-2-methoxy-2-phenylethyl)amino)-5-methyl-2-((*R*)-2-phenylpropyl)thieno[2,3-
27
28 *d*]pyrimidine-6-carboxylate **54** (precursor)

29
30 Isolated 67 mg (65% yield) as a colorless syrup. ¹H NMR (300 MHz, CDCl₃) δ 7.46 – 7.32 (m,
31 5H), 7.30 – 7.19 (m, 4H), 7.13 (dt, *J* = 9.3, 4.2 Hz, 1H), 6.11 (br. t, NH), 4.39 (m, 3H), 4.06 (ddd,
32 *J* = 13.7, 7.0, 4.1 Hz, 1H), 3.57 – 3.44 (m, 2H), 3.31 (s, 3H), 3.08 (m, 2H), 2.87 (s, 3H), 1.38 (t, *J*
33 = 6.2 Hz, 3H), 1.27 (d, *J* = 6.9 Hz, 3H). ¹³C NMR (75 MHz, CDCl₃) δ 163.33, 158.78, 147.22,
34 139.29, 138.35, 128.97, 128.57, 128.47, 127.26, 126.88, 126.12, 115.37, 82.06, 61.45, 57.24,
35 47.06, 39.28, 36.93, 22.18, 15.68, 14.55. MS (ESI): calcd. 490.22; found 490.33 [M+H]⁺.
36
37
38
39
40
41
42
43
44
45
46
47

48 4-(((*S*)-2-Methoxy-2-phenylethyl)amino)-5-methyl-2-((*R*)-2-phenylpropyl)thieno[2,3-
49
50 *d*]pyrimidine-6-carboxylic acid (**54**)

51
52 Isolated 42 mg (74% yield) as a yellow solid. ¹H NMR (500 MHz, DMSO) δ 7.41 – 7.36 (m, 2H),
53 7.34 – 7.29 (m, 3H), 7.26 – 7.19 (m, 4H), 7.12 – 7.08 (m, 1H), 7.00 (br. t, *J* = 5.5 Hz, NH), 4.54
54 (dd, *J* = 7.6, 5.1 Hz, 1H), 3.76 – 3.70 (m, 1H), 3.69 – 3.62 (m, 1H), 3.18 (s, 3H), 2.96 (m, 3H),
55
56
57
58
59
60

1
2
3 2.75 (s, 3H), 1.20 (d, $J = 7.0$ Hz, 3H). ^{13}C NMR (126 MHz, DMSO) δ 167.12, 165.02, 159.09,
4
5 147.68, 140.96, 139.62, 129.62, 129.43, 129.04, 127.96, 127.75, 127.10, 122.45, 115.91, 82.02,
6
7 68.17, 57.70, 47.71, 39.55, 23.20, 16.25. HRMS (ESI): calcd. 462.18514 for $\text{C}_{26}\text{H}_{28}\text{N}_3\text{O}_3\text{S}$; found
8
9 462.1847 $[\text{M}+\text{H}]^+$.

10
11
12
13
14 *Ethyl (S)-2-(4-acetamidophenethyl)-4-((2-methoxy-2-phenylethyl)amino)-5-methylthieno[2,3-*
15
16 *d]pyrimidine-6-carboxylate* **55** (precursor)

17
18
19 Isolated 40 mg (82% yield, over two steps) as a white powder. ^1H NMR (300 MHz, CDCl_3) δ 7.55
20
21 (s, 1H), 7.41 (m, 7H), 7.15 (d, $J = 8.4$ Hz, 2H), 6.16 (br. m, NH), 4.43 (dd, $J = 8.6, 3.8$ Hz, 1H),
22
23 4.34 (q, $J = 7.1$ Hz, 2H), 4.14 (ddd, $J = 14.0, 7.0, 4.3$ Hz, 1H), 3.54 (ddd, $J = 13.7, 8.7, 3.8$ Hz,
24
25 1H), 3.31 (s, 3H), 3.07 (m, 4H), 2.88 (s, 3H), 2.12 (s, 3H), 1.38 (t, $J = 7.1$ Hz, 4H). ^{13}C NMR (75
26
27 MHz, CDCl_3) δ 163.32, 158.91, 150.73, 137.95, 129.11, 128.98, 126.87, 120.18, 115.46, 84.48,
28
29 61.49, 57.24, 47.08, 41.08, 33.87, 24.72, 15.72, 14.55. MS (ESI): calcd. 533.22; found
30
31 533.27 $[\text{M}+\text{H}]^+$.

32
33
34
35
36
37
38 *(S)-2-(4-Acetamidophenethyl)-4-((2-methoxy-2-phenylethyl)amino)-5-methylthieno[2,3-*
39
40 *d]pyrimidine-6-carboxylic acid* (**55**)

41
42
43 Isolated 24 mg (63% yield) as a white powder. ^1H NMR (500 MHz, DMSO) δ 9.81 (s, NHAc),
44
45 7.43 (d, $J = 8.5$ Hz, 2H), 7.39 – 7.28 (m, 5H), 7.12 (d, $J = 8.5$ Hz, 2H), 6.98 (br. t, $J = 5.2$ Hz,
46
47 NH), 4.54 (dd, $J = 7.7, 5.0$ Hz, 1H), 3.80 (m, 1H), 3.67 (m, 1H), 3.18 (s, 3H), 2.98 (m, 4H), 2.79
48
49 (s, 3H), 1.98 (s, 3H). ^{13}C NMR (126 MHz, DMSO) δ 169.15, 167.82, 165.09, 159.21, 141.02,
50
51 139.66, 138.37, 137.11, 129.61, 129.55, 129.00, 127.75, 122.32, 120.10, 115.96, 82.14, 57.69,
52
53 47.66, 41.28, 33.91, 25.08, 16.33. HRMS (ESI): calcd. 505.19095 for $\text{C}_{27}\text{H}_{29}\text{N}_4\text{O}_4\text{S}$; found
54
55 505.1916 $[\text{M}+\text{H}]^+$.

1
2
3
4
5 *Protein expression and purification:*
6

7 The heterologous expression of PglD was accomplished using the *E. coli* BL-21(DE3) strain
8 (Stratagene). Cells were transformed with pETNO-construct plasmids and grown to an A600 of
9 0.6 absorbance units at 37 °C in Lysogeny broth; the cultures were cooled to 16 °C and then
10 induced by the addition of 0.5 mM isopropyl-D-thiogalactopyranoside (IPTG). The pETNO
11 plasmid is based on the pET30a plasmid modified to include a His₈TEV (purification tag/protease
12 cleavage site) in place of the existing His₆-thrombin site. Twenty hours after induction the cells
13 were harvested by centrifugation and resuspended in ice-cold buffer composed of 50 mM HEPES
14 pH 7.1, 10 mM imidazole, 150 mM NaCl, at 1/20 the original culture volume. Maintaining a
15 working temperature of 4 °C, the cells were lysed by sonication, and the lysate was cleared by
16 centrifugation in a Type 45 Ti rotor (Beckman/Coulter) at 35,000 rpm. The extract was bound to
17 Ni-NTA (Qiagen) in batch mode using 1 mL of resin per liter of culture for 1h with gentle
18 tumbling. The protein-bound resin was washed with 25 column volumes of lysis buffer containing
19 50 mM imidazole, and the protein was eluted in lysis buffer containing 250 mM imidazole. The
20 hexahistidine tag was removed by TEV cleavage, and after the digest reached completion, the
21 reaction was dialyzed twice against 4 L 20 mM HEPES pH 7.1, 150 mM NaCl with a 10,000
22 MWCO Snakeskin (Thermo Scientific). Further purification was performed by size exclusion
23 chromatography using a Superdex 200 XK16–60 column (GE Healthcare) in a running buffer of
24 20 mM HEPES pH 7.1, 100 mM NaCl.
25
26
27
28
29
30
31
32
33
34
35
36
37
38
39
40
41
42
43
44
45
46
47
48
49

50
51
52 *High-throughput screening – Broad Institute MLPCN*
53

54 To a Nunc 384-well black-clear bottom plate (Thermo Scientific) was added 200 nL of compound
55 in neat DMSO (final assay concentration = 10 μM) and 20 μL of enzyme solution (final assay
56
57
58
59
60

1
2
3 concentrations: 6 nM PglD, 50 mM HEPES pH 7.4, 0.001% Triton, 0.05% BSA, 100 μ M
4
5 AcCoA). Solution dispensing was accomplished utilizing a Multidrop Combi (Thermo Scientific).
6
7 This mixture was allowed to incubate at room temperature for a duration of 45 minutes. The
8
9 reaction was started by the addition of 10 μ L reaction solution (final assay concentrations: 50 mM
10
11 HEPES pH7.4, 100 μ M UDP-4-aminosugar). The reaction was quenched after 30 minutes with
12
13 the addition of 30 μ L stop solution (final assay concentrations: 2 mM DTNB, 1 mM EDTA, 20%
14
15 1-propanol). The plates were allowed to develop for 5 minutes before reading at a $\lambda = 405$ nm.
16
17
18
19

20 21 *Enzymatic inhibition assay*

22
23 Kinetic characterization of PglD inhibition was carried out by monitoring CoASH release
24
25 resulting from the acetyltransferase reaction with Ellman's reagent (DTNB) in a continuous
26
27 fashion. To a flat, clear bottom 96-well plate (Falcon) was added sequentially the inhibitor as a
28
29 DMSO stock solution, followed by PglD in 50 mM HEPES pH 7.8, 1 mM $MgCl_2$, 0.05 mg/mL
30
31 BSA, 0.001% Triton X-100. Inhibitors and enzyme were pre-incubated 30 min at RT, followed by
32
33 addition of substrate and Ellman's reagent cocktail to final concentrations of 3 nM PglD, 500 μ M
34
35 4-amino-sugar, 300 μ M AcCoA, 2 mM DTNB and 3% DMSO in 150 μ L volume. Initial rates
36
37 were measured in the linear portion of the reaction curve over a 5 min time period at RT,
38
39 measuring absorbance at 412 nm on a Synergy H1 hybrid plate reader from Biotek.
40
41
42
43
44
45
46

47 *Dynamic Light Scattering*

48
49 Samples were prepared in buffer 50 mM HEPES 7.5, 100 mM NaCl and a final concentration of
50
51 3% DMSO; the concentration of *C jejuni* PglD was 25 μ M with or without 250 μ M inhibitor **57**.
52
53
54
55 DLS data was acquired on a Wyatt DynaPro Nanostar Light Scatterer by measuring scattering at a 90°
56
57
58
59
60

1
2
3 angle with a 685 nm laser and analyzed with a Rayleigh scattering model using the Dynamics 7.1.9
4
5 software package.
6
7
8

9 10 *Differential Scanning Fluorimetry*

11
12 Samples were prepared to a final volume of 25 μL containing 10 μM PglD protein and 100 μM
13
14 inhibitor in a buffer containing 50 mM HEPES 7.5, 150 mM NaCl, 0.001 % Triton X-100, 10x
15
16 Sypro orange (diluted from a commercial stock solution of 5000X; Invitrogen) and a final
17
18 concentration of 3% DMSO. All samples were prepared in duplicate. Fluorescence was measured
19
20 using a Roche Lightcycler 480 RT-PCR instrument while increasing the temperature gradient
21
22 from 30 to 95°C in increments of 4.4°C/60 s. The midpoint temperature of the unfolding protein
23
24 transition (T_m) was calculated using the built-in functionality of the instrument software package.
25
26
27
28
29
30

31 *Crystallization of C. jejuni PglD in complex with inhibitor 17*

32
33 Initial crystallization screening was performed by sitting drop vapor diffusion using intelli-plate[®]
34
35 from Hampton Research with 50 μL /well solution, which was dispensed as a 0.15 μL drop
36
37 followed 0.15 μL of 10 mg/mL PglD solution in SEC buffer. Screens used were PEG suite 1, PEG
38
39 suite 2, PACT and ProComp from Qiagen, and drops were set up using an Art Robbins Phoenix
40
41 robot. Diffraction quality crystals were formed via hanging drop vapor diffusion by mixing 1.5
42
43 μL of protein solution with 1.5 μL of reservoir solution (15% PEG-3350, 0.1M NaF and 10%
44
45 glycerol) and incubation at 22 °C.
46
47
48

49
50 Ligand soaking: Wells were carefully opened and 50 μL of DMSO was added directly to the well;
51
52 0.75 μL of a solution containing 10 mM inhibitor **17** in reservoir solution (final concentration of
53
54 10% DMSO) was added directly to the drops on the slide. The crystals were then incubated for 30
55
56
57
58
59
60

1
2
3 min to 3 days, and then looped and flash frozen in liquid nitrogen without the need of separate
4
5 cryoprotection.
6
7

8
9
10 *Data Collection, Processing, and Structure Refinement*

11
12 Diffraction data was collected either at a home source (Rigaku Saturn 944 with MicroMax-007
13
14 HF and VariMax HF generator) or at the Advanced Photon Source (APS) at Argonne National
15
16 Laboratory (in Argonne, Illinois, USA) national synchrotron on the NECAT-24ID beamline.

17
18 The diffraction data were indexed and scaled with either HKL2000. The initial structure model
19
20 was built by applying molecular replacement methods with a ligand/solvent-omitted input model
21
22 generated from the PDB model 3BSY. The initial models were further improved through iterative
23
24 rounds of manual and automated refinement with COOT.⁵⁶ The final structure has been deposited
25
26 into the Protein Data Bank PDB ID 5T2Y. Data collection and refinement statistics are presented
27
28
29 in in the supporting information **Table S3**
30
31
32
33
34
35
36
37
38
39
40
41
42
43
44
45
46
47
48
49
50
51
52
53
54
55
56
57
58
59
60

Supporting Information

Supporting information accompanying this paper includes NMR spectra and LC-MS chromatograms of selected inhibitors, molecular formula strings table, enzyme inhibition studies, DLS studies, and X-ray crystallography data.

PDB IDs: 5T2Y and 5TYH The atomic coordinates and experimental data will be released on the PDB upon article publication.

Corresponding Author Information

Phone: +1-617-253-1838

Email: imper@mit.edu

Author Contributions

J.P.M., M.J.M. and A.C. were involved in the initial stages of the project, including enzyme expression and assay development, fragment screening and determination of the 5TYH structure, MLPCN screening and thienopyrimidinone hit validation. J.W.D. S. synthesized the thienopyrimidine series compounds, carried out biochemical and biophysical assays and determined the 5T2Y structure. J.W.D. S. and B.I. wrote the paper and all authors contributed to editing the final manuscript.

Conflict of interests

The authors declare that there is no conflict of interests

Acknowledgements

1
2
3 We thank Dr. K. Rajashankar and the staff at NECAT-24ID (APS) for facilitating X-ray data
4
5 collection for the 5T2Y structure and Dr. Alexei Soares (BNL) for the 5TYH structure, Dr. Robert
6
7 Grant (MIT) and Dr. Nelson Olivier for technical assistance with protein crystallography and data
8
9 processing and Dr. James Spoonamore (Broad Institute) for the MLPCN screening. We also thank
10
11 Drs. Amael Madec and Cristina Zamora for their valuable assistance with the preparation of this
12
13 manuscript. Financial support for this work was provided by NIH (R01-GM097241 & R03-
14
15 MH096549 to BI), the Belgian American Education Foundation (fellowship to J.W.D.S.) and the
16
17 Homerton College, Cambridge (Junior Research Fellowship to A.C.). Part of this work is based
18
19 upon research conducted at the Northeastern Collaborative Access Team beamline 24-ID-E,
20
21 which is funded by the National Institute of General Medical Sciences from the National
22
23 Institutes of Health (P41 GM103403). This research used resources of the Advanced Photon
24
25 Source, a U.S. Department of Energy (DOE) Office of Science User Facility operated for the
26
27 DOE Office of Science by Argonne National Laboratory under Contract No. DE-AC02-
28
29 06CH11357.
30
31
32
33
34
35
36
37

38 **Abbreviations**

39
40 AcCoA: acetyl coenzyme A

41
42 BOP: (Benzotriazol-1-yloxy)tris(dimethylamino)phosphonium hexafluorophosphate

43
44 DBU: 1,8-Diazabicyclo[5.4.0]undec-7-ene

45
46 diNAcBac: 2,4-diacetamido-2,4,6-trideoxy- α -D-glucose

47
48 PyBOP: (Benzotriazol-1-yloxy)tripyrrolidinophosphonium hexafluorophosphate

49
50 DSF: Differential scanning fluorimetry

51
52 dynamic light scattering (DLS)

53
54 PLP: Pyridoxal 5'-phosphate
55
56
57
58
59
60

1
2
3
4
5
6
7
8
9
10
11
12
13
14
15
16
17
18
19
20
21
22
23
24
25
26
27
28
29
30
31
32
33
34
35
36
37
38
39
40
41
42
43
44
45
46
47
48
49
50
51
52
53
54
55
56
57
58
59
60

STD: saturation transfer difference

UndP: undecaprenyl phosphate

References

- (1) Silver, L. L., Challenges of Antibacterial Discovery, *Clin. Microbiol. Rev.* **2011**, *24*, 71-109.
- (2) Clatworthy, A. E.; Pierson, E.; Hung, D. T., Targeting Virulence: A New Paradigm for Antimicrobial Therapy, *Nat. Chem. Biol.* **2007**, *3*, 541-548.
- (3) Baron, C., Antivirulence Drugs to Target Bacterial Secretion Systems, *Curr. Opin. Microbiol.* **2010**, *13*, 100-105.
- (4) Barczak, A. K.; Hung, D. T., Productive Steps Toward an Antimicrobial Targeting Virulence, *Curr. Opin. Microbiol.* **2009**, *12*, 490-496.
- (5) Cegelski, L.; Marshall, G. R.; Eldridge, G. R.; Hultgren, S. J., The Biology and Future Prospects of Antivirulence Therapies, *Nat. Rev. Micro.* **2008**, *6*, 17-27.
- (6) Ohtsubo, K.; Marth, J. D., Glycosylation in Cellular Mechanisms of Health and Disease, *Cell* **2006**, *126*, 855-867.
- (7) Nothaft, H.; Szymanski, C. M., Bacterial Protein N-glycosylation: New Perspectives and Applications, *J. Biol. Chem.* **2013**, *288*, 6912-6920.
- (8) Aas, F. E.; Vik, Å.; Vedde, J.; Koomey, M.; Egge-Jacobsen, W., Neisseria gonorrhoeae O-linked Pilin Glycosylation: Functional Analyses Define Both the bBosynthetic Pathway and Glycan Structure, *Mol. Microbiol.* **2007**, *65*, 607-624.
- (9) Benz, I.; Schmidt, M. A., Never Say Never Again: Protein Glycosylation in Pathogenic Bacteria, *Mol. Microbiol.* **2002**, *45*, 267-276.
- (10) Szymanski, C. M.; Wren, B. W., Protein Glycosylation in Bacterial Mucosal Pathogens, *Nat. Rev. Micro.* **2005**, *3*, 225-237.

- 1
2
3 (11) Vik, Å.; Aas, F. E.; Anonsen, J. H.; Bilsborough, S.; Schneider, A.; Egge-Jacobsen,
4
5 W.; Koomey, M., Broad Spectrum O-Linked Protein Glycosylation in the Human Pathogen
6
7 *Neisseria gonorrhoeae*, *Proc. Natl. Acad. Sci. U. S. A.* **2009**, *106*, 4447-4452.
8
9
10 (12) Szymanski, C. M.; Yao, R.; Ewing, C. P.; Trust, T. J.; Guerry, P., Evidence for a
11
12 System of General Protein Glycosylation in *Campylobacter jejuni*, *Mol. Microbiol.* **1999**, *32*,
13
14 1022-1030.
15
16
17 (13) Nothaft, H.; Szymanski, C. M., Protein Glycosylation in Bacteria: Sweeter Than
18
19 Ever, *Nat. Rev. Micro.* **2010**, *8*, 765-778.
20
21
22 (14) Scott, N. E.; Parker, B. L.; Connolly, A. M.; Paulech, J.; Edwards, A. V. G.;
23
24 Crossett, B.; Falconer, L.; Kolarich, D.; Djordjevic, S. P.; Højrup, P.; Packer, N. H.; Larsen, M.
25
26 R.; Cordwell, S. J., Simultaneous Glycan-Peptide Characterization Using Hydrophilic Interaction
27
28 Chromatography and Parallel Fragmentation by CID, Higher Energy Collisional Dissociation, and
29
30 Electron Transfer Dissociation MS Applied to the N-Linked Glycoproteome of *Campylobacter*
31
32 *jejuni*, *Mol. Cell. Proteomics* **2011**, *10*, M000031-MCP000201.
33
34
35 (15) Schmidt, M. A.; Riley, L. W.; Benz, I., Sweet New World: Glycoproteins in
36
37 Bacterial Pathogens, *Trends Microbiol.* **2003**, *11*, 554-561.
38
39
40 (16) Sharon, N., Celebrating the Golden Anniversary of the Discovery of Bacillosamine,
41
42 the Diamino Sugar of a Bacillus, *Glycobiology* **2007**, *17*, 1150-1155.
43
44
45 (17) Morrison, M. J.; Imperiali, B., The Renaissance of Bacillosamine and Its
46
47 Derivatives: Pathway Characterization and Implications in Pathogenicity, *Biochemistry* **2014**, *53*,
48
49 624-638.
50
51
52 (18) Olivier, N. B.; Chen, M. M.; Behr, J. R.; Imperiali, B., In Vitro Biosynthesis of
53
54 UDP-N,N'-Diacetylbacillosamine by Enzymes of the *Campylobacter jejuni* General Protein
55
56 Glycosylation System†, *Biochemistry* **2006**, *45*, 13659-13669.
57
58
59
60

- 1
2
3 (19) Hartley, M. D.; Morrison, M. J.; Aas, F. E.; Børud, B.; Koomey, M.; Imperiali, B.,
4
5 Biochemical Characterization of the O-Linked Glycosylation Pathway in *Neisseria gonorrhoeae*
6
7 Responsible for Biosynthesis of Protein Glycans Containing N,N'-Diacetylbaucillosamine,
8
9 *Biochemistry* **2011**, *50*, 4936-4948.
10
11
12 (20) Morrison, M. J.; Imperiali, B., Biosynthesis of UDP-N,N'-Diacetylbaucillosamine in
13
14 *Acinetobacter baumannii*: Biochemical Characterization and Correlation to Existing Pathways,
15
16 *Arch. Biochem. Biophys.* **2013**, *536*, 72-80.
17
18
19 (21) Kelly, J.; Jarrell, H.; Millar, L.; Tessier, L.; Fiori, L. M.; Lau, P. C.; Allan, B.;
20
21 Szymanski, C. M., Biosynthesis of the N-Linked Glycan in *Campylobacter jejuni* and Addition
22
23 onto Protein through Block Transfer, *J. Bacteriol.* **2006**, *188*, 2427-2434.
24
25
26 (22) Hendrixson, D. R.; DiRita, V. J., Identification of *Campylobacter jejuni* Genes
27
28 Involved in Commensal Colonization of the Chick Gastrointestinal Tract, *Mol. Microbiol.* **2004**,
29
30 *52*, 471-484.
31
32
33 (23) Szymanski, C. M.; Burr, D. H.; Guerry, P., *Campylobacter* Protein Glycosylation
34
35 Affects Host Cell Interactions, *Inf. Immun.* **2002**, *70*, 2242-2244.
36
37
38 (24) Larsen, J. C.; Szymanski, C.; Guerry, P., N-Linked Protein Glycosylation Is
39
40 Required for Full Competence in *Campylobacter jejuni* 81-176, *J. Bacteriol.* **2004**, *186*, 6508-
41
42 6514.
43
44
45 (25) Elmi, A.; Watson, E.; Sandu, P.; Gundogdu, O.; Mills, D. C.; Inglis, N. F.; Manson,
46
47 E.; Imrie, L.; Bajaj-Elliott, M.; Wren, B. W.; Smith, D. G.; Dorrell, N., *Campylobacter jejuni*
48
49 Outer Membrane Vesicles Play an Important Role in Bacterial Interactions with Human Intestinal
50
51 Epithelial Cells, *Infect. Immun.* **2012**, *80*, 4089-4098.
52
53
54 (26) Ellis, T. N.; Kuehn, M. J., Virulence and Immunomodulatory Roles of Bacterial
55
56 Outer Membrane Vesicles, *Microbiol. Mol. Biol. Rev.* **2010**, *74*, 81-94.
57
58
59
60

- 1
2
3 (27) Jennings, M. P.; Jen, F. E. C.; Roddam, L. F.; Apicella, M. A.; Edwards, J. L.,
4
5 Neisseria gonorrhoeae Pilin Glycan Contributes to CR3 Activation During Challenge of Primary
6
7 Cervical Epithelial Cells, *Cell. Microbiol.* **2011**, *13*, 885-896.
8
9
10 (28) Olivier, N. B.; Imperiali, B., Crystal Structure and Catalytic Mechanism of PglD
11
12 from *Campylobacter jejuni*, *J. Biol. Chem.* **2008**, *283*, 27937-27946.
13
14 (29) Rangarajan, E. S.; Ruane, K. M.; Sulea, T.; Watson, D. C.; Proteau, A.; Leclerc, S.;
15
16 Cygler, M.; Matte, A.; Young, N. M., Structure and Active Site Residues of PglD, an N-
17
18 Acetyltransferase from the Bacillosamine Synthetic Pathway Required for N-Glycan Synthesis in
19
20 *Campylobacter jejuni*, *Biochemistry* **2008**, *47*, 1827-1836.
21
22
23 (30) Vetting, M. W.; LP, S. d. C.; Yu, M.; Hegde, S. S.; Magnet, S.; Roderick, S. L.;
24
25 Blanchard, J. S., Structure and Functions of the GNAT Superfamily of Acetyltransferases, *Arch.*
26
27 *Biochem. Biophys.* **2005**, *433*, 212-226.
28
29
30 (31) Aspinall, G. O.; McDonald, A. G.; Pang, H.; Kurjanczyk, L. A.; Penner, J. L.,
31
32 Lipopolysaccharides of *Campylobacter jejuni* Serotype O:19: Structures of Core Oligosaccharide
33
34 Regions from the Serostrain and Two Bacterial Isolates from Patients with the Guillain-Barre
35
36 Syndrome, *Biochemistry* **1994**, *33*, 241-249.
37
38
39 (32) Allos, B. M.; Lippy, F. T.; Carlsen, A.; Washburn, R. G.; Blaser, M. J.,
40
41 *Campylobacter jejuni* Strains from Patients with Guillain-Barre Syndrome, *Emerg. Infect. Disease*
42
43 **1998**, *4*, 263-268.
44
45
46 (33) Luangtongkum, T.; Jeon, B.; Han, J.; Plummer, P.; Logue, C. M.; Zhang, Q.,
47
48 Antibiotic Resistance in *Campylobacter*: Emergence, Transmission and Persistence, *Fut.*
49
50 *Microbiol.* **2009**, *4*, 189-200.
51
52
53 (34) Scott, D. E.; Coyne, A. G.; Hudson, S. A.; Abell, C., Fragment-Based Approaches
54
55 in Drug Discovery and Chemical Biology, *Biochemistry* **2012**, *51*, 4990-5003.
56
57
58
59
60

- 1
2
3 (35) Silvestre, H. L.; Blundell, T. L.; Abell, C.; Ciulli, A., Integrated Biophysical
4 Approach to Fragment Screening and Validation for Fragment-Based Lead Discovery, *Proc. Natl.*
5 *Acad. Sci. U. S. A.* **2013**, *110*, 12984-12989.
6
7
8
9
10 (36) Ellman, G. L., Tissue Sulfhydryl Groups, *Arch. Biochem. Biophys.* **1959**, *82*, 70-77.
11
12 (37) NCBI. Inhibition of Glycoprotein Biosynthesis in Gram-Negative Pathogens
13 Inhibitor Probe Project, <https://pubchem.ncbi.nlm.nih.gov/bioassay/602402>, Deposit Date: 2012-
14 03-15.
15
16
17
18
19 (38) Friesner, R. A.; Murphy, R. B.; Repasky, M. P.; Frye, L. L.; Greenwood, J. R.;
20 Halgren, T. A.; Sanschagrín, P. C.; Mainz, D. T., Extra Precision Glide: Docking and Scoring
21 Incorporating a Model of Hydrophobic Enclosure for Protein–Ligand Complexes, *J. Med. Chem.*
22 **2006**, *49*, 6177-6196.
23
24
25
26
27
28 (39) James, C. E.; Mahendran, K. R.; Molitor, A.; Bolla, J. M.; Bessonov, A. N.;
29 Winterhalter, M.; Pagès, J. M., How β -Lactam Antibiotics Enter Bacteria: A Dialogue with the
30 Porins, *PLoS ONE* **2009**, *4*, e5453.
31
32
33
34
35 (40) Doak, B. C.; Zheng, J.; Dobritzsch, D.; Kihlberg, J., How Beyond Rule of 5 Drugs
36 and Clinical Candidates Bind to Their Targets, *J. Med. Chem.* **2016**, *59*, 2312-2327.
37
38
39
40 (41) Hann, M. M.; Keseř, G. M., Finding the Sweet Spot: The Role of Nature and
41 Nurture in Medicinal Chemistry, *Nat. Rev. Drug. Discov.* **2012**, *11*, 355-365.
42
43
44 (42) Wan, Z.-K.; Wacharasindhu, S.; Binnun, E.; Mansour, T., An Efficient Direct
45 Amination of Cyclic Amides and Cyclic Ureas, *Org. Lett.* **2006**, *8*, 2425-2428.
46
47
48 (43) Albe, K. R.; Butler, M. H.; Wright, B. E., Cellular Concentrations of Enzymes and
49 their Substrates, *J. Theor. Biol.* **1990**, *22143*, 163-195.
50
51
52
53
54
55
56
57
58
59
60

- 1
2
3 (44) Seidler, J.; McGovern, S. L.; Doman, T. N.; Shoichet, B. K., Identification and
4
5 Prediction of Promiscuous Aggregating Inhibitors among Known Drugs, *J. Med. Chem.* **2003**, *46*,
6
7 4477-4486.
8
9
10 (45) Pantoliano, M. W.; Petrella, E. C.; Kwasnoski, J. D.; Lobanov, V. S.; Myslik, J.;
11
12 Graf, E.; Carver, T.; Asel, E.; Springer, B. A.; Lane, P.; Salemme, F. R., High-Density
13
14 Miniaturized Thermal Shift Assays as a General Strategy for Drug Discovery, *J. Biomol. Screen.*
15
16 **2001**, *6*, 429-440.
17
18
19 (46) Wallace, A. C.; Laskowski, R. A.; Thornton, J. M., LIGPLOT: a program to
20
21 generate schematic diagrams of protein-ligand interactions, *Protein Eng* **1995**, *8*, 127-134.
22
23
24 (47) Dunford, J. E.; Kwaasi, A. A.; Rogers, M. J.; Barnett, B. L.; Ebetino, F. H.;
25
26 Russell, R. G. G.; Oppermann, U.; Kavanagh, K. L., Structure–Activity Relationships Among the
27
28 Nitrogen Containing Bisphosphonates in Clinical Use and Other Analogues: Time-Dependent
29
30 Inhibition of Human Farnesyl Pyrophosphate Synthase, *J. Med. Chem.* **2008**, *51*, 2187-2195.
31
32
33 (48) Morrison, M. J.; Imperiali, B., Biochemical Analysis and Structure Determination
34
35 of Bacterial Acetyltransferases Responsible for the Biosynthesis of UDP-N,N'-
36
37 Diacetylbaucillosamine, *J. Biol. Chem.* **2013**, *288*, 32248-32260.
38
39
40 (49) Lertpiriyapong, K.; Gamazon, E. R.; Feng, Y.; Park, D. S.; Pang, J.; Botka, G.;
41
42 Graffam, M. E.; Ge, Z.; Fox, J. G., *Campylobacter jejuni* Type VI Secretion System: Roles in
43
44 Adaptation to Deoxycholic Acid, Host Cell Adherence, Invasion, and in vivo Colonization, *PLoS*
45
46 *ONE* **2012**, *7*, e42842.
47
48
49 (50) Isabella, Vincent M.; Campbell, Arthur J.; Manchester, J.; Sylvester, M.; Nayar,
50
51 Asha S.; Ferguson, Keith E.; Tommasi, R.; Miller, Alita A., Toward the Rational Design of
52
53 Carbapenem Uptake in *Pseudomonas aeruginosa*, *Chem. Biol.* **2015**, *22*, 535-547.
54
55
56
57
58
59
60

1
2
3 (51) Lo, A. W. H.; Van de Water, K.; Gane, P. J.; Chan, A. W. E.; Steadman, D.;
4
5 Stevens, K.; Selwood, D. L.; Waksman, G.; Remaut, H., Suppression of Type 1 Pilus Assembly in
6
7 Uropathogenic *Escherichia coli* by Chemical Inhibition of Subunit Polymerization, *J. Antimicrob.*
8
9 *Chemother.* **2014**, *69*, 1017-1026.

10
11 (52) Adams, L. A.; Sharma, P.; Mohanty, B.; Ilyichova, O. V.; Mulcair, M. D.;
12
13 Williams, M. L.; Gleeson, E. C.; Totsika, M.; Doak, B. C.; Caria, S.; Rimmer, K.; Horne, J.;
14
15 Shouldice, S. R.; Vazirani, M.; Headey, S. J.; Plumb, B. R.; Martin, J. L.; Heras, B.; Simpson, J.
16
17 S.; Scanlon, M. J., Application of Fragment-Based Screening to the Design of Inhibitors of
18
19 *Escherichia coli* DsbA, *Angew. Chem. Int. Ed. Engl.* **2015**, *54*, 2179-2184.

20
21 (53) Moore, J. D.; Rossi, F. M.; Welsh, M. A.; Nyffeler, K. E.; Blackwell, H. E., A
22
23 Comparative Analysis of Synthetic Quorum Sensing Modulators in *Pseudomonas aeruginosa*:
24
25 New Insights into Mechanism, Active Efflux Susceptibility, Phenotypic Response, and Next-
26
27 Generation Ligand Design, *J. Am. Chem. Soc.* **2015**, *137*, 14626-14639.

28
29 (54) Ménard, R.; Schoenhofen, I. C.; Tao, L.; Aubry, A.; Bouchard, P.; Reid, C. W.;
30
31 Lachance, P.; Twine, S. M.; Fulton, K. M.; Cui, Q.; Hogues, H.; Purisima, E. O.; Sulea, T.;
32
33 Logan, S. M., Small-Molecule Inhibitors of the Pseudaminic Acid Biosynthetic Pathway:
34
35 Targeting Motility as a Key Bacterial Virulence Factor, *Antimicrob. Agents. Chemother.* **2014**, *58*,
36
37 7430-7440.

38
39 (55) Curtis, M. M.; Russell, R.; Moreira, C. G.; Adebisin, A. M.; Wang, C.; Williams,
40
41 N. S.; Taussig, R.; Stewart, D.; Zimmern, P.; Lu, B.; Prasad, R. N.; Zhu, C.; Rasko, D. A.;
42
43 Huntley, J. F.; Falck, J. R.; Sperandio, V., QseC Inhibitors as an Antivirulence Approach for
44
45 Gram-Negative Pathogens, *mBio.* **2014**, *5*, e02165.

46
47 (56) Emsley, P.; Cowtan, K., Coot: Model-Building Tools for Molecular Graphics, *Acta*
48
49 *Cryst. Sect. D* **2004**, *60*, 2126-2132.

1
2
3
4
5
6
7
8
9
10
11
12
13
14
15
16
17
18
19
20
21
22
23
24
25
26
27
28
29
30
31
32
33
34
35
36
37
38
39
40
41
42
43
44
45
46
47
48
49
50
51
52
53
54
55
56
57
58
59
60

Table of Contents Graphic

